

VU Research Portal

Visualizing the Shrinking Brain: Longitudinal MR Studies in the Spectrum of Cognitive Decline

Sluimer, J.D.

2011

document version

Publisher's PDF, also known as Version of record

[Link to publication in VU Research Portal](#)

citation for published version (APA)

Sluimer, J. D. (2011). *Visualizing the Shrinking Brain: Longitudinal MR Studies in the Spectrum of Cognitive Decline*. [PhD-Thesis - Research and graduation internal, Vrije Universiteit Amsterdam].

General rights

Copyright and moral rights for the publications made accessible in the public portal are retained by the authors and/or other copyright owners and it is a condition of accessing publications that users recognise and abide by the legal requirements associated with these rights.

- Users may download and print one copy of any publication from the public portal for the purpose of private study or research.
- You may not further distribute the material or use it for any profit-making activity or commercial gain
- You may freely distribute the URL identifying the publication in the public portal ?

Take down policy

If you believe that this document breaches copyright please contact us providing details, and we will remove access to the work immediately and investigate your claim.

E-mail address:

vuresearchportal.ub@vu.nl

VISUALIZING THE SHRINKING BRAIN:
LONGITUDINAL MR STUDIES
IN THE SPECTRUM OF COGNITIVE DECLINE

Jasper Daniël Sluimer

The studies described in this thesis were carried out in the Image Analysis Center of the department of Radiology, and the Alzheimer Center of the department of Neurology at the VU University Medical Center.

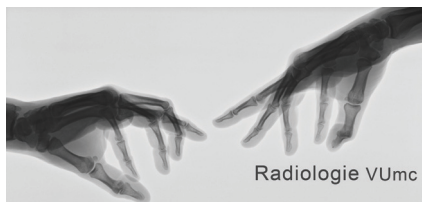
Funding of this research project was kindly provided by:



Project number 03514



Image Analysis Center



Voor mijn naasten

© Jasper D. Sluimer, Amsterdam, The Netherlands

All rights reserved. No part of this thesis may be reproduced or transmitted in any form or by any means without the prior written permission of the copyright holder.

ISBN: 978-94-91211-16-4

The studies described in this thesis were carried out at the Alzheimer Center VUmc. The Alzheimercenter VUmc is supported by unrestricted grants from AEGON Nederland NV, Ars Donandi Kas Bank Welzijnsfonds, Heer en Mw Capitain, Heineken Nederland NV, ING Private Banking, Janssen, Kroonenberg Groep, KLM Royal Dutch Airlines, KPN/Talk & Vision, Krafft stichting, Novartis, Nutricia Nederland, Pfizer Nederland, Soroptimisten Bussum e.o, Stichting ITON, Stichting De Merel, Stichting Alzheimer Nederland, Stichting Dioraphte, Stichting VitaValley, Stichting Mooiste Contact Fonds KPN, Twentse Kabel Holding, Ton aan de Stegge, Unilever Nederland, van Leeuwen-Rietberg stichting, Vereniging AEGON

Publication of this thesis has been accomplished with greatly acknowledged financial support, provided by R Emmert Adriaan Laan fonds, van Leersum fonds, Image Analysis Center, Alzheimercentrum, Alzheimer Nederland, Philips Healthcare Benelux, Danone Research – Centre for Specialised Nutrition, Firma Janssen, Novartis Pharma, Lundbeck, Sanofi-Aventis, Internationale Stichting Alzheimer Onderzoek, Guerbet, GE Healthcare, the Alzheimer Research Centrum, and



The author has no disclosures to report. At the time of writing and printing of this thesis, the author did not own stock options or have any financial interests in the aforementioned companies.

Lay-out and cover by: Nicole Coenen-van den Hout
 www.proefschriftvormgeven.nl

Printed by: Ipskamp Drukkers, Enschede

VRIJE UNIVERSITEIT

**Visualizing the Shrinking Brain:
Longitudinal MR Studies
in the Spectrum of Cognitive Decline**

ACADEMISCH PROEFSCHRIFT

ter verkrijging van de graad Doctor aan
de Vrije Universiteit Amsterdam,
op gezag van de rector magnificus
prof.dr. L.M. Bouter,
in het openbaar te verdedigen
ten overstaan van de promotiecommissie
van de faculteit der Geneeskunde
op donderdag 28 april 2011 om 13.45 uur
in de aula van de universiteit,
De Boelelaan 1105

door

Jasper Daniël Sluimer

geboren te Vlaardingen

promotoren: prof.dr. F. Barkhof
 prof.dr. Ph. Scheltens

copromotoren: dr. W.M. van der Flier
 dr. H. Vrenken

‘Always look on the bright side of life’

Brian, 33 AD

CONTENTS

| | |
|--|-----|
| LIST OF ABBREVIATIONS | 12 |
| CHAPTER 1 Introduction | 15 |
| CHAPTER 2 Amnesic mild cognitive impairment: Structural MRI findings predictive of conversion to Alzheimer's disease American Journal of Neuroradiology 2008 | 25 |
| CHAPTER 3 Whole-brain atrophy and cognitive decline: A longitudinal MRI study of memory clinic patients Radiology 2008 | 45 |
| CHAPTER 4 Accelerating regional atrophy rates in the progression from normal aging to Alzheimer's disease. European Radiology 2009 | 65 |
| CHAPTER 5 Added value over whole-brain volume measures Neurology 2009 | 85 |
| CHAPTER 6 Whole-brain atrophy rate in Alzheimer's disease: Identifying fast progressors Neurology 2008 | 105 |
| CHAPTER 7 Whole-brain atrophy rate and CSF biomarker levels in MCI and AD: A longitudinal study Neurobiology of Aging 2010 | 123 |
| CHAPTER 8 General Discussion, Summary & Future perspectives | 141 |
| NEDERLANDSE SAMENVATTING | 154 |
| CURRICULUM VITAE | 158 |
| LIST OF PUBLICATIONS | 159 |
| THESES ALZHEIMERCENTRUM | 161 |
| DANKWOORD / ACKNOWLEDGEMENTS | 163 |

List of Abbreviations

| | |
|---------------------------|--|
| 3D | 3-dimensional |
| A β ₁₋₄₂ | Beta-amyloid 1-42 |
| AAL | Automated Anatomical Labeling |
| AD | Alzheimer's disease |
| ANOVA | Analysis of variance |
| APOE | Apolipoprotein E genotype |
| ASL | Arterial spin labeling |
| BET | Brain extraction tool |
| CDR | Clinical dementia rating |
| CI | Confidence interval |
| CSF | Cerebrospinal Fluid |
| CV | Coefficient of variation |
| DBC | Differential bias correction |
| DLB | Dementia with Lewy bodies |
| dof | Degrees of freedom |
| FAST | FMRIB's Automated Segmentation Tool |
| FDR | False discovery rate |
| FLAIR | Fluid attenuation inversion recovery |
| FLIRT | FMRIB's Linear Image Registration Tool |
| FSL | FMRIB Software Library |
| FTLD | Frontal-temporal lobar degeneration |
| FWHM | Full-width at half maximum |
| GM | Grey matter |
| HR | Hazard ratio |
| IDL | Interface Description Language |
| LP | Lumbar puncture |
| MCI | Mild Cognitive Impairment |
| MMSE | Mini-mental state examination |
| MNI-152 | Montreal neurological institute-152 (standard brain image) |
| MP-RAGE | Magnetization prepared rapid acquisition gradient echo |

| | |
|----------------------|---|
| MRI | Magnetic Resonance Imaging |
| MTA | Medial temporal lobe atrophy |
| NBV | Normalized Brain Volume |
| NFT | Neurofibrillary tangles |
| NINCDS-ADRDA | National Institute of Neurological and Communicative Diseases and Stroke/Alzheimer's Disease and Related Disorders Association |
| NINDS-AIREN | National Institute of Neurological Disorders and Stroke and Association Internationale pour la Recherche et l'Enseignement en Neurosciences |
| NYU | NYU paragraph recall tests |
| PBVC | Percentage Brain Volume Change (whole-brain atrophy rate) |
| PET | Positron Emission Tomography |
| P-tau ₁₈₁ | Tau phosphorylated at threonine-181 |
| ROI | Region of interest |
| SIENA | Structural Image Evaluation using Normalisation of Atrophy |
| SIENAX | Structural Image Evaluation using Normalisation of Atrophy Cross-sectional |
| SPAM | Statistical probability anatomical maps |
| SPECT | Single Photon Emission Computed Tomography |
| SPM | Statistical Parametric Mapping |
| SPSS | Statistical Package for the Social Sciences |
| VaD | Vascular dementia |
| VAT | Visual association test |
| VBM | Voxel-based morphometry |
| WM | White matter |

Chapter 1

Introduction

Purpose and motivation

Alzheimer's disease (AD) is a growing socio-economic problem, due to an increase in population and the longer average lifespan. The changes associated with this neurodegenerative disease start years before the clinical diagnosis can be made.¹ The pathological hallmark of AD is an accumulation of amyloid plaques and neurofibrillary tangles, which are associated with neuronal loss.² It is believed that neurons have very limited regenerative abilities. As a result it is imperative to prevent neuronal loss as early in the disease as possible, and future treatments should be given in the earliest possible stages.³ So far no single diagnostic modality or biomarker is available with high enough sensitivity and specificity to establish an accurate diagnosis in the individual patient. Consequently there is a need for biomarkers to detect the disease at an earlier stage in the individual.

Magnetic Resonance Imaging (MRI) offers the possibility to visualize structural changes associated with neurodegenerative disease *in vivo*. The use of neuroimaging in clinical practice has shifted from excluding other causes of cognitive complaints (e.g. hemorrhage, tumors, hydrocephalus), to early detection (e.g. AD versus normal ageing) and nosological diagnosis (e.g. AD versus FTLD).⁴ Nevertheless, the diagnostic accuracy leaves room for improvement, partly because cross-sectional analysis has the disadvantage of confounding influence of inter-individual variability in brain structure and ageing. Furthermore, there is need for prognostic factors that can accurately track disease progression. Longitudinal imaging might not have these restrictions, and can possibly be used to determine brain tissue loss (atrophy) in the individual *in vivo*.⁵

This thesis aspires to expand insights in the use of longitudinal whole-brain and regional MR imaging in the early detection, diagnosis and prognosis of AD. Furthermore, it explores the association of these atrophy markers with clinical, genetic and cerebrospinal fluid (CSF) biomarkers, aiming to develop a better understanding of the course of the disease, eventually improving the effectiveness of patient management.

General introduction

Alzheimer's disease and MCI

Alzheimer's disease is characterised by an insidious onset of progressive cognitive decline. The term mild cognitive impairment (MCI) has been introduced to describe patients who do not fulfil clinical criteria for dementia, but who do have objective evidence of memory deficits.¹ MCI patients are at an increased risk of developing AD, with about 10-15% progressing to AD per year. In these subjects MCI may be considered to be a transitional phase for AD.³ However, not all patients diagnosed with MCI progress to AD: some develop another type of dementia, while others improve or remain clinically stable.⁶ The course of AD itself is also variable: not all patients progress at the same rate and the factors that influence or predict progression are not well known.⁷ Neuropathological studies suggest that Alzheimer's pathology spreads throughout the brain in a relatively predictable fashion, starting well before clinical onset of the disease. Accumulation has pathologically been observed to start at the medial temporal lobe and to gradually affect other parts of the cerebral cortex in later stages.² However, by definition, neuropathological studies are post hoc and cross-sectional in design, and clearly cannot track disease progression in the individual. Hence, clinical, biologic, and imaging markers are needed to detect the earliest stage of underlying pathology in *vivo*. Most commonly, diagnosis requires impaired cognition, and progression of the disease is measured by change in cognition over time.⁸ Nonetheless, clinical and neuropsychological measures may lack sensitivity to change, are subject to day-to-day variability, and are influenced by behavioral fluctuations, intercurrent illness, and medication.

Magnetic Resonance Imaging

Structural MR imaging allows atrophy to be assessed in *vivo*. Neuroimaging markers provide an alternative and objective assessment of diagnosis and progression.⁴ Many studies in AD focussed on the medial temporal lobe, known to be affected early in the disease, but tissue loss is not limited to this region. Neocortical loss and enlargement of the ventricles have also been reported at an early stage.^{7,9,10}

Most of the previous MR imaging studies were cross-sectional by design, which has the disadvantage of confounding influence of inter-individual variability. It has been suggested that longitudinal atrophy rates are more sensitive to the earliest disease changes than brain volume measurement at a single time point.^{7,11} Therefore, longitudinal MR imaging might provide more sensitive and specific diagnostic measures, and be able to track the brain changes over time.

Computational Neuroanatomy

A standard feature of modern MRI scanners is the acquisition of three-dimensional images (3D volume). Faster computers and parallel computer networks allow for the implementation of algorithms developed for powerful analysis and comprehensive comparison of these 3D volumes. Using the following unbiased neurocomputational analyses, we calculated whole-brain as well as regional atrophy measures:

VBM (voxel-based morphometry), is an unbiased method to analyze 3D volumes at the voxel level.¹⁰ It consists of a registration step to spatially align the 3D images -often this is an affine linear registration (12 degrees of freedom)-, followed by a segmentation of the image to identify the grey matter, white matter and CSF. Then, a statistical analysis is performed, where a voxel-wise comparison between or within groups can be made. Outcome measures are statistical parametric maps, and when quantified within standard normalized brain regions, whole-brain and regional volumes.

SIENAX (Structural Image Evaluation, using Normalisation, of Atrophy; Cross-sectional)¹² is a cross-sectional measure of whole-brain volume, used to quantify global brain atrophy. It automatically segments brain from non-brain tissue; subsequently it estimates brain volume and applies a normalization factor to correct for head size. The normalization factor is acquired by registering the patients scan to the Montreal neurological institute 152 (MNI152) standard brain image using the skull to normalize spatially. The corrected brain volume is expressed as Normalized Brain Volume (NBV), from now on referred to as brain volume (ml).

SIENA (Structural Image Evaluation, using Normalisation, of Atrophy)¹² is a method to measure the loss of brain volume over time. SIENA aligns the baseline and follow-up scan using the skull as scale and skew constraint. Next,

the displacement of the brain edge for each point is estimated. Finally, all edge points are taken together to calculate the overall Percentage Brain Volume Change (PBVC) expressed as a single value, further referred to as whole-brain atrophy rate (%/year).

Fluid is a non-linear registration algorithm, which is based on the principles of fluid dynamics (Navier-Stokes equations), developed at the Dementia Research Centre (University College London).¹³ Before non-linear registration can take place, a number of preprocessing steps have to be executed to spatially align the baseline and follow-up 3D volumes of a single individual, and normalize image intensity by eliminating scanner related bias-fields artifacts. Subsequently the fluid algorithm performs an intensive non-linear registration based on voxel intensity. The voxelwise volumetric contraction or expansion, derived from the transformations imposed by the Fluid registration, is used as the outcome measure. By quantifying the total change in a specific region, whole-brain and regional atrophy rates are obtained.

Biomarkers in cerebrospinal fluid

CSF biomarkers are increasingly used to detect and characterise brain changes associated with AD *in vivo*. In CSF, decreased beta-amyloid 1–42 ($A\beta_{1-42}$) levels, and increased tau, and tau phosphorylated at threonine-181 ($P\text{-tau}_{181}$) levels are thought to reflect the presence of AD pathology.¹⁴ These CSF biomarkers have been shown to differentiate patients with AD from control subjects with reasonable accuracy.¹⁵ Moreover, these changes can be detected in patients with MCI who will progress to AD.¹⁶ Although both MRI and CSF biomarkers have been shown to be valuable markers of disease in MCI and AD, the relation between these markers has been less extensively studied. In cross-sectional studies, CSF biomarkers have been reported not to be related to MRI measures of atrophy, suggesting that these markers reflect different aspects of Alzheimer type neuropathology.¹⁷ However, longitudinal studies are needed, to clarify the relationship between these markers. The few studies that have reported CSF biomarkers and MRI measures in a longitudinal design, have used relatively small sample sizes, and have shown conflicting results in terms of whether or not these markers are associated.^{17,18} The relation between CSF biomarkers and MRI derived atrophy measures remains unclear.

Cohort

The studies described in this thesis are based on a cohort of 147 patients who underwent repeated MRI. Between 2004 and 2006, patients visiting the memory outpatient clinic of the Alzheimercentre (VU University Medical Center) were approached to participate. At baseline patients underwent a standardized clinical assessment including medical history, physical and neurological examination, psychometric evaluation, and brain MR examination. Diagnoses were established during a multidisciplinary consensus meeting according to the Petersen criteria for MCI,¹⁹ the NINCDS-ADRDA criteria (National Institute of Neurological and Communicative Diseases and Stroke/Alzheimer's Disease and Related Disorders Association) for probable AD,⁸ and according to published consensus criteria for frontal-temporal lobar degeneration (FTLD),²⁰ vascular dementia (VaD),²¹ and dementia with Lewy bodies (DLB).²² When all clinical investigations were normal (i.e. MCI criteria were not fulfilled), patients were considered to have subjective complaints. Additionally, we included normal controls without cognitive complaints, recruited from caregivers, who were willing to undergo the same diagnostic procedure as patients attending our memory clinic. At follow-up patients were re-examined, and underwent a second MR examination. If they were willing, patients also underwent a second lumbar puncture. Non-demented subjects (patients with MCI and patients with subjective complaints) visited the memory clinic annually; diagnostic classification was re-evaluated at follow-up. Patients were included only if they had two MR examinations of adequate quality, performed on the same scanner using the same imaging protocol. MR examinations were reviewed by a radiologist to exclude non-neurodegenerative pathology that could explain the cognitive impairment. NINDS-AIREN criteria were used to exclude patients with vascular dementia.²¹

Aims of this thesis

The objective of this thesis was to examine *in vivo* atrophy patterns using serial MRI, calculated with advanced neurocomputational analyses. The application of longitudinal whole-brain and regional atrophy rates in research and clinical practice was investigated in a cohort that covers the spectrum of cognitive decline, from normal ageing to AD. Firstly this thesis focuses on accurate and early detection of AD, by prospectively determining atrophy rates in MCI and

AD, and its association with cognitive decline. Secondly, it tries to identify the prognostic value of atrophy rates within MCI and AD by exploring if whole-brain and regional atrophy rates are suitable as markers for disease progression, as well as investigate the risk of progression to dementia in initially non-demented patients. Finally, the association of the MRI derived atrophy rates with clinical parameters, genetic factors, and CSF biomarkers was studied.

Outline per chapter

In chapter 2 we used VBM to find out whether structural differences on MR imaging offer insight in the development of clinical AD in patients with amnesic MCI at 3-year follow-up.

In chapter 3, we prospectively determined baseline brain volume and whole-brain atrophy rate in the aforementioned cohort, using SIENAX and SIENA respectively. We assessed its association with cognitive decline, as well as investigated the risk of progression to dementia in initially non-demented patients, based on baseline brain volume and whole-brain atrophy rate.

In chapter 4, we used Fluid, a robust and accurate non-linear registration algorithm, to calculate regional atrophy rates. Our objective was to track the regional lobar atrophy pattern in the progression from normal aging to Alzheimer's disease.

In chapter 5, we looked into the added value of hippocampal atrophy rates over whole brain atrophy measurements. We examined the applicability of different types of measurements of regional hippocampal and whole-brain atrophy by comparing their ability to distinguish between controls, MCI and AD, and their ability to predict progression to AD within controls and MCI. Finally, we compared cross-sectional and longitudinal measurement of the hippocampus and whole brain.

In chapter 6, we evaluated which baseline clinical and MRI measures influence rate of progression within AD, using whole-brain atrophy rates measured from serial MR imaging, derived with SIENA as outcome measure.

In chapter 7 we investigated associations between cross-sectional and longitudinal CSF biomarker levels and MRI-based whole-brain atrophy rate in MCI and AD.

Finally, in chapter 8, results are summarized and discussed.

Reference list

1. Petersen, R. C. et al. Current concepts in mild cognitive impairment. *Arch Neurol.* 2001 Dec;58(12):1985-92.
2. Braak, H. & Braak, E. Neuropathological staging of Alzheimer-related changes. *Acta Neuropathol (Berl).* 1991;82(4):239-59.
3. Gauthier, S. et al. Mild cognitive impairment. *Lancet.* 2006 Apr 15;367(9518):1262-70.
4. Scheltens, P., Fox, N., Barkhof, F. & De, C. C. Structural magnetic resonance imaging in the practical assessment of dementia: beyond exclusion. *Lancet Neurol.* 2002 May;1(1):13-21.
5. Jack, C. R. et al. Brain atrophy rates predict subsequent clinical conversion in normal elderly and amnesic MCI. *Neurology* 65, 1227-1231
6. Visser, P. J., Kester, A., Jolles, J. & Verhey, F. Ten-year risk of dementia in subjects with mild cognitive impairment. *Neurology.* 2006 Oct 10;67(7):1201-7.
7. Fox, N. C., Scahill, R. I., Crum, W. R. & Rossor, M. N. Correlation between rates of brain atrophy and cognitive decline in AD. *Neurology.* 1999 May 12;52(8):1687-9.
8. McKhann, G. et al. Clinical diagnosis of Alzheimer's disease: report of the NINCDS-ADRDA Work Group under the auspices of Department of Health and Human Services Task Force on Alzheimer's Disease. *Neurology.* 1984 Jul;34(7):939-44.
9. Carmichael, O. T. et al. Ventricular volume and dementia progression in the Cardiovascular Health Study. *Neurobiol. Aging* 28, 389-397
10. Karas, G. B. et al. A comprehensive study of gray matter loss in patients with Alzheimer's disease using optimized voxel-based morphometry. *Neuroimage.* 2003 Apr;18(4):895-907.
11. Jack, C. R. et al. Comparison of different MRI brain atrophy, rate measures with clinical disease progression in AD. *Neurology* 62, 591-600.
12. Smith, S. M. et al. Accurate, robust, and automated longitudinal and cross-sectional brain change analysis. *Neuroimage.* 2002 Sep;17(1):479-89.
13. Fox, N. C. et al. Imaging of onset and progression of Alzheimer's disease with voxel-compression mapping of serial magnetic resonance images. *Lancet.* 2001 Jul 21;358(9277):201-5.
14. Blennow, K. & Hampel, H. CSF markers for incipient Alzheimer's disease. - *Lancet Neurol.* 2003 Oct;2(10):605-13.
15. Wiltfang, J. et al. Consensus paper of the WFSBP Task Force on Biological Markers of Dementia: the role of CSF and blood analysis in the early and differential diagnosis of dementia. *World J Biol Psychiatry.* 2005;6(2):69-84.

16. Bouwman, F. H. et al. CSF biomarkers and medial temporal lobe atrophy predict dementia in mild cognitive impairment. *Neurobiol Aging*. 2007 Jul;28(7):1070-4.
17. Schoonenboom, N. S. et al. CSF and MRI markers independently contribute to the diagnosis of Alzheimer's disease. *Neurobiol Aging*. 2008 May;29(5):669-75.
18. Schonknecht, P. et al. Cerebrospinal fluid tau levels in Alzheimer's disease are elevated when compared with vascular dementia but do not correlate with measures of cerebral atrophy. *Psychiatry Res*. 2003 Oct 15;120(3):231-8.
19. Petersen, R. C. et al. Practice parameter: early detection of dementia: mild cognitive impairment (an evidence-based review). Report of the Quality Standards Subcommittee of the American Academy of Neurology. *Neurology*. 2001 May 8;56(9):1133-42.
20. Neary, D. et al. Frontotemporal lobar degeneration: a consensus on clinical diagnostic criteria. *Neurology*. 1998 Dec;51(6):1546-54.
21. van Straaten, E. C. et al. Operational definitions for the NINDS-AIREN criteria for vascular dementia: an interobserver study. *Stroke*. 2003 Aug;34(8):1907-12.
22. McKeith, I. G. et al. Diagnosis and management of dementia with Lewy bodies: third report of the DLB Consortium. *Neurology*. 2005 Dec 27;65(12):1863-72.

Chapter 2

Amnestic mild cognitive impairment: Structural MRI findings predictive of conversion to Alzheimer's disease

American Journal of Neuroradiology 2008

G.B. Karas
J.D. Sluimer
R. Goekoop
W.M. van der Flier
S.A.R.B. Rombouts
Ph. Scheltens
F. Barkhof

Abstract

Background and Purpose: Mild cognitive impairment (MCI) is by many considered a prodromal phase of Alzheimer's disease (AD). We used voxel-based morphometry (VBM) to find out whether structural differences on MRI could offer insight about the development of clinical AD in patients with amnesic MCI at three years follow-up.

Methods: Twenty-four amnesic MCI patients were included. After three years 46% had progressed to AD (n=11, age [72.7, SD 4.8]; sex [women/men] 8/3). For 13 patients (age [72.4, SD 8.6]; sex [women/men] 10/3) the diagnosis remained MCI. Baseline MRI at 1.5T included a coronal heavily T1-weighted 3D gradient echo sequence. Localized grey matter differences were assessed with VBM.

Results: The converters had less grey matter volume in medial (including the hippocampus) and lateral temporal lobe structures, parietal lobe structures and lateral temporal lobe structures. After correction for age, gender, total grey matter volume and neuropsychological evaluation, left-sided atrophy remained statistically significant. Specifically, converters had more left parietal atrophy (angular gyrus and inferior parietal lobule) and left lateral temporal lobe atrophy (superior and middle temporal gyrus) than stable MCI patients.

Conclusion: By studying two MCI populations, converters versus non-converters, we found atrophy beyond the medial temporal lobe to be characteristic of MCI patients who will progress to dementia. Atrophy of structures such as the left lateral temporal lobe and left parietal cortex may independently predict conversion.

Introduction

The term mild cognitive impairment was coined to describe individuals not yet fulfilling the criteria of Alzheimer's disease, but who evidently do not have a normal cognitive profile compared to their contemporaries.¹ The annual conversion rate of MCI patients is generally believed to lie around 10-15%, meaning that by three years half of the patients with MCI will probably have developed clinical AD.² If drugs become available that could influence the course of the disease, it is evident that these should be administered at the earliest stage at which a diagnosis can be made with certainty. Hence, clinical, biological and imaging markers are needed to detect that earliest stage of underlying pathology.

Previous MRI studies assessing the predictive value of structural brain changes for AD focused on medial temporal lobe atrophy (MTA).^{3,4} Brains of patients with Alzheimer's disease exhibit more atrophy in the medial temporal lobe, thalamus, superior temporal gyrus, parietal association cortex and cingulate gyrus, than patients with MCI.⁵⁻⁸ Some of these brain atrophy locations might provide additional independent information about risk of conversion⁹; conversion from MCI to AD has already been associated with hippocampal and entorhinal volume loss¹⁰ and with hippocampal shape changes.¹¹ We adopted a longitudinal approach, in which we followed up a study group for three years and then compared the baseline MRI scans. Voxel-based morphometry was chosen as the post-processing method in order to avoid a priori hypotheses.

Patients and Methods

Patient inclusion

Twenty-five amnesic MCI patients were prospectively selected from the Alzheimer Center at the VU Medical Center, Amsterdam, The Netherlands. Due to image pipeline failure one patient had to be excluded, leaving 24 patients for analysis. MCI patients were diagnosed according to the Petersen criteria with a slowly progressive memory decline without the involvement of another domain of cognitive function, that did not interfere significantly with activities of daily living.² Inclusion of an individual in the study required mini-mental state examination (MMSE) score of 24 and higher.¹² Follow-up ending for this study was set at three years after inclusion and diagnosis of AD was made according to the NINCDS-ARDRA criteria.¹³ All patients received a diagnostic battery comprising of mini-mental state examination - MMSE¹², clinical dementia rating - CDR¹⁴ and NYU-paragraph recall tests, which were used for cognitive profiling. The study had approval of the review board of the committee of medical ethics of the VU University Medical Center in Amsterdam, The Netherlands. All patients provided informed consent according to the Declaration of Helsinki under supervision of a lawful caretaker during a screening visit in which the procedure was explained and contraindications were checked.

MRI Data Acquisition

Imaging was carried out on a 1.5 T Sonata scanner (Siemens AG, Erlangen, Germany), using a standard circularly polarized head coil with foam padding to restrict head motion. A heavily T1-weighted structural 3D sequence was employed to obtain high resolution images (MP-RAGE; inversion time: 300s, TR = 15 ms; TE = 7 ms; flip angle = 8°; 160 coronal slices, 1x1x1.5 mm voxel dimensions). Additional to the structural MRI protocol the patients also received FLAIR and gradient-echo weighted sequences to exclude significant vascular pathology or microbleeds which might interfere with either the diagnosis of pure amnesic MCI or cause the segmentation of the T1-weighted images to be sub-optimal.

Visual Scoring

In order to have an absolute and not a relative measure of hippocampal atrophy the MTA was visually scored on the coronal images using a well validated scale, medial temporal atrophy scale.^{15,16} According to the scale, MTA scores evaluate the medial temporal lobe structures, encompassing the hippocampus proper, dentate gyrus, subiculum, parahippocampal gyrus and the volume of the surrounding cerebrospinal fluid (CSF) spaces, especially the temporal horn of the lateral ventricle and the choroid fissure. MTA scores range from 0 (no atrophy) to 4 (severe atrophy) on each side. Visual scores from left and right were averaged. The rater (J.S.) was blinded to diagnosis or other clinical variables of the patients, and trained using our standard training set (19 brains, none belonging to the study's dataset) to meet consistency requirements according to our standard operating procedure. The intrarater weighted Cohen's kappa was 0.93 and interrater weighted Cohen's kappa was 0.91 (against internally established gold-standard).

SIENAX

Global grey matter volume was estimated with a cross-sectional atrophy estimation method called SIENAX.¹⁷ Briefly, scans were affinely (12 parameters) registered to standard Montreal Neurological Institute space (average template of 152 healthy adult brains), the skull was extracted and grey matter was segmented based on signal intensity and a voxel-connectivity algorithm. Subsequently, global grey matter volumes were corrected for scaling and scanner errors by using the extracted skull as a constant variable and partial volume effects were incorporated into the model. The resulting grey matter volumes were then expressed as cubic centimeters (cm³).

Voxel-based Morphometry

Preprocessing

Localized grey matter differences were assessed with VBM¹⁸, implemented as described previously.^{8,19} A detailed algorithm with the image processing settings of the proposed VBM scheme is shown in table 1. MRI scans were brought into standard reference anatomical space using an affine 12-parameter registration and with the MNI template as target. We chose not to perform nonlinear registration since Jacobian analysis of SPM-basis function warped images showed mainly expansion/contraction of the lateral ventricles without little change of gyri or sulci. At this step the scalp was removed using the automated skull-stripping algorithm brain extraction tool (BET).²⁰

Subsequently, scans were segmented into grey matter (GM), white matter (WM) and CSF, based on a segmentation algorithm implemented in SPM5 (<http://www.fil.ion.ucl.ac.uk/spm/software/spm5/>) producing statistical probability anatomical maps (SPAMs). We found that this algorithm outperformed the previous SPM implementations, especially in subjects with enlarged ventricles.

SPAMs values range from 0% to 100% probability of a voxel belonging to a tissue class (GM, WM, and CSF). Registration accuracy was enhanced by aligning and scaling with advanced registration methods spreading registration bias among the whole group – transformation matrix averaging by projection on a manifold.^{8,21} Finally, grey matter volumes were smoothed with a Gaussian

kernel of 12 mm (full-width at half maximum-FWHM), a kernel which seems to perform well in studies of simulated atrophy (best kernels being in the range of 10-15mm).²²

Image level Statistics: statistical parametric mapping (SPM)

Initially an SPM two-sample t-test was applied to search for grey matter differences between the two groups. Statistics were run within a brain mask excluding the cerebellum (mask created with the 'aal' toolbox, see below). Since the baseline clinical measures were unbalanced at baseline we further refined the statistical model by including age, gender, and NYU and SIENAX global grey matter volume in the model (model: "single-subject, conditions and covariates" with the modeled variables introduced as nuisance variables). NYU was preferred over MMSE since in a logistic regression model with NYU and MMSE as predictors and conversion as outcome, it was only NYU which remained significantly independent ($p_{\text{NYU}}=0.05[\text{OR } 2.3, 1-5.2]$ versus $p_{\text{MMSE}}=0.15[\text{OR } 2.8, 0.7-11]$). CDR was not entered in the model since it practically represents a binary outcome. Visual scoring of MTA was also not included in the model since it is highly correlated with SPAM data (both derived from the same source images). Our threshold for statistical significance was set to $p<0.001$ uncorrected for multiple comparisons, subsequently suprathreshold voxels were further filtered to $p<0.1$ corrected with FDR (false discovery rate) for multiple comparisons and cluster height $p<0.1$ corrected for multiple comparisons.

Variable level Statistics

T-tests were performed where appropriate. Monte-Carlo nonparametric statistical simulation was applied to test for differences in visual scores, and NYU score (exact p values). Fisher's exact test was used to compare sex proportions between the two groups.

Table 1. VBM method protocol.

| VBM | Action | Algorithm |
|---------------|---|-----------------------|
| Step 1: | Affine register to MNI template | SPM5 |
| preprocessing | Skull strip images | BET |
| | Segment grey matter | SPM5 |
| | Manifold additional affine registration | air, define_commonair |
| Step 2: | 1. Simple t-test between converters and non-converters | SPM5 |
| Statistics | 2. Model with covariates | SPM5 |
| | Condition: conversion or not | |
| | Nuisance variables: age, sex, global grey matter, NYU | |
| | MMSE not included due to significant interaction with NYU | |
| | 3. Reporting of results at $p < 0.1$ corrected Aal and anatomical percentages | |

SPM: Statistical Parametric Mapping (software, versions SPM2 and SPM5), air: automated image registration, MNI: Montreal Neurological Institute, BET: brain extraction tool, NYU: delayed New York paragraph recall, MMSE: mini-mental state examination, aal: automatic anatomic labeling toolbox.

Technical Issues

(<http://www.fil.ion.ucl.ac.uk/spm/software/spm2/>) running under Matlab 6.5 (The Mathworks, MA). The segmentation algorithm was performed with SPM5 (<http://www.fil.ion.ucl.ac.uk/spm/software/spm5/>). Custom image processing steps and batch analysis were coded in IDL 6.1 (Research Systems, CO). Cluster extraction was performed with the SPM plug-in 'marsbar' version 0.38.2.²³ Calculation of cluster locations was performed with the 'aal' toolbox.²⁴ The 'aal' toolbox parcellates statistical parametric clusters to sub-clusters according to standard-space anatomical boundaries and gives percentage points of each sub-cluster. Conversion of MNI to Talairach coordinates was performed with the mni2tal.m script in Matlab. Special Matlab, IDL and UNIX shell scripts were used to batch process the analysis. All extra scripts and source code is freely available upon request from the author. Conventional statistics were performed with SPSS 13.

Results

Baseline Demographics

At the end of the three-year follow-up period 46% of the MCI patients had converted to AD. There were no differences between groups in age or sex (Table 2). MMSE values were relatively high in both groups (above 25), but the patients who progressed to AD differed significantly from the patients who remained stable MCI in terms of lower MMSE and NYU.

Table 2. Demographics and clinical findings at baseline.

| | MCI non-Converters | MCI Converters |
|------------------------|---------------------------------|--|
| Sample size | 13 | 11 |
| Sex (women/men) | 10/3 | 8/3 (ns) |
| Age mean (SD, range) | 72.4 (8.6, 54-82) | 72.7 (4.8, 66-79) |
| MMSE score (SD, range) | 27.5(1.4, 26-30) | 25.9(0.9, 24-28)* |
| NYU score (SD, range) | 4.4(3, 0-10) | 0.7(1.3, 0-4)* |
| CDR (n subjects) | 2 with CDR 0 11 with CDR 0.5 | 5 with CDR 0 4 with CDR 0.5 2 with CDR 1 |

MCI = mild cognitive impairment, MMSE = mini-mental scale examination, NYU = delayed New York paragraph recall, ns= not significant. * $p < 0.01$

MTA and cortical atrophy

The converters exhibited more medial temporal lobe atrophy already at baseline, according to visual scoring of medial temporal lobe atrophy by using a well-validated method.^{15,16} The median difference was one step on the MTA rating scale, with the non-converters displaying a median score of 1 and the converters a median score of 2. Global brain grey matter volumes as evaluated by SIENAX demonstrated 5% less total grey matter volume in the converters.

Table 3. Descriptive MRI results.

| | MCI non-Converters | MCI Converters |
|---|--------------------|--------------------|
| Medial Temporal Lobe Atrophy score, Left | 1 (1.5) | 2 (2)* |
| Medial Temporal Lobe Atrophy score, Right | 1 (1.5) | 2 (1)* |
| Grey Matter volume in cm ³ | 695 (51, 624-805) | 657 (34, 597-709)* |

The first two variables are expressed as median with interquartile range (quartile-3 minus quartile-1). The last two variables are expressed as mean with standard deviation and range.

* p <0.05

VBM results

The patients who progressed to AD were found to have more atrophic left medial and lateral temporal lobe structures, left parietal lobe structures and right lateral temporal lobe structures (figure 1). Anatomical parcellation of the clusters allowed evaluation of percentage of clusters of significant differences according to anatomical regions (Table 4). The left medial temporal lobe structures involved were the hippocampus, parahippocampal gyrus, fusiform gyrus and amygdala (highest percentage for the hippocampus and parahippocampal gyrus). The involved left lateral temporal lobe structures included the superior and middle temporal gyrus, and the superior and middle temporal pole (highest percentages for the superior and middle temporal gyrus). The left parietal lobe structures involved were the angular gyrus, inferior parietal lobule and the supramarginal gyrus (highest percentages for the angular gyrus and the inferior parietal lobule). The involved right lateral

temporal lobe structures included the superior, middle and inferior temporal gyrus, and the superior and middle temporal lobe (highest percentages for the middle and superior temporal gyrus). Figure 1 shows the unthresholded VBM maps (with a color-coded significance scale).

After correction for age, gender, global grey matter volume, and delayed NYU the overall statistical significance declined with only left-sided atrophy surviving the statistical threshold, namely parietal atrophy (angular gyrus and inferior parietal lobule) and lateral temporal lobe atrophy (superior and middle temporal gyrus). These results indicate that location of (more) atrophy in those regions carries independent predictive value for conversion to AD.

Table 4. VBM results of contrast between MCI converters and MCI non-converters.

| MNI Max | pCluster | K | T | pFDR | Cluster % | R/L | Location |
|------------|----------|-------------------|-----|------|-----------|-------|--------------------------|
| -58 0 -15 | 0.0001 | 5240 (5.2 cm3) | 5.1 | 0.04 | 46.51 | Left | Superior Temporal Gyrus |
| | | | | | 40.88 | Left | Middle Temporal Gyrus |
| | | | | | 6.16 | Left | Superior Temporal Pole |
| | | | | | 5.23 | Left | Middle Temporal Pole |
| -24 -4 -24 | 0.002 | 3220 (3.2 cm3) | 4.7 | 0.04 | 57.30 | Left | Hippocampus |
| | | | | | 21.46 | Left | Parahippocampal Gyrus |
| | | | | | 10.09 | Left | Fusiform Gyrus |
| | | | | | 6.27 | Left | Amygdala |
| -52 -64 38 | 0.05 | 1524 (1.5 cm3) | 4.7 | 0.04 | 4.41 | Left | Middle Temporal Pole |
| | | | | | 67.78 | Left | Angular Gyrus |
| | | | | | 29.27 | Left | Inferior Parietal Lobule |
| 56 12 -17 | 0.04 | 1627 (1.6 cm3) | 4.5 | 0.04 | 2.95 | Left | Supramarginal Gyrus |
| | | | | | 47.80 | Right | Middle Temporal Gyrus |
| | | | | | 22.54 | Right | Superior Temporal Pole |
| | | | | | 16.40 | Right | Inferior Temporal Gyrus |
| | | | | | 6.63 | Right | Superior Temporal Gyrus |
| | | | | | 5.12 | Right | Middle Temporal Pole |

Statistics calculated within a brain mask excluding cerebellum. Thresholding was performed at $p < 0.0001$ (uncorrected) and subsequently only the cluster surviving corrected thresholds reported (p cluster corrected (pCluster) = 0.1, p false discovery rate (pFDR) voxel corrected=0.1, cluster extent = 70 = 0.7 cm3

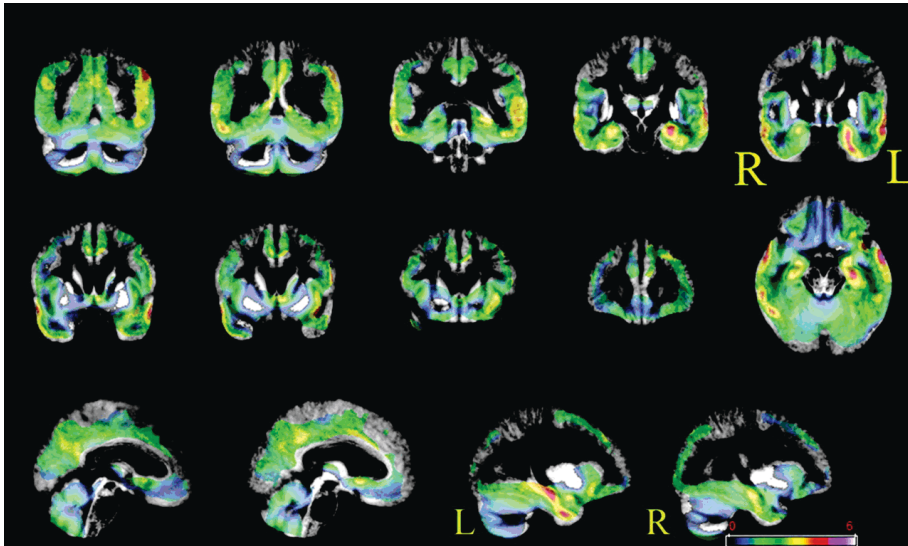


Figure 1. VBM contrast between converters and non-converters using a simple t-test (no covariates). Areas with more atrophy in converters are superimposed on the average grey matter template. No threshold is applied, so that the full extent of the results can be appreciated. Converters have more atrophy of the medial and lateral temporal lobes bilaterally, of frontal lobes and parietal lobes. Thresholded results and corrected for multiple comparisons using random field theory are displayed in tables 4 and 5.

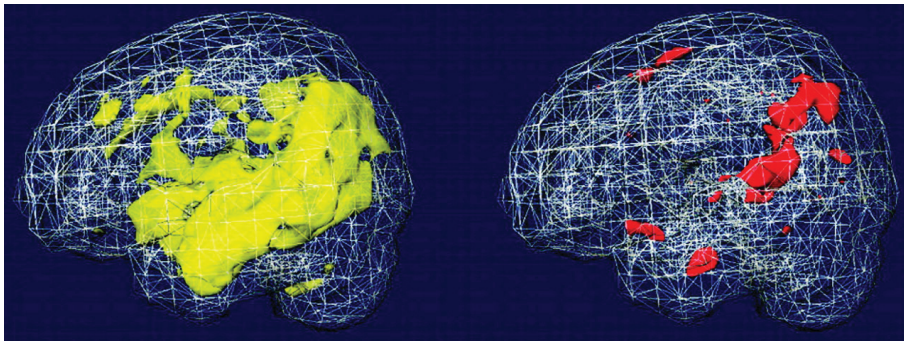


Figure 2. Rendering of the simple t-test and full model (corrected for age, sex, NYU and global grey matter) between MCI converters and non-converters. The big yellow area on the left hemisphere denotes less gray matter (more atrophy) in the converters group, compared to non-converters, as captured by the t-test. After correcting for age, sex, global grey matter atrophy and a neuropsychological measure which is a good predictor of conversion to AD (NYU), atrophy in the left lateral temporal lobe and left parietal regions remains statistically significant, depicted as red. Results were thresholded at $p=0.001$ uncorrected for multiple comparisons for display purposes.

Table 5. VBM results of the comparison between MCI converters and MCI non-converters adjusting for gender, age, global grey matter volume and delayed NYU paragraph recall.

| MNI Max | pCluster | K | T | pFDR | Cluster % | R/L | Location |
|------------|----------|------------------|-----|------|----------------|--------------|--|
| -34 -57 51 | 0.07 | 931 (0.9 cm3) | 5 | 0.06 | 70.03 29.22 | Left Left | Angular Gyrus Inferior Parietal Lobule |
| -54 -42 10 | 0.06 | 941 (0.9 cm3) | 4.4 | 0.06 | 81.08 18.92 | Left Left | Superior Temporal Gyrus Middle Temporal Gyrus |

Statistics calculated within a brain mask comprising only of temporal and parietal lobes. Thresholding was performed at $p < 0.0001$ (uncorrected) and subsequently only the cluster surviving corrected thresholds reported (p cluster corrected = 0.1 (pCluster), p false discovery rate (pFDR) voxel-level corrected=0.1, cluster extent = 70 = 0.7 cm3).

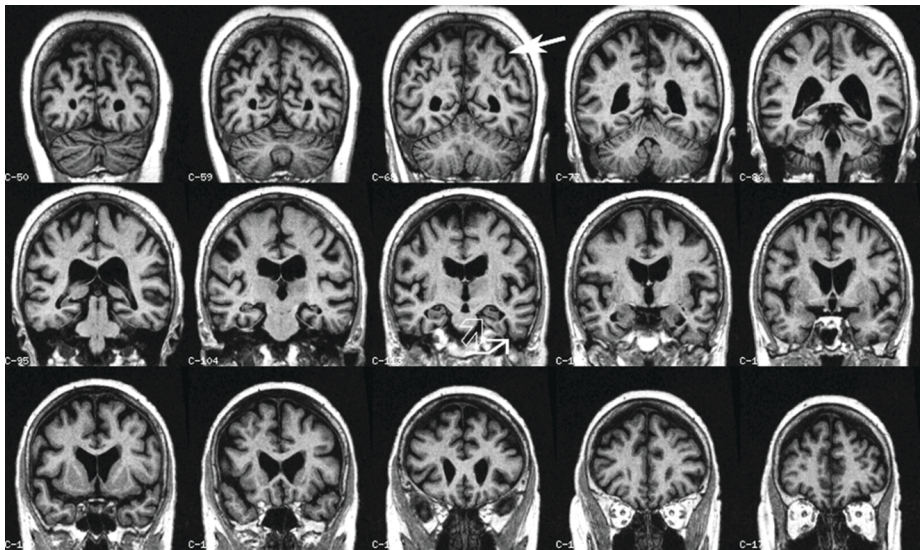


Figure 3. Coronal multiplanar reconstructions of a structural T1-weighted MRI volume. There is slight hippocampal atrophy (open arrow) with concomitant widening of the collateral sulcus (closed kinked arrow), both signs of progressive medial temporal lobe atrophy. We additionally notice slight parietal atrophy (closed arrow), which adds independent predictive value for conversion from mild cognitive impairment to Alzheimer's disease.

Discussion

Our goal in this study was to test whether prediction of conversion by utilization of clinical variables can be augmented by incorporating structural imaging data. Almost half (46%) of the MCI amnesic population had deteriorated to fulfill diagnostic criteria for AD, comparable with previous studies on the conversion rate in MCI.² We found that medial and lateral temporal lobe atrophy as well as parietal cortex atrophy on MRI characterized converters (figure 1). After correction for clinical variables, left lateral temporal and left parietal cortex atrophy conveyed independent predictive value to distinguish converters from non-converters (figures 2 and 3). Of note, hippocampal atrophy was not significant after correction for the above variables. The importance of lateral parietal cortex atrophy might be significant since it is believed to be mainly involved at a later stage of the disease and not in MCI. Introduction of a visual scoring method for evaluation of medial temporal lobe atrophy might appear coarse, but its use offers robustness to our findings since the visual scale used has been well validated.^{15,16}

The finding of medial and lateral temporal lobe atrophy in the patients who progressed to AD is in agreement with previous MRI studies.^{4, 16, 25-28} Involvement of both medial and lateral temporal lobes corresponds to neuropathological Braak stages III and IV, the time when there is disruption between the two hemispheres and cognitive deterioration first becomes apparent.²⁹ There are only few published studies using VBM to study MCI conversion. One study (n=18) with a conversion rate of 39% over 18 months, found more atrophy of medial and lateral temporal lobe structures, and frontal lobe gyri in converters²⁵. Another study (n=9) with a conversion rate of 44% at 45.7 months, found more atrophy of medial and lateral temporal lobe structures and the frontal lobe in converters.²⁶ We did not notice frontal lobe atrophy to the extent described in the other two VBM studies. A possible explanation might be that frontal lobe atrophy did not survive the statistical threshold: it is visible on the unthresholded VBM maps (figure 1).

Moving further away from the temporal lobe, we also noted parietal atrophy. Especially after correcting our data for a measure of disease severity it was only left-sided parietal atrophy and lateral temporal atrophy which distinguished

converters from non-converters. Parietal atrophy is known to characterize AD. Neuropathologically, involvement of the parietal cortex corresponds to Braak stages V and VI of neurofibrillary tangles (NFTs) deposition, at the time usually the diagnosis of AD is made.²⁹ It seems that functional changes in the parietal cortex might even precede tissue loss.³⁰ The first data of parietal cortex involvement in MCI developing AD came from studies utilizing PET and SPECT.^{6, 31-34} A goal for future research might be to correlate *in vivo* data, pathological data and clinical status of MCI patients to determine the precise contribution of parietal atrophy or hypometabolism to MCI status.

The strength of this study lies in the unbiased way of identifying atrophic brain regions. Additionally, we showed that even after accounting for clinical variables there remained brain atrophy to discriminate patients who would later develop AD. One could argue that the two groups were already clinically different at baseline and that we simply detected AD patients at different stages of the disease. That may very well be true and putting arbitrary cutoffs on a continuum might indeed be controversial. On the other hand, our main goal was not to find isolated regions of brain atrophy in patients with equal cognitive status; clinical scales are well known for their strong predictive ability and it might be naive to think that structural MRI is able to discriminate among the very mild patients. More relevant is the survival of brain atrophy locations after correcting for the predictive ability of clinical scales. As our sample size was relatively small a larger study is needed to confirm the findings and usefulness of lateral temporal and parietal atrophy. Moreover, VBM has caused controversy^{35,36}, and additional studies utilizing a different post-processing approach are needed to corroborate our findings. Unfortunately a region of interest approach (considered the gold standard for the hippocampus) might be problematic for the parietal region due to high sulcal variability in that region.³⁷ VBM smoothes gyri, thereby reducing this variability and enabling comparisons. Another strength of this study is the relatively long follow-up of 3 years and ascertainment of conversion. Nevertheless, one could argue that with even longer follow-up more MCI patients would deteriorate; most likely those will have less severe disease. A more elegant approach would have been to implement survival analysis in VBM and utilize time to conversion and not

a dichotomous criterion. Unfortunately, no such algorithm implementation of survival models in VBM exists to our knowledge and is beyond the capabilities and resources of our research group.

Conclusion

By studying two MCI populations, converters versus non-converters, we found atrophy beyond the medial temporal lobe to be characteristic of MCI patients who will progress to dementia. Atrophy of structures such as the left lateral temporal lobe and left parietal cortex may independently predict conversion.

Reference list

1. Petersen RC. Mild cognitive impairment as a diagnostic entity. *J Intern Med* 2004;256:183-194
2. Petersen RC, Doody R, Kurz A, et al. Current concepts in mild cognitive impairment. *Arch Neurol* 2001;58:1985-1992
3. Grundman M, Jack CR, Jr., Petersen RC, et al. Hippocampal volume is associated with memory but not nonmemory cognitive performance in patients with mild cognitive impairment. *J Mol Neurosci* 2003;20:241-248
4. Jack CR, Jr., Shiung MM, Weigand SD, et al. Brain atrophy rates predict subsequent clinical conversion in normal elderly and amnesic MCI. *Neurology* 2005;65:1227-1231
5. Baron JC, Chetelat G, Desgranges B, et al. *In vivo* mapping of gray matter loss with voxel-based morphometry in mild Alzheimer's disease. *Neuroimage* 2001;14:298-309
6. Chetelat G, Desgranges B, De La Sayette V, Viader F, Eustache F, Baron JC. Mild cognitive impairment: Can FDG-PET predict who is to rapidly convert to Alzheimer's disease? *Neurology* 2003;60:1374-1377
7. Pennanen C, Testa C, Laakso MP, et al. A voxel based morphometry study on mild cognitive impairment. *J Neurol Neurosurg Psychiatry* 2005;76:11-14
8. Karas GB, Scheltens P, Rombouts SA, et al. Global and local gray matter loss in mild cognitive impairment and Alzheimer's disease. *Neuroimage* 2004;23:708-716
9. van der Flier WM, van den Heuvel DM, Weverling-Rijnsburger AW, et al. Magnetization transfer imaging in normal aging, mild cognitive impairment, and Alzheimer's disease. *Ann Neurol* 2002;52:62-67
10. Devanand DP, Pradhaban G, Liu X, et al. Hippocampal and entorhinal atrophy in mild cognitive impairment: prediction of Alzheimer disease. *Neurology* 2007;68:828-836
11. Apostolova LG, Dutton RA, Dinov ID, et al. Conversion of mild cognitive impairment to Alzheimer disease predicted by hippocampal atrophy maps. *Arch Neurol* 2006;63:693-699
12. Folstein MF, Folstein SE, McHugh PR. "Mini-mental state". A practical method for grading the cognitive state of patients for the clinician. *J Psychiatr Res* 1975;12:189-198
13. McKhann G, Drachman D, Folstein M, Katzman R, Price D, Stadlan EM. Clinical diagnosis of Alzheimer's disease: report of the NINCDS-ADRDA Work Group under the auspices of Department of Health and Human Services Task Force on Alzheimer's Disease. *Neurology* 1984;34:939-944

14. Morris JC. Clinical dementia rating: a reliable and valid diagnostic and staging measure for dementia of the Alzheimer type. *Int Psychogeriatr* 1997;9 Suppl 1:173-176; discussion 177-178
15. Scheltens P, Leys D, Barkhof F, et al. Atrophy of medial temporal lobes on MRI in "probable" Alzheimer's disease and normal ageing: diagnostic value and neuropsychological correlates. *J Neurol Neurosurg Psychiatry* 1992;55:967-972
16. Korf ES, Wahlund LO, Visser PJ, Scheltens P. Medial temporal lobe atrophy on MRI predicts dementia in patients with mild cognitive impairment. *Neurology* 2004;63:94-100
17. Smith SM, Zhang Y, Jenkinson M, et al. Accurate, robust, and automated longitudinal and cross-sectional brain change analysis. *Neuroimage* 2002;17:479-489
18. Ashburner J, Friston KJ. Voxel-based morphometry--the methods. *Neuroimage* 2000;11:805-821
19. Karas GB, Burton EJ, Rombouts SA, et al. A comprehensive study of gray matter loss in patients with Alzheimer's disease using optimized voxel-based morphometry. *Neuroimage* 2003;18:895-907
20. Smith SM. Fast robust automated brain extraction. *Hum Brain Mapp* 2002;17:143-155
21. Woods RP. Characterizing volume and surface deformations in an atlas framework: theory, applications, and implementation. *Neuroimage* 2003;18:769-788
22. Davatzikos C, Genc A, Xu D, Resnick SM. Voxel-based morphometry using the RAVENS maps: methods and validation using simulated longitudinal atrophy. *Neuroimage* 2001;14:1361-1369
23. Brett M, Anton JL, Valabregue R, Poline JB. Region of interest analysis using an SPM toolbox. 8th International Conference on Functional Mapping of the Human Brain. Sendai, Japan; 2002
24. Tzourio-Mazoyer N, Landeau B, Papathanassiou D, et al. Automated anatomical labeling of activations in SPM using a macroscopic anatomical parcellation of the MNI MRI single-subject brain. *Neuroimage* 2002;15:273-289
25. Chetelat G, Landeau B, Eustache F, et al. Using voxel-based morphometry to map the structural changes associated with rapid conversion in MCI: a longitudinal MRI study. *Neuroimage* 2005;27:934-946
26. Bell-McGinty S, Lopez OL, Meltzer CC, et al. Differential cortical atrophy in subgroups of mild cognitive impairment. *Arch Neurol* 2005;62:1393-1397

27. deToledo-Morrell L, Stoub TR, Bulgakova M, et al. MRI-derived entorhinal volume is a good predictor of conversion from MCI to AD. *Neurobiol Aging* 2004;25:1197-1203
28. Killiany RJ, Hyman BT, Gomez-Isla T, et al. MRI measures of entorhinal cortex vs hippocampus in preclinical AD. *Neurology* 2002;58:1188-1196
29. Braak E, Griffling K, Arai K, Bohl J, Bratzke H, Braak H. Neuropathology of Alzheimer's disease: what is new since A. Alzheimer? *Eur Arch Psychiatry Clin Neurosci* 1999;249 Suppl 3:14-22
30. Chetelat G, Desgranges B, De La Sayette V, et al. Dissociating atrophy and hypometabolism impact on episodic memory in mild cognitive impairment. *Brain* 2003;126:1955-1967
31. Borroni B, Anchisi D, Paghera B, et al. Combined 99mTc-ECD SPECT and neuropsychological studies in MCI for the assessment of conversion to AD. *Neurobiol Aging* 2006;27:24-31
32. Drzezga A, Grimmer T, Riemenschneider M, et al. Prediction of individual clinical outcome in MCI by means of genetic assessment and (18)F-FDG PET. *J Nucl Med* 2005;46:1625-1632
33. Drzezga A, Lautenschlager N, Siebner H, et al. Cerebral metabolic changes accompanying conversion of mild cognitive impairment into Alzheimer's disease: a PET follow-up study. *Eur J Nucl Med Mol Imaging* 2003;30:1104-1113
34. Anchisi D, Borroni B, Franceschi M, et al. Heterogeneity of brain glucose metabolism in mild cognitive impairment and clinical progression to Alzheimer disease. *Arch Neurol* 2005;62:1728-1733
35. Ashburner J, Friston KJ. Why voxel-based morphometry should be used. *Neuroimage* 2001;14:1238-1243
36. Bookstein FL. "Voxel-based morphometry" should not be used with imperfectly registered images. *Neuroimage* 2001;14:1454-1462
37. Thompson PM, Mega MS, Woods RP, et al. Cortical change in Alzheimer's disease detected with a disease-specific population-based brain atlas. *Cereb Cortex* 2001;11:1-16

Chapter 3

Whole-brain atrophy and cognitive decline: A longitudinal MRI study of memory clinic patients

Radiology 2008

J.D. Sluimer
W.M. van der Flier
G.B. Karas
N.C. Fox
Ph. Scheltens
F. Barkhof
H. Vrenken

Abstract

Purpose: To prospectively determine the whole-brain atrophy rate in mild cognitive impairment (MCI) and Alzheimer's disease (AD) and its association with cognitive decline, as well as investigate the risk of progression to dementia in initially non-demented patients based on baseline brain volume and whole-brain atrophy rate.

Materials & Methods: Our study had institutional ethical committee approval; written informed consent was obtained from all participants. We included 65 patients with AD (age-range, sex(f/m): 52-81y, 38/27), 45 patients with MCI (56-80y, 22/23), 27 patients with subjective complaints (50-87y, 12/15) and 10 normal controls (53-80y, 6/4). Two MR scans were acquired, with an average interval of 1.8 ± 0.7 years. Baseline brain volume and whole-brain atrophy rates were measured from 3D T1-weighted MR imaging (1.0T; single slab, 168 slices; matrix size 256x256; FOV 250mm; voxel size 1x1x1.5 mm; TR=15ms; TE=7ms; TI=300ms; flip angle 15°). Associations were assessed using partial correlations. Cox proportional hazards models were used to estimate risk of developing dementia.

Results: Baseline brain volume was lowest in AD, but did not differ significantly between the MCI, subjective complaints and control groups ($p > 0.38$). Whole-brain atrophy rates were higher in AD (mean \pm SD $-1.9 \pm 0.9\%/y$) than MCI ($-1.2 \pm 0.9\%/y$; $p = 0.003$), who in turn had higher whole-brain atrophy rates than patients with subjective complaints ($-0.7 \pm 0.7\%/y$; $p = 0.03$) and controls ($-0.5 \pm 0.5\%/y$; $p = 0.05$). Whole-brain atrophy rate correlated with annualized mini-mental state examination (MMSE) change ($r = 0.48$, $p < 0.001$), while baseline volume did not ($r = 0.11$, $p = 0.22$). Cox proportional hazard models showed that -after correction for age, sex, and baseline MMSE- a higher whole-brain atrophy rate was associated with an increased risk of progression to dementia (highest vs lowest tertile (hazard ratio 3.6, 95% confidence interval 1.2-11.4)).

Conclusions: Whole-brain atrophy rate was strongly associated with cognitive decline. In non-demented participants a high whole-brain atrophy rate was associated with an increased risk of progression to dementia.

Introduction

Alzheimer's disease is characterised by an insidious onset of progressive cognitive decline. The term mild cognitive impairment is used to describe patients who do not fulfil clinical criteria for dementia, but who do have objective evidence of memory deficits. MCI patients are at an increased risk of developing AD¹; however, not all patients diagnosed with MCI progress to AD, some develop another type of dementia, while others improve or remain clinically stable.^{2,3}

Structural MR imaging allows tissue loss (atrophy) to be assessed *in vivo*.⁴ Many studies in AD focussed on the medial temporal lobe, known to be affected early in the disease.^{5,8} However, development of atrophy is not limited to this region. Neocortical loss and enlargement of the ventricles have been reported at an early stage.^{9,10} It has been suggested that whole-brain atrophy rate is more sensitive to the earliest disease changes than brain volume measurement at a single time point.^{11,14} Reported whole-brain atrophy rates in AD range from 1% to 4% per year,^{15,18} while healthy elderly have (age-related) atrophy rates ranging from 0.2 % to 0.7 % per year.^{19,20} Relatively few studies have addressed the issue of whole-brain atrophy rates across the cognitive spectrum of normal cognition, MCI and AD.^{21,23}

Thus, the purpose of this study was to prospectively determine the whole-brain atrophy rate in mild cognitive impairment and Alzheimer's disease and its association with cognitive decline, as well as to investigate the risk of progression to dementia in initially non-demented patients based on baseline brain volume and whole-brain atrophy rate.

Material and methods

Patients

Baseline clinical assessment

The study was approved by the institutional ethical review board. All participants (or caregivers) gave written informed consent. We included 65 patients with AD (age-range, sex (f/m): 52-81y, 38/27), 45 patients with MCI (56-80y, 22/23), and 27 patients with subjective complaints (50-87y, 12/15). Patients underwent a standardized clinical assessment including medical history, physical and neurological examination, psychometric evaluation, and brain MRI. The mini-mental state examination (MMSE) was used as a measure of general cognitive function²⁴). Diagnoses were established during a multidisciplinary consensus meeting according to the Petersen criteria for MCI²⁵ and the NINCDS-ADRDA (National Institute of Neurological and Communicative Diseases and Stroke/Alzheimer's Disease and Related Disorders Association) criteria for probable AD²⁶. When all clinical investigations were normal (i.e. MCI criteria were not fulfilled), patients were considered to have subjective complaints. Additionally, we included 10 normal individuals without cognitive complaints (controls (53-80y, 6/4)), recruited from caregivers, who were willing to undergo the same diagnostic procedure as patients attending our memory clinic.

Clinical assessment at follow-up

Non-demented participants (MCI and subjective complaints) visited the memory clinic annually. Diagnostic classification was re-evaluated at follow-up. The clinical diagnosis of dementia was determined according to published consensus criteria^{25,29}. Within the MCI group, 17 patients had remained stable, 23 progressed to AD, two to fronto-temporal lobar degeneration (FTLD)²⁷, two to vascular dementia (VaD)²⁸ and one to dementia with Lewy bodies (DLB)²⁹. Within the group of patients with subjective complaints, three patients progressed to MCI, three to AD and one to FTLD while 20 patients remained stable. All normal controls without complaints remained stable.

MRI and Evaluation

Between 2004 and 2006 all patients attending our memory clinic were invited for a repeat MR scan. Follow-up time is defined as time between the two MRI scans (mean interval 1.8 years, standard deviation 0.7; range 11m-4y2m). MR imaging was performed on a 1.0-T Siemens Magnetom Impact Expert System (Siemens AG, Erlangen, Germany) and included coronal T1-weighted 3D MPRAGE volumes (magnetization prepared rapid acquisition gradient echo; single slab, 168 slices; matrix size 256x256; FOV 250x250mm; voxel size 1x1x1.5 mm; TR=15ms; TE=7ms; TI=300ms; flip angle 15°). A total of 159 patients agreed to undergo 2 MR scans (71 AD, 49 MCI, 29 subjective complaints, 10 controls). Participants were included only: 1. if they had two scans of adequate quality, performed on the same scanner using the same imaging protocol. 2. if non-neurodegenerative pathology that could explain the cognitive impairment was present, as judged by one radiologist with 15 years experience in dementia field (FB). 3. if fully-automated SIENA(X) (Structural Image Evaluation, using Normalisation, of Atrophy, (X-sectional)) processing output did not yield errors, as checked for errors by a rater who was blinded to the diagnosis (JS, 4 years experience in dementia field, MR imaging and image analysis). Consequently we excluded 12 patients; two because of movement artefacts in the original MRI data, seven participants had non-neurodegenerative pathology associated with cognitive impairment (one hydrocephalus, one tumor, one hemorrhage, and four patients fulfilled NINDS-AIREN criteria for vascular dementia). Finally, three scans were excluded from analysis, because of remaining non-brain tissue after processing. A total of 147 participants were included (65 AD, 45 MCI, 27 subjective complaints, 10 controls)

Normalized baseline brain volume (NBV) and percentage brain volume change (PBVC) between two time-points were measured from the MPRAGE images using SIENAX, and SIENA, two fully automated techniques that are part of FSL (for a detailed explanation see: www.fmrib.ox.ac.uk/analysis/research/siena).^{30,31}

Whole-brain atrophy rate was measured with SIENA. Briefly, the brain was extracted using the brain extraction tool.³¹ Compared to standard SIENAX and SIENA, the procedure to remove non-brain tissue was slightly modified, because the brain extraction tool often leaves substantial amounts of non-brain tissue

when using a single slab 3D MPRAGE sequence, while also removing cortex in some areas.³² To remove all non-brain tissue without losing cortex, we incorporated registration of a template mask to the individual scan. After brain extraction the two brain images were aligned to each other, using the skull images to constrain the registration scaling. Both brain images were resampled into the space halfway between the two. Next, tissue-type segmentation was performed in order to find brain / non-brain edge points, and for each edge point perpendicular edge displacement between baseline and repeat scan was measured. The mean edge displacement was automatically converted into a global estimate of PBVC between the two time points

Baseline brain volume, normalized for subject head size, was measured with a cross-sectional modification of SIENA called SIENAX. Briefly, after brain extraction, tissue-type segmentation with partial volume estimation was carried out in order to calculate total volume of brain tissue. In addition, to correct for interindividual differences in head size, a volumetric scaling factor was obtained by registering the brain image to MNI152 space, using an affine transformation (i.e., a linear transformation with 12 degrees of freedom), and using the skull to constrain the registration scaling. Baseline brain volume, normalized for subject head size, was then obtained by multiplying the volume of brain tissue by the volumetric scaling factor. We used the baseline normalized brain volume as a cross-sectional measure, and whole-brain atrophy rate (PBVC) as a longitudinal measure of atrophy.

Statistical Analysis

Statistical analysis was performed with SPSS 12.0 (2003, Chicago, Illinois). PBVC and change in MMSE were annualized by dividing by the intermediate time interval between observations in years. Diagnostic groups were compared with chi-squared tests for sex. For continuous variables (age, MMSE, MMSE change, MR scan interval, normalized baseline brain volume, whole-brain atrophy rate) we used analysis of variance (ANOVA), with age and sex as covariates. Post-hoc comparisons were performed using Bonferroni tests. Box-and-whisker plots of baseline brain volume and whole-brain atrophy rate, by diagnostic group were constructed. Associations of baseline brain volume and whole-brain atrophy rate with MMSE and MMSE change were assessed using

partial correlations, corrected for age and sex. Scatter plots of baseline brain volume and whole-brain atrophy rate versus annual change in MMSE were created. Within the group of initially non-demented participants we assessed the predictive value of baseline brain volume and whole-brain atrophy rate, by using Cox proportional hazards models, which account for variability in length of follow-up. Among those initially non-demented, baseline brain volume and whole-brain atrophy rate were categorized into tertiles and entered as categorical variables in the model. Hazard ratios (HRs) with 95% confidence interval (CI) are presented. First (model 1), unadjusted HRs are presented. In model 2, sex and age were corrected for, and in model 3 baseline MMSE was added as an additional covariate. Main outcome was progression to dementia, second outcome was progression to AD, which excludes six cases who developed a different kind of dementia. Time-to-event curves were constructed with the Kaplan-Meier method. Statistical analysis was performed by JS and WF. Statistical significance was set at $p < 0.05$.

Results

Brain volume, Whole-brain atrophy rate

There were group differences for both baseline brain volume and whole-brain atrophy rate (Table 1, Figure 1). Post-hoc Bonferroni-corrected tests illustrated that brain volume at baseline was lowest for the AD group (vs MCI $p = 0.09$; vs subjective complaints $p < 0.001$; vs controls $p < 0.01$), but the MCI group did not differ from either the subjective complaints ($p = 0.38$) or control groups ($p = 0.48$). No difference between patients with subjective complaints and controls was found ($p = 1.00$).

By contrast, annualized whole-brain atrophy rates (PBVC) did not only differentiate the AD group from all other groups, but also showed differences between the other groups. AD patients had higher whole-brain atrophy rates compared to MCI ($p = 0.003$), who in turn had higher whole-brain atrophy rates compared to subjective complaints ($p = 0.025$) and controls ($p = 0.05$). No difference was found between subjective complaints and controls ($p = 1.00$) (Figure 2).

Table 1. Demographics and clinical variables

| | Controls | Subjective complaints | MCI | AD | F _{df,df} (p-value) |
|--|------------|---------------------------------------|-------------------------------|-----------------------------|--------------------------------|
| Number of participants | 10 | 27 | 45 | 65 | |
| Number converted | 10 stable | 20 stable 3 MCI 3 AD 1 other | 17 stable 23 AD 5 other | - | |
| Age-at-diagnosis (y) | 69 (7) | 66 (9) | 71 (6) | 67 (8) ^c | 3.0 _{3,143} (0.03) |
| Sex (f/m) | 6 / 4 | 12 / 15 | 22 / 23 | 38 / 27 | 2.1 _{3,3} (0.56) |
| MMSE baseline* | 28 (2) | 28 (1) | 26 (3) ^b | 22 (4) ^{f,g,h} | 27.0 _{3,141} (<0.001) |
| MMSE annual decline*+ | 0.3 (0.9) | -0.2 (1.4) | -1.5 (2.5) ^{a,b} | -2.1 (2.1) ^{d,g} | 7.9 _{3,128} (<0.001) |
| MR scan interval (y) * | 2.3 (0.5) | 1.7 (0.9) | 1.9 (0.7) | 1.7 (0.6) | 2.5 _{3,141} (0.06) |
| Normalized baseline brain volume (ml) * | 1541 (99) | 1536 (91) | 1483 (78) | 1453 (88) ^{d,g} | 8.0 _{3,141} (<0.001) |
| Annualized whole-brain atrophy rate (%/y) * | -0.5 (0.5) | -0.7 (0.7) | -1.2 (0.9) ^{a,b} | -1.9 (0.9) ^{f,g,e} | 18.0 _{3,141} (<0.001) |

Table 1. Group difference for sex (f/m) was calculated with Pearson Chi-Square. Other data in this table is displayed as mean (sd). F-value is displayed with degrees of freedom for contrast and error, respectively. Differences between groups were assessed using ANOVA (*age and sex as covariates, post-hoc Bonferroni correction $p < 0.05$). + available for $n=134$; a $p < 0.05$ compared to controls; b $p < 0.05$ compared to subjective complaints; c $p < 0.05$ compared to MCI; d $p < 0.01$ compared to controls; e $p < 0.01$ compared to MCI; f $p < 0.001$ compared to controls; g $p < 0.001$ compared to subjective complaints; h $p < 0.001$ compared to MCI; MCI=mild cognitive impairment; AD=Alzheimer's disease; MMSE=mini-mental state examination

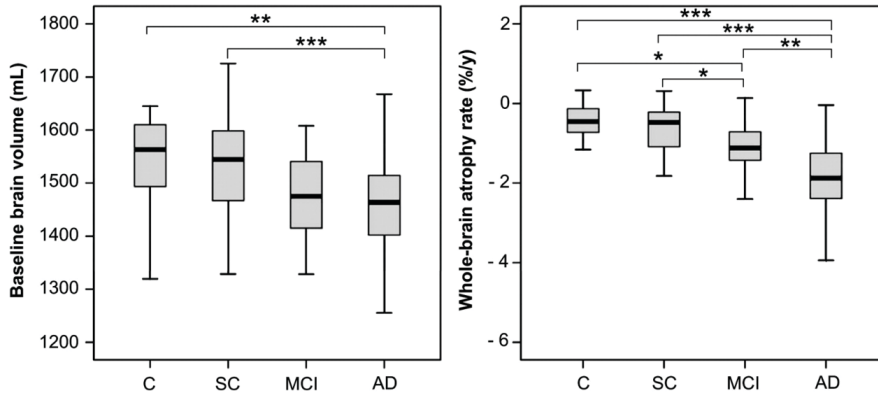


Figure 1. Box-and-whisker plot of (left) baseline brain volume and (right) whole-brain atrophy rate, by diagnostic group (C=controls, SC=subjective complaints, MCI = mild cognitive impairment, AD = Alzheimer's disease). Horizontal line inside box is median value. Differences between groups were assessed using ANOVA (age and sex as covariates, post-hoc Bonferroni correction), and are indicated by asterisks:

* $p < 0.05$; ** $p < 0.01$; *** $p < 0.001$

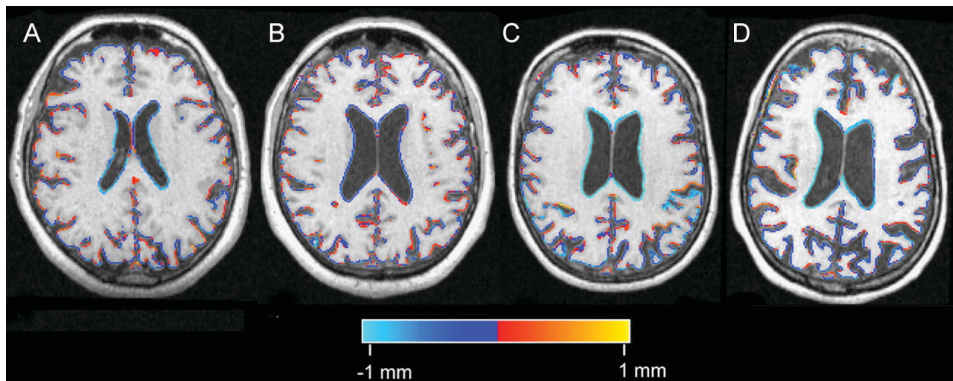


Figure 2. Four examples of individual edge-displacement maps, overlaid on baseline axial MR images. Dark-blue to light-blue represents mild to severe local contraction respectively, which implies atrophy. Red to yellow indicates mild to severe expansion of brain tissue. Note that for display purposes, edge motion was truncated at 1 mm in this figure. (A) patient with subjective complaints (age, normalised baseline brain volume, whole-brain atrophy rate: 74 y, 1471mL, -0.7%/y), (B) a patient with Mild Cognitive Impairment, who did not progress to AD (80y, 1607mL, -0.6%/y), (C) a patient with Mild Cognitive Impairment, who progressed to AD (67 y, 1548 mL, -1.9 %/y) and (D) a patient diagnosed with Alzheimer's disease at baseline (63 y, 1286mL, -4.2%/y).

Cognitive decline

To investigate whether baseline brain volume and whole-brain atrophy rate reflected cognitive decline, we assessed associations with baseline MMSE and annualized MMSE change (Figure 3). Partial correlations corrected for age and sex showed that across the whole sample, baseline brain volume correlated with baseline MMSE ($r=0.32$, $p<0.001$), but not with annualized change in MMSE ($r=0.11$, $p=0.22$). Whole-brain atrophy rate (PBVC) however, was associated with both baseline MMSE ($r=0.48$, $p<0.001$) and change in MMSE ($r=0.48$, $p<0.001$). Further evaluation of correlations within diagnostic groups showed that baseline brain volume was not associated with either MMSE or MMSE change within any of the groups. By contrast, whole-brain atrophy rate was associated both with MMSE and MMSE change within the AD group ($r=0.37$, $p<0.01$; $r=0.34$, $p<0.01$). Within the MCI group whole-brain atrophy rate was associated with MMSE change ($r=0.33$, $p<0.05$) but not with baseline MMSE ($r=0.09$, $p=0.61$). No such associations were found among patients with subjective complaints or controls.

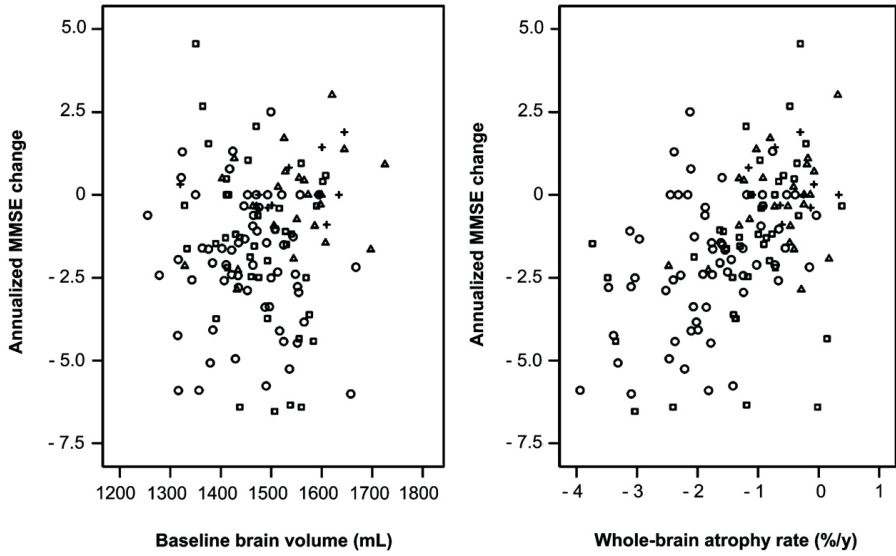


Figure 3. Scatterplots of (left) baseline brain volume and (right) whole-brain atrophy rate by annual change in mini-mental state examination (MMSE). Data for the entire spectrum of cognitive decline are presented. No association between baseline brain volume and annual MMSE decline was found (Figure 3a; partial correlation, correcting for age and sex: $r=0.11$, $p=0.22$). By contrast, whole-brain atrophy rate was associated with annualized MMSE change (Figure 3b; $r=0.48$, $p<0.001$). Subsequent evaluation of correlations within diagnostic groups showed that whole-brain atrophy rate was associated with annualized MMSE change within the AD group ($r=0.34$, $p<0.01$), and within the MCI group ($r=0.33$, $p<0.05$). No associations were found among normal controls or subjective memory complaints.

+ = normal controls; Δ = subjective memory complaints; □ = MCI; ○ = AD

Prediction of Progression to Dementia

Finally, we assessed the predictive value of baseline brain volume and whole-brain atrophy rate for progression to dementia in initially non-demented patients ($n=82$), using tertiles of MRI measures (Figure 4, Table 2). Baseline brain volumes were $1603\pm40\text{mL}$ in the large, $1512\pm26\text{mL}$ in the middle, and $1410\pm46\text{mL}$ in the small tertile. Whole-brain atrophy rates ($\%/y$) were -0.2 ± 0.2 in the lowest, -0.8 ± 0.2 in the moderate and -1.8 ± 0.8 in the high tertile. Compared with a large baseline brain volume, a small volume was associated with a threefold increased risk of progression to dementia in the unadjusted model. However, after adjusting for age, sex and baseline MMSE, this effect largely disappeared. Patients in the moderate whole-brain atrophy rate tertile had a twofold - though not significantly - increased risk of progression to dementia, in comparison with patients with a low whole-brain atrophy rate. A high whole-brain atrophy rate (highest tertile) was associated with a more than fourfold increased risk of progression to dementia. These results remained significant after correction for age, sex and baseline MMSE. When the analysis was restricted to progression to AD (i.e. excluding the six patients who progressed to another type of dementia), all results were essentially unchanged: corrected for age, sex and baseline MMSE (model 3), smaller baseline brain volumes were associated with a modest - although not significantly - increased risk (middle: $\text{HR}(95\%\text{CI})= 1.8(0.5-6.6)$; small: $\text{HR}(95\%\text{CI})= 1.9(0.5-7.3)$), while whole-brain atrophy rate was associated with a more strongly increased risk of progression to AD (moderate: $\text{HR}(95\%\text{CI})= 1.3(0.4-4.8)$; high: $\text{HR}(95\%\text{CI})= 3.5(1.1-11.2)$).

Whole-brain atrophy and cognitive decline

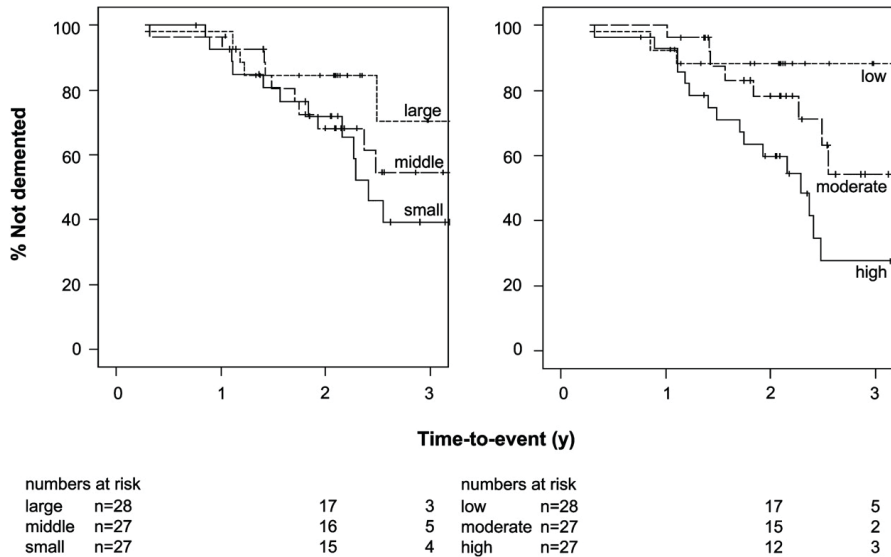


Figure 4. Kaplan-Meier curve of time-to-conversion in initially non-demented patients (n=82) depends on (left) baseline brain volume and (right) whole-brain atrophy rate. Baseline brain volume and whole-brain atrophy rate were divided into tertiles. Numbers at risk are displayed below graph. Participants reaching end of follow-up period without progression to dementia were censored. + = censored

Table 2. Hazard ratios (HR) and 95 % confidence interval (CI) of progression to dementia

| HR (CI) | Model 1: univariate | Model 2: age, sex | Model 3: age, sex, baseline MMSE |
|---------------------------------------|------------------------|----------------------|-------------------------------------|
| Baseline brain volume (mL) | | | |
| Large | 1 (-) | 1 (-) | 1 (-) |
| Middle | 1.7 (0.6 - 5) | 1.7 (0.5 - 5.2) | 1.2 (0.4 - 3.9) |
| Small | 3 (1.1 - 8.4) | 2.9 (0.9 - 9) | 1.6 (0.5 - 5.1) |
| Whole-brain atrophy rate (%/y) | | | |
| Low | 1 (-) | 1 (-) | 1 (-) |
| Moderate | 2.2 (0.7 - 7.2) | 2 (0.6 - 7) | 1.8 (0.5 - 6.1) |
| High | 4.6 (1.5 - 13.6) | 4.3 (1.4 - 13.5) | 3.6 (1.2 - 11.4) |

Table 2. Baseline brain volume and whole-brain atrophy rate were categorized into tertiles. Data are shown as Hazard ratios (HRs) with 95% confidence interval (CI). In model 1 unadjusted HRs are presented. In model 2 sex and age were corrected for, and in model 3 baseline MMSE was added as an additional covariate.

Discussion

Our study results show that while baseline brain volume was significantly lower in AD than in patients with subjective complaints and controls, it did not distinguish AD from MCI, nor could MCI be distinguished from subjective complaints and controls using baseline brain volume. By contrast, whole-brain atrophy rates were able to separate AD from MCI and MCI from subjective memory complaints and controls, illustrating that whole-brain atrophy rate is more sensitive than cross-sectional brain volume. The clinical relevance of this marker was demonstrated by the association of whole-brain atrophy rate with baseline cognition and rate of cognitive decline. Finally, for initially non-demented patients a high whole-brain atrophy rate was associated with increased risk of progression to dementia.

Our results confirm previous studies showing an increased whole-brain atrophy rate in AD versus controls. Our control group had a whole-brain atrophy rate of 0.5 % per year, which is in the middle of the previously reported range of rates of 0.2 % to 0.7 % per year.^{19,33} The AD patients had an annualized whole-brain atrophy rate of 1.9 %, almost four fold higher than controls. This is similar to previously reported rates in AD which are most typically around 2 % per year^{15,34}, although reported whole-brain atrophy rates in AD range from 1 % to 4 %, probably depending on the characteristics of the AD population, and method of atrophy rate calculation.^{17,35-37} We extend those earlier findings showing that while there was no difference in baseline brain volume, the whole-brain atrophy rate for the MCI group with 1.2 % per year was twice higher than among controls. This value is somewhat higher than the 0.7 % per year observed in a previous study.²¹ That study used BSI (boundary shift integral) to assess whole-brain atrophy, and is the only other study that assessed the risk of progression to dementia in the non-demented. They report a slightly increased risk of progression to dementia. Two other studies used brain segmentation to measure whole-brain atrophy rates.^{22,23} One of these studies assessed association of whole-brain atrophy rates with age, but not with cognitive decline.²² Both studies did not assess risk of progression to dementia. Our study adds to these previous observations by investigating a large cohort, recruited in a clinical setting, that covers the entire cognitive spectrum. We have used a well defined, easily accessible, fully automated

atrophy measurement technique. Furthermore, we used the MMSE, the most commonly used clinical cognition test, to check for associations with whole-brain atrophy rates. Finally, we assessed the risk of progression to dementia, and found a more than three-fold risk of progression to dementia for participants with a higher rate of atrophy.

Whole-brain atrophy rate was more sensitive than baseline brain volume in distinguishing the diagnostic groups. Whole-brain atrophy rate showed a clear distinction between groups, while baseline brain volume could only distinguish AD. A higher sensitivity of longitudinal atrophy in the detection of subtle differences in whole-brain and localized atrophy rates has been reported previously in AD and other neurodegenerative disease.^{38,40} The higher sensitivity of whole-brain atrophy rate can in part be attributed to the fact that when a subject is compared with him/herself instead of with a standard brain template, the confounding influence of inter-individual variability is reduced, reducing the measurement error.

Among non-demented patients, a higher whole-brain atrophy rate was associated with a greater risk of progression to dementia. A small brain volume was associated with a threefold increased risk of progression to dementia, although this effect largely disappeared when correcting for age, sex, and baseline MMSE. By contrast, a high whole-brain atrophy rate was associated with a more than fourfold increased risk of progression to dementia, which remained significant after correcting for age, sex and baseline MMSE.

Our study included the entire cognitive spectrum: patients with AD and MCI, patients with subjective complaints (who in fact can be considered normal at baseline, since all baseline clinical investigations were normal) and individuals without complaints. No differences were found between patients with subjective complaints and controls. Pooling these two groups would not have altered the results of this study. Furthermore we included a relatively large number of participants from one center. All participants have been carefully defined using a standardized diagnostic battery. As a consequence, they are characterized in a uniform manner and the diagnosis was determined by a multidisciplinary team. MR imaging was always performed on the same scanner using the same protocol.

A limitation of our study is that MR imaging of our participants was available for only two time points. In future studies, more than two MR scans per patient could be obtained to increase power and sensitivity, and to monitor the course of the disease. Furthermore, since no post mortem verification of diagnosis was available –which is considered the gold standard for diagnosing AD- we cannot exclude the possibility that some of our AD patients were misdiagnosed. However, all patients fulfilled NINDS-ADRDA clinical criteria for probable AD, which was confirmed both at baseline and at follow-up in multidisciplinary consensus meetings.

Our study confirms that whole-brain atrophy rate discriminates between diagnostic groups, better than cross-sectional brain volume. The clinical relevance of whole-brain atrophy rate is demonstrated by the association with cognition and cognitive decline. Since individuals with higher whole-brain atrophy rate had greater risks of progression to dementia, repeat MRI scans may be helpful in the diagnostic work-up of patients suspected of dementia.

Reference list

1. Petersen RC, Doody R, Kurz A et al. - Current concepts in mild cognitive impairment. - Arch Neurol 2001 Dec;58(12):1985-92.
2. Gauthier S, Reisberg B, Zaudig M et al. - Mild cognitive impairment. - Lancet 2006 Apr 15;367(9518):1262-70.
3. Visser PJ, Kester A, Jolles J, Verhey F. - Ten-year risk of dementia in subjects with mild cognitive impairment. - Neurology 2006 Oct 10;67(7):1201-7.
4. Scheltens P, Fox N, Barkhof F, De CC. - Structural magnetic resonance imaging in the practical assessment of dementia: beyond exclusion. - Lancet Neurol 2002 May;1(1):13-21.
5. Mungas D, Reed BR, Jagust WJ et al. - Volumetric MRI predicts rate of cognitive decline related to AD and cerebrovascular disease. - Neurology 2002 Sep 24;59(6):867-73.
6. Jack CR, Jr., Petersen RC, Xu Y et al. - Rates of hippocampal atrophy correlate with change in clinical status in aging and AD. - Neurology 2000 Aug 22;55(4):484-89.
7. Rusinek H, De SS, Frid D et al. - Regional brain atrophy rate predicts future cognitive decline: 6-year longitudinal MR imaging study of normal aging. - Radiology 2003 Dec;229(3):691-6.
8. Tapiola T, Pennanen C, Tapiola M et al. - MRI of hippocampus and entorhinal cortex in mild cognitive impairment: A follow-up study. - Neurobiol Aging 2006 Nov 9.
9. Karas GB, Scheltens P, Rombouts S et al. - Global and local gray matter loss in mild cognitive impairment and Alzheimer's disease. Neuroimage 2004; 23:708-716.
10. Kaye JA, Moore MM, Dame A et al. - Asynchronous regional brain volume losses in presymptomatic to moderate AD. - J Alzheimers Dis 2005 Sep;8(1):51-6.
11. Fotenos AF, Snyder AZ, Girton LE, Morris JC, Buckner RL. - Normative estimates of cross-sectional and longitudinal brain volume decline in aging and AD. - Neurology 2005 Mar 22;64(6):1032-9.
12. Freeborough PA, Fox NC. - The boundary shift integral: an accurate and robust measure of cerebral volume changes from registered repeat MRI. - IEEE Trans Med Imaging 1997 Oct;16(5):623-9.
13. Preboske GM, Gunter JL, Ward CP, Jack CR. - Common MRI acquisition non-idealities significantly impact the output of the boundary shift integral method of measuring brain atrophy on serial MRI. Neuroimage 2006; 30:1196-1202.
14. Smith SM, Zhang Y, Jenkinson M et al. - Accurate, robust, and automated longitudinal and cross-sectional brain change analysis. - Neuroimage 2002 Sep;17(1):479-89.

Chapter 3

15. Schott JM, Price SL, Frost C, Whitwell JL, Rossor MN, Fox NC. Measuring atrophy in Alzheimer disease - A serial MRI study over 6 and 12 months. *Neurology* 2005; 65:119-124.
16. Fox NC, Scahill RI, Crum WR, Rossor MN. - Correlation between rates of brain atrophy and cognitive decline in AD. - *Neurology* 1999 May 12;52(8):1687-9.
17. Jack CR, Shiung MM, Gunter JL et al. Comparison of different MRI brain atrophy, rate measures with clinical disease progression in AD. *Neurology* 2004; 62:591-600.
18. Wang D, Chalk JB, Rose SE et al. - MR image-based measurement of rates of change in volumes of brain structures. Part II: application to a study of Alzheimer's disease and normal aging. - *Magn Reson Imaging* 2002 Jan;20(1):41-8.
19. Enzinger C, Fazekas F, Matthews PM et al. Risk factors for progression of brain atrophy in aging - Six-year follow-up of normal subjects. *Neurology* 2005; 64:1704-1711.
20. Scahill RI, Frost C, Jenkins R, Whitwell JL, Rossor MN, Fox NC. - A longitudinal study of brain volume changes in normal aging using serial registered magnetic resonance imaging. - *Arch Neurol* 2003 Jul;60(7):989-94.
21. Jack CR, Shiung MM, Weigand SD et al. Brain atrophy rates predict subsequent clinical conversion in normal elderly and amnesic MCI. *Neurology* 2005; 65:1227-1231.
22. Fotenos AF, Snyder AZ, Girton LE, Morris JC, Buckner RL. - Normative estimates of cross-sectional and longitudinal brain volume decline in aging and AD. - *Neurology* 2005 Mar 22;64(6):1032-9.
23. Mungas D, Harvey D, Reed BR et al. Longitudinal volumetric MRI change and rate of cognitive decline. *Neurology* 2005; 65:565-571.
24. Folstein MF, Folstein SE, McHugh PR. - "Mini-mental state". A practical method for grading the cognitive state of patients for the clinician. - *J Psychiatr Res* 1975 Nov;12(3):189-98.
25. Petersen RC, Stevens JC, Ganguli M, Tangalos EG, Cummings JL, DeKosky ST. - Practice parameter: early detection of dementia: mild cognitive impairment (an evidence-based review). Report of the Quality Standards Subcommittee of the American Academy of Neurology. - *Neurology* 2001 May 8;56(9):1133-42.
26. McKhann G, Drachman D, Folstein M, Katzman R, Price D, Stadlan EM. - Clinical diagnosis of Alzheimer's disease: report of the NINCDS-ADRDA Work Group under the auspices of Department of Health and Human Services Task Force on Alzheimer's Disease. - *Neurology* 1984 Jul;34(7):939-44.

27. Neary D, Snowden JS, Gustafson L et al. - Frontotemporal lobar degeneration: a consensus on clinical diagnostic criteria. - *Neurology* 1998 Dec;51(6):1546-54.
28. van Straaten EC, Scheltens P, Knol DL et al. - Operational definitions for the NINDS-AIREN criteria for vascular dementia: an interobserver study. - *Stroke* 2003 Aug;34(8):1907-12
29. McKeith IG, Dickson DW, Lowe J et al. - Diagnosis and management of dementia with Lewy bodies: third report of the DLB Consortium. - *Neurology* 2005 Dec 27;65(12):1863-72
30. Smith SM, Zhang Y, Jenkinson M et al. - Accurate, robust, and automated longitudinal and cross-sectional brain change analysis. - *Neuroimage* 2002 Sep;17(1):479-89.
31. Smith SM, Jenkinson M, Woolrich MW et al. - Advances in functional and structural MR image analysis and implementation as FSL. - *Neuroimage* 2004;23 Suppl 1:S208-19.
32. Hartley SW, Scher AI, Korf ESC, White LR, Launer LJ. Analysis and validation of automated skull stripping tools: A validation study based on 296 MR images from the Honolulu Asia aging study. *Neuroimage* 2006; 30:1179-1186.
33. Scahill RI, Frost C, Jenkins R, Whitwell JL, Rossor MN, Fox NC. - A longitudinal study of brain volume changes in normal aging using serial registered magnetic resonance imaging. - *Arch Neurol* 2003 Jul;60(7):989-94.
34. Fox NC, Freeborough PA. - Brain atrophy progression measured from registered serial MRI: validation and application to Alzheimer's disease. - *J Magn Reson Imaging* 1997 Nov-Dec;7(6):1069-75.
35. Fox NC, Black RS, Gilman S et al. Effects of A beta immunization (AN1792) on MRI measures of cerebral volume in Alzheimer disease. *Neurology* 2005; 64:1563-1572.
36. Wang D, Chalk JB, Rose SE et al. - MR image-based measurement of rates of change in volumes of brain structures. Part II: application to a study of Alzheimer's disease and normal aging. - *Magn Reson Imaging* 2002 Jan;20(1):41-8.
37. Bradley KM, Bydder GM, Budge MM et al. - Serial brain MRI at 3-6 month intervals as a surrogate marker for Alzheimer's disease. - *Br J Radiol* 2002 Jun;75(894):506-13.
38. O'Brien JT, Paling S, Barber R et al. - Progressive brain atrophy on serial MRI in dementia with Lewy bodies, AD, and vascular dementia. - *Neurology* 2001 May 22;56(10):1386-8.
39. Paviour DC, Price SL, Jahanshahi M, Lees AJ, Fox NC. Longitudinal MRI in progressive supranuclear palsy and multiple system atrophy: rates and regions of atrophy. *Brain* 2006; 129:1040-1049.
40. Sormani MP, Rovaris M, Valsasina P, Wolinsky JS, Comi G, Filippi M. - Measurement error of two different techniques for brain atrophy assessment in multiple sclerosis. - *Neurology* 2004 Apr 27;62(8):1432-4.

Chapter 4

Accelerating regional atrophy rates in the progression from normal aging to Alzheimer's disease.

European Radiology 2009

J.D. Sluimer
W.M. van de Flier
G.B. Karas
R. van Schijndel
J. Barnes
R.G. Boyes
K.S. Cover
S.D. Olabarriaga
N.C. Fox
Ph. Scheltens
H. Vrenken
F. Barkhof

Abstract

We investigated progression of atrophy in *vivo*, in Alzheimer's disease (AD), and Mild Cognitive Impairment (MCI).

We included 64 patients with AD, 44 with MCI, and 34 controls with serial MRI examinations (interval 1.8 ± 0.7 y). A non-linear registration algorithm (fluid) calculated atrophy rates in six regions: frontal, medial temporal, temporal (extra-medial), parietal, occipital lobes, and insular cortex.

In MCI, the highest atrophy rate was observed in the medial temporal lobe, comparable to AD. AD patients showed even higher atrophy rates in the extra-medial temporal lobe. Additionally, atrophy rates in frontal, parietal and occipital lobes were increased. Cox proportional hazard models showed that all regional atrophy rates predicted conversion to AD. Hazard ratios varied between 2.6 (95% confidence interval=(1.1 - 6.2)) for occipital atrophy, and 15.8 (95%CI=(3.5 - 71.8)) for medial temporal lobe atrophy.

In conclusion, atrophy spreads through the brain with development of AD. MCI is marked by temporal lobe atrophy. In AD, atrophy rate in the extra-medial temporal lobe was even higher. Moreover, atrophy rates also accelerated in parietal, frontal, insular and occipital lobes. Finally, in non-demented elderly, medial temporal lobe atrophy was most predictive of progression to AD, demonstrating the involvement of this region in the development of AD.

Introduction

Alzheimer's disease is a neurodegenerative disease, characterised by progressive cognitive decline and cerebral atrophy. Patients with mild cognitive impairment have measurable cognitive deficits, but do not fulfil criteria for dementia.¹ Subjects with MCI are at an increased risk of developing AD with about 10-15% progressing to AD per year: in these subjects MCI may be considered to be a transitional phase for AD.²

Neuropathological studies suggest that Alzheimer's pathology spreads throughout the brain in a relatively predictable fashion and starts well before clinical onset of disease.³ However, by definition, neuropathological studies are post hoc and cross-sectional in design, and clearly cannot track disease progression in the individual. Magnetic resonance imaging (MRI) of the brain shows atrophy *in vivo*, particularly involving the medial temporal lobe, early in the disease.⁴ In contrast to neuropathological studies, serial MRI is feasible and enables *in vivo* study of progression of the disease throughout the brain.^{4,5} Serial measures allow each subject to act as their own control and thereby avoid the wide variability in brain morphology between subjects. In particular hippocampal atrophy rates have shown to be sensitive markers of AD, and predict progression of cognitive decline more accurately than cross-sectional volumes.⁶⁻⁸ However, whole-brain atrophy rates also distinguish patients with AD and MCI from controls, suggesting the additional early involvement of brain regions other than the hippocampus.^{5,9,10}

We studied progression of atrophy in six lobar brain regions AD, MCI and control subjects. We hypothesised that atrophy rates of MCI patients would be highest in the medial temporal lobes, consistent both with this region's early pathological involvement and its association with memory function – often the presenting symptom.³ With advancing disease, we expected atrophy rates of AD patients to increase in other brain regions as well. This study aimed to compare the pattern of regional atrophy rates in AD, MCI and controls. In addition, we investigated associations between regional atrophy rates and clinical progression to AD in initially non-demented patients.

Material and methods

Patients

Baseline clinical assessment

We included 64 patients with probable AD, 44 patients with MCI, and 34 controls. All patients underwent a standardised clinical assessment including medical history, physical and neurological examination, and psychometric evaluation. All subjects had serial volumetric MR imaging. The mini-mental state examination (MMSE) was used as a measure of general cognitive function.¹¹ Diagnoses were established during a multidisciplinary consensus meeting according to the Petersen criteria for MCI¹² and the NINCDS-ADRDA (National Institute of Neurological and Communicative Diseases and Stroke/Alzheimer's Disease and Related Disorders Association) criteria for probable AD.¹³ The control group consisted of 26 patients who presented at our memory clinic with subjective complaints, but who had normal clinical investigations and did not have significant cognitive deficits (i.e. MCI criteria were not fulfilled). Additionally, we included eight volunteers without cognitive complaints, who were willing to undergo the same diagnostic procedure as patients attending our memory clinic. The study was approved by the institutional ethical review board. All participants (or caregivers) gave written informed consent.

Clinical assessment at follow-up

Diagnostic classification of non-demented participants (MCI and controls) was re-evaluated at follow-up. The clinical diagnosis of dementia was determined according to published consensus criteria.¹²⁻¹⁶ Within the MCI group, 16 patients had remained stable, 23 progressed to AD, two to frontal-temporal lobar degeneration (FTLD)¹⁴, two to vascular dementia (VaD)¹⁵, and one to dementia with Lewy bodies (DLB)¹⁶. Within the group of controls, three progressed to MCI, three to AD and one to FTLD whilst 27 controls remained stable.

MRI

MR imaging was performed on a 1.0-T Siemens Magnetom Impact Expert System (Siemens AG, Erlangen, Germany) and included coronal T1-weighted 3D MPRAGE volumes (magnetization prepared rapid acquisition gradient echo; single slab, 168 slices; matrix size 256x256; FOV 250mm; voxel size 1x1x1.5 mm; TR=15ms; TE=7ms; TI=300ms; flip angle 15°). For inclusion subjects

had to have had two MR examinations without artefacts, performed on the same MR system using the same imaging protocol. Images were reviewed by a neuro-radiologist to exclude non-neurodegenerative pathology that could explain the cognitive impairment. Patients with baseline MR examinations that fulfilled radiological criteria of the NINDS-AIREN for vascular dementia were excluded.¹⁵

Regional atrophy rates between two time-points were measured from the 3D-T1 MPRAGE images using fluid registration, a non-linear matching algorithm.^{17,18} This algorithm requires the baseline and repeat image to be aligned, and intensity to be normalised within and between volumes. We used the following pre-processing steps:

- All images were bias-corrected using N3 software (<http://www.bic.mni.mcgill.ca/software/N3/>).¹⁹
- Images from the two time-points of each subject were linearly co-registered to a halfway position, using the skull-based scaling constraint as implemented in the SIENA software (structural brain change analysis, for estimating brain atrophy), part of the FSL suite (<http://www.fmrib.ox.ac.uk/fsl/>).²⁰
- Residual bias field differences between the two time-points were then removed using differential bias collection (DBC) as described by Lewis and Fox.²¹
- A brain mask was extracted from the resulting images using BET (Brain Extraction Tool) combined with registration of a standard mask using FLIRT (FMRIB's Linear Image Registration Tool).²²
- The brain mask was expanded to induce a Gaussian signal drop-off in space around the brain tissue.

After pre-processing, non-linear registration between the registered baseline and repeat images was performed, using a non-linear voxel-compression technique (fluid).¹⁷ This technique uses a viscous fluid model to compute the transformation required to bring one image in register with the other, using cross correlation as a similarity function. The data analysis for the whole data set required around 1,200 computing hours, and was performed in the GRID infrastructure provided by the Virtual Laboratory for e-Sciences project (www.vl-e.nl). By using trivially parallel computing the entire dataset could be processed in a single weekend. Visual inspection of the results confirmed that in all cases the registration had succeeded (i.e. all image pairs were

well matched and the algorithm had succeeded in deforming the latter MR examinations compared with the baseline – effectively removing the effects of atrophy). From the transformation field created by each registration, we generated a map of Jacobian determinants; these are a measure of the volume change (compression or expansion) at each voxel required to match the examinations precisely. Examples of these voxel-compression (Jacobian) maps are shown in Figure 1.

We then defined six lobar regions as follows: first brain tissue was separated from non-brain using FAST (FMRIB's Automated Segmentation Tool)²²; secondly, the AAL mask (Automated Anatomical Labeling)²³ was co-registered to the individual data. We used the subdivisions of the AAL mask of six 6 pre-defined lobar regions: frontal, medial temporal (hippocampus, parahippocampal gyrus, and amygdala), temporal (excluding medial temporal), parietal, occipital lobes, and insular cortex. For every patient, we averaged the relative volume change over all voxels in each region, and divided by the follow-up time in years between MR examinations to obtain annualized regional atrophy rates.

Statistical Analysis

Statistical analysis was performed with SPSS 12.0 (2003, Chicago, Illinois). Follow-up time was defined as the interval in years between baseline and repeat MR examinations. Diagnostic groups were compared with chi-squared tests for sex. For continuous variables we used analysis of variance (ANOVA), with age and sex as covariates. Post-hoc comparisons were performed using Bonferroni tests. Differences in regional atrophy rates between groups were assessed using ANOVA for repeated measures with region as within-subjects factor, diagnosis as between-subjects factor, and age and sex as covariates. In addition, within the group of initially non-demented participants we assessed the predictive value of regional atrophy rates, by using Cox proportional hazards models, which account for variability in length of follow-up. Results are presented as Hazard ratios (HRs) with 95% confidence interval (CI). The main outcome was progression to dementia, while the secondary outcome was progression to AD, which excludes six cases who developed a different type of dementia. Regional atrophy rates (dichotomized into high and low rates of atrophy, based on the median) were used as independent variables in separate models, adjusted for age and sex. Time-to-event curves were constructed with the Kaplan-Meier method. Statistical significance was set at $p < 0.05$.

Results

Demographics and clinical data are presented by patient group in Table 1. No between-group difference in sex or follow-up time was found. MCI patients were older than AD patients and controls. Frontal, medial temporal, temporal (excluding medial temporal), parietal, occipital, and insular atrophy rates are given in Table 1.

Table 1. Demographic and clinical variables by diagnostic group

| | Controls | MCI | AD | Overall p-value |
|--|------------------------------|-------------------------------|---------------------------|-----------------|
| Number of participants | 34 | 44 | 64 | |
| Outcome – numbers remaining stable or converting | 30 stable 3 AD 1 other | 16 stable 23 AD 5 other | - | |
| Sex, w/m | 16 / 18 | 21 / 23 | 38 / 26 | p=0.37 |
| Age, y | 67 (9) ^b | 71 (6) | 67 (8) ^b | p<0.001 |
| MMSE baseline | 28 (2) | 26 (3) ^a | 22 (5) ^{c,d} | p<0.001 |
| MR examination interval, y | 1.9 (0.9) | 1.9 (0.7) | 1.7 (0.6) | p=0.39 |
| Regional atrophy rates, %/ y | | | | |
| Frontal | -0.6 (0.7) | -0.9 (0.7) | -1.3 (0.8) ^c | p<0.001 |
| Medial temporal | -0.6 (0.7) | -1.5 (0.7) ^c | -1.5 (0.7) ^c | p<0.001 |
| Temporal (extra-medial) | -0.6 (0.5) | -1.4 (0.8) ^c | -2.2 (1.0) ^{c,d} | p<0.001 |
| Parietal | -0.5 (0.5) | -0.9 (0.7) ^a | -1.7 (0.9) ^{c,d} | p<0.001 |
| Occipital | -0.4 (0.4) | -0.8 (0.6) ^c | -1.4 (1.0) ^{c,d} | p<0.001 |
| Insular cortex | -0.3 (0.7) | -0.7 (0.6) | -0.8 (0.8) ^c | p<0.001 |

Table 1. Data are displayed as mean (sd). Differences between groups were assessed using ANOVA (age & sex as covariates where appropriate) with post-hoc Bonferroni tests. Group difference for sex (w/m) was calculated with Pearson Chi-Square. Medial temporal lobe is defined as hippocampus, parahippocampal gyrus, and amygdala. Temporal lobe is defined as temporal lobe excluding medial temporal lobe. ^a p<0.05 compared to controls; ^b p<0.05 compared to MCI; ^c p<0.001 compared to controls; ^d p<0.001 compared to MCI; MCI=mild cognitive impairment; AD=Alzheimer's disease; MMSE=mini-mental state examination

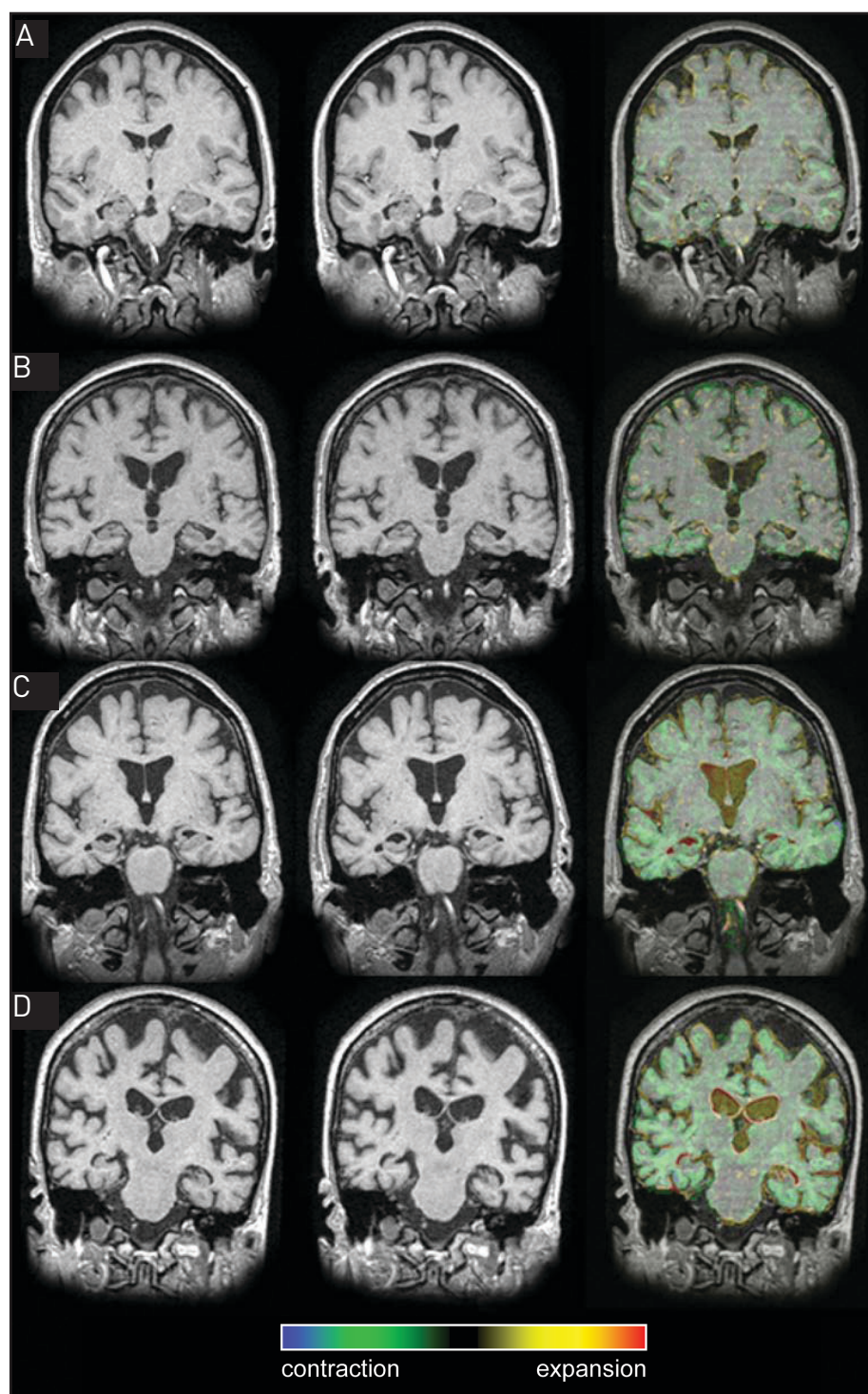


Figure 1 (previous page). Examples: baseline MR examination (left), repeat MR examination (middle) and colour overlay overlaid on the baseline examination (right) of four individual patients. Baseline and repeat examinations were affine-registered. The result of the non-linear registration is presented as a colour overlay applied to the baseline examination (representing the local Jacobian of the calculated deformation field), in order to highlight regions of structural expansion and contraction. Green and blue represent moderate to severe contraction (atrophy), yellow and red moderate to severe expansion. The overlay image was masked with a dilated mask to also show expansion of peripheral CSF spaces. [A] A 50 year old control subject, who presented at the memory clinic with subjective memory complaints [B] A 72 year old MCI patient who remained stable during follow-up; [C] A 69 year old MCI patient who progressed to AD during follow-up; [D] A 64 year old, moderately demented AD patient.

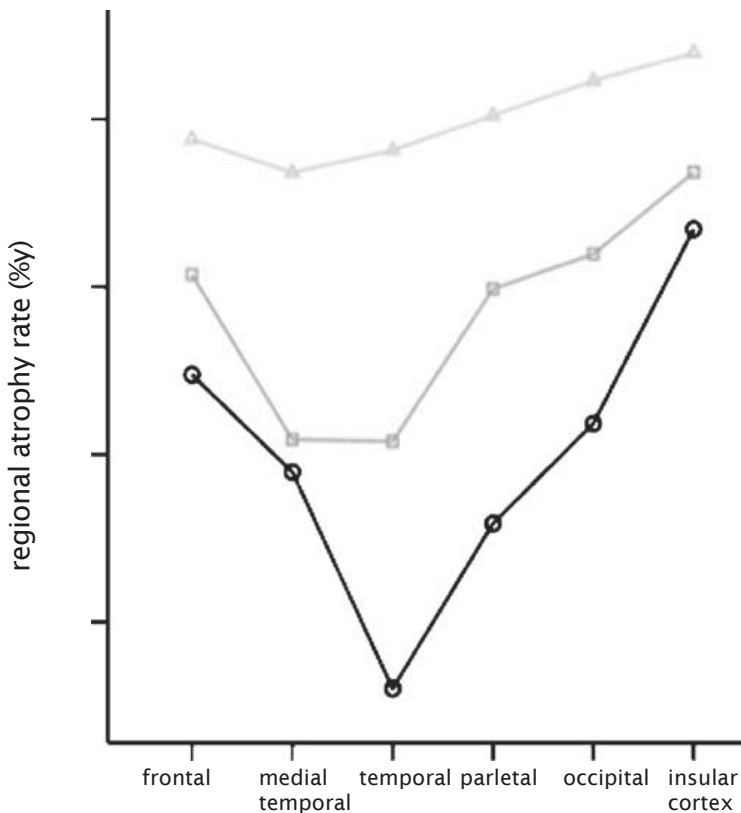


Figure 2. Regional atrophy rate in six pre-defined lobar regions are presented by diagnostic group: Frontal, medial temporal (hippocampus, amygdala, parahippocampal gyrus), temporal (extra-medial), parietal, occipital and insular lobe. In controls, atrophy rates are around 0.5%/y for each region. In MCI patients, atrophy rates start to accelerate mainly in the medial temporal, and remaining temporal lobe (extra-medial), and to a lesser extent in the other regions. AD is characterised by a further increase in atrophy rate in the remainder of the temporal lobe, parietal, frontal, occipital and insular lobe. Medial temporal lobe atrophy rates appear to be at a maximum, in the preclinical stage, since the rate is comparable to that of MCI patients.

Δ = controls (light gray line); □ = MCI (dark gray line); o = AD (black line)

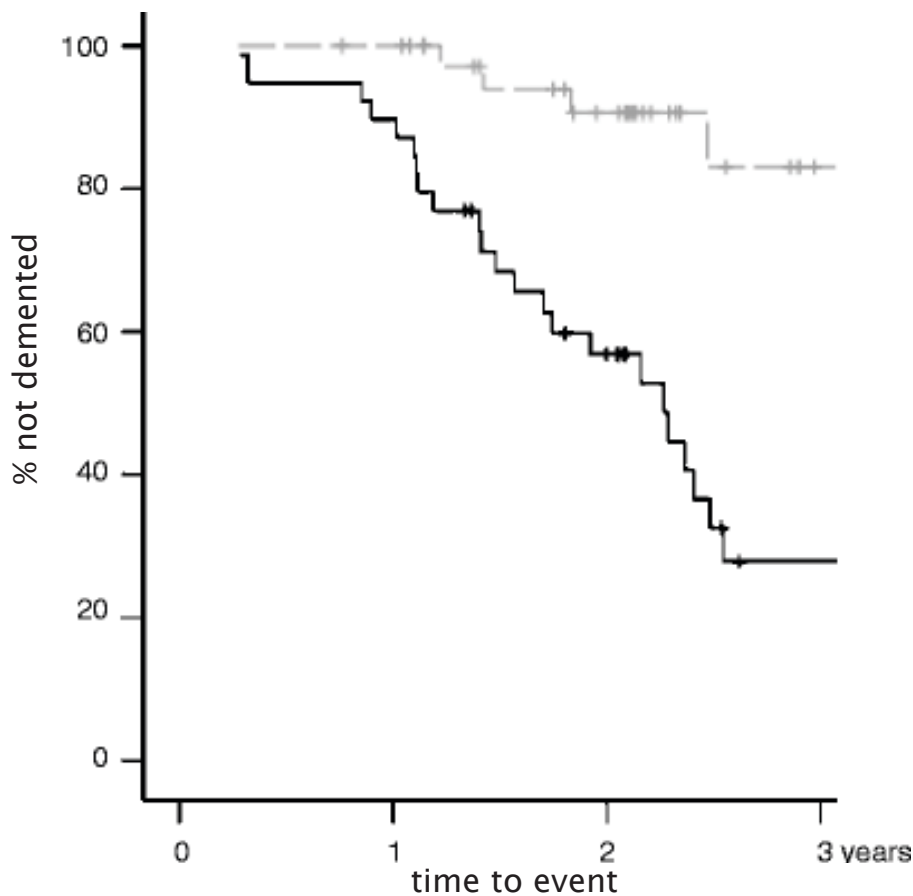
ANOVA for repeated measures with region as within-subjects factor, group as between-subjects factor, and age and sex as covariates showed main effects of diagnostic group ($p<0.001$) and region ($p<0.001$), and an interaction between diagnosis and region ($p<0.001$), indicating different patterns of regional atrophy rates according to diagnostic group. Figure 2 shows that for MCI patients, the highest annualized atrophy rates were observed not only in the medial temporal lobe, but also in the remaining (extra-medial) part of the temporal lobe. With progression of the disease, the atrophy appears to spread more widely through the brain, with patients with clinically established AD showing higher atrophy rates in temporal, frontal, parietal and occipital lobes. The atrophy rate in the medial temporal lobe appears to already have reached its maximum at a stage prior to clinical diagnosis, as this rate did not increase further in patients with AD when compared with MCI patients.

Subsequently, we assessed the predictive value of regional atrophy rates for the prediction of dementia in initially non-demented patients (controls and MCI, $n=78$). Thirty-two patients progressed to dementia, while 46 patients remained stable. No differences were found between patients progressing to dementia and patients who remained stable during follow-up, for sex (w/m 17/15 versus 20/26; $p=0.57$), age (mean \pm sd 71 \pm 6 versus 68 \pm 9; $p=0.14$) or duration of follow-up (1.8 \pm 0.7y versus 1.9 \pm 0.8y; $p=0.53$). There was a difference in baseline MMSE score between progressing and stable patients (26 \pm 3 versus 28 \pm 2; $p<0.001$). Age and sex adjusted Cox proportional hazard models showed that atrophy rates in all regions were associated with an increased risk of progression to dementia (Table 2). Risk estimates varied between 2.0 (95% confidence interval, CI=(0.9 – 4.4)) for occipital lobe atrophy rate and 6.4 (95% CI=(2.4 -17.3) for medial temporal lobe atrophy rate. As an example, Figure 3 shows the Kaplan Meier survival curve for the medial temporal lobe. When the analysis was repeated and restricted to progression to AD (excluding six patients who developed other types of dementia) the risk estimates were even higher. Atrophy rates in the medial temporal lobe remained the best predictor in model, HR 15.8 (95% CI = 3.5 - 71.8). In addition, the temporal lobe (non-medial) and parietal lobe were good predictors of progression to AD. When we repeated the analysis with additional adjustment for baseline MMSE, results remained largely unaltered (data not shown).

Table 2. Risk of progression to dementia associated with regional atrophy measures

| | Median Atrophy Rate %/year (IQ range) | Outcome dementia (n=78) HR (CI) | = Outcome AD (n=72) HR (CI) |
|----------------------|--|--|--|
| Frontal lobe | - 0.8 (-1.2 – -0.4) | 2.2 (1.0 – 4.9) | 2.8 (1.1 – 6.8) |
| Medial Temporal lobe | -0.9 (-1.5 – -0.3) | 6.4 (2.4 – 17.3) | 15.8 (3.5 – 71.8) |
| Temporal lobe | -0.9 (-1.4 – -0.4) | 3.9 (1.7 – 9.2) | 6.3 (2.2 – 18.7) |
| Parietal lobe | -0.6 (-1.0 – -0.2) | 3.4 (1.4 – 8.3) | 5.1 (1.8 – 14.8) |
| Occipital lobe | -0.5 (-0.9 – -0.2) | 2.0 (0.9 – 4.4) | 2.6 (1.1 – 6.2) |
| Insular cortex | -0.4 (-0.9 – 0) | 2.5 (1.1 – 5.9) | 2.9 (1.2 – 7.3) |

Median atrophy rate is displayed as median (interquartile range). Other data are presented as age and sex adjusted hazard ratios (HR) and 95 % confidence interval (CI). In the third column, six patients who progressed to another type of dementia were excluded.



Numbers at risk (n=78):

| | | |
|--------------------------|----|---|
| Low atrophy rate (n=39) | 25 | 7 |
| High atrophy rate (n=39) | 19 | 5 |

Figure 3. Kaplan-Meier curve of time-to-conversion in initially non-demented patients (n=78) dependent on medial temporal lobe atrophy rate. Non-demented patients were dichotomised into either the high or the low category, based on median medial temporal lobe atrophy rate ($-0.9\%/y$). Numbers at risk are displayed below graph. Participants reaching end of follow-up period without progression to dementia were censored.

--- = low atrophy rate (gray line); — = high atrophy rate of the medial temporal lobe (black line)
+ = censored

Discussion

The main finding of our study is that the pattern of regional atrophy rates differs in patients with MCI and AD when compared to controls. These data suggest how atrophy rates accelerate through the brain with the progression of cognitive decline. In MCI, the temporal lobe shows the greatest atrophy rate, but atrophy already extends beyond the medial temporal lobe, with atrophy rates in the extra-medial part of the temporal lobe even at this stage appear equally high. Atrophy rates in the medial temporal lobe were no higher in the AD patients than in the MCI patients, implying that rate of neurodegeneration in this region is already maximal prior to clinical diagnosis. The progression to AD is characterised by increasing atrophy rates in the rest of the temporal lobe, and atrophy also accelerating in parietal, frontal and occipital lobes. Nonetheless, medial temporal lobe atrophy was most predictive of progression to dementia in initially non-demented patients. Mainly subjects with a higher than median atrophy rate were associated with a 15-fold higher risk of developing AD, when compared to those with a lower than median atrophy rate during follow-up.

Previous studies report increased cerebral atrophy rates and ventricular enlargement in AD versus controls.^{9,24} Most cross-sectional MRI studies have focussed on atrophy of medial temporal lobe structures, commonly using volumetric measures. These studies have shown that hippocampal volumes at the time of clinical diagnosis are on average 18 percent lower when compared to controls.^{6,25} Whole-brain volumes are decreased in AD also, and tend to be around 5 percent lower – this volume loss cannot be accounted for by medial temporal lobe damage and implies widespread atrophy beyond this region.¹⁰ Voxel-based morphometry studies have shown using cross-sectional comparisons that in addition to atrophy of medial temporal lobe structures, temporal-parietal atrophy is prominent in AD.²⁶⁻²⁸ In MCI patients progressing to AD versus stable MCI patients atrophy of the temporal lobe, and to a lesser extent of the parietal and frontal lobe was shown.²⁹⁻³¹ Longitudinal measures of atrophy, which allow changes within the individual to be assessed, have been shown to be more sensitive at detecting group differences than cross-sectional volumes, in part because they are less susceptible to inter-subject variability.^{4,32,33} A number of studies described the pattern of longitudinal

atrophy in relatively small groups of sporadic and familial AD patients. They found increased atrophy in the medial temporal lobe over time, but also more widespread throughout the brain, in the parietal and frontal lobe.^{17,34} Longitudinal studies report that hippocampal atrophy rates increase in MCI.⁶⁻⁸ We extend these findings, by providing rates of atrophy, in six brain regions. Our study confirms that the medial temporal lobe is affected at an early stage of the disease. Additionally, we found the mean atrophy rate in the remainder of the temporal lobe to be increased at an early stage as well, before a clinical diagnosis could be made with certainty. Regional atrophy rates in the remainder of the cortex further accelerated in AD.

Among the limitations of our study is the fact that the control group included individuals with subjective complaints. At baseline, we found no differences between healthy volunteers and patients with subjective complaints, and we therefore pooled these subjects in one control group. However, patients presenting at a memory clinic with subjective complaints are known to have a higher risk of developing AD.^{35,36} In fact, three patients converted to AD and one to FTLD. One could argue that these patients should have been excluded, as they did not remain control-like throughout the study. However, we feel that, since they fulfilled initial inclusion criteria, excluding these patients would bias the results. Looking back at the regional atrophy rates, the patients who progressed to AD showed high atrophy rates, congruent with their clinical progression. Regional (including frontal) atrophy rates of the patient who progressed to FTLD were not remarkable. A second limitation was that no post mortem verification of diagnosis -which is considered the gold standard for diagnosing AD- was available. We therefore cannot exclude the possibility that some of our patients were misdiagnosed. Even though our MCI patients fulfilled the Petersen criteria, generally regarded as predictive of AD, five patients progressed to another type of dementia. When we visually inspected the individual data, the FTLD progressors showed relatively high frontal atrophy rates, while the pattern was more generalized for the two patients with VaD and the patient who progressed to DLB. Remarkably, none of these five patients showed predominant medial temporal lobe atrophy, as was generally observed in MCI patients progressing to AD.

Among the strengths of our study was the relatively large sample, in which we studied regional atrophy rates, using a robust method. We used fluid registration, a non-linear registration algorithm to match two MR examinations of each individual. This fully-automated voxel-compression technique has the advantage that changes at a lobar level can be assessed without time-consuming manual measurement of regional volumes. Furthermore, the non-linear registration matches examinations with shape change as well as volume loss. This means that the structural readjustments, that are an inevitable consequence of neurodegeneration, do not confound assessment of the distribution of loss.

The results of our study are in agreement with what has been published about the progression of atrophy through the brain in neuropathological studies regarding AD.^{3,37-40} Neuropathological studies report that AD pathology spreads through the brain in a relatively predictable fashion³. For neurofibrillary tangles the progression can be separated into six stages: Stages I-II show alterations in the transentorhinal regions, stages III-IV are known as the limbic stage, while stage V-VI are marked by widespread isocortical involvement. The accumulation of amyloid deposits can be divided in three stages: Stage A shows initial deposits in the basal portions of the isocortex, stage B shows amyloid in virtually all isocortical association areas, but the hippocampal formation is only mildly involved, while in stage C end-stage deposits can be observed throughout the isocortex. This study demonstrated that the pattern of atrophy, observed *in vivo* using serial MRI, more closely resembles the pattern of accumulating neurofibrillary tangles. Furthermore, the early involvement of the medial temporal lobe, as observed in neuropathological studies, has shown to be of clinical importance in the detection of incipient AD in this study.

Reference List

1. Petersen RC, Doody R, Kurz A et al (2001) Current concepts in mild cognitive impairment. *Arch Neurol* 58:1985-92
2. Gauthier S, Reisberg B, Zaudig M et al (2006) Mild cognitive impairment. *Lancet* 367:1262-70
3. Braak H and Braak E (1991) Neuropathological staging of Alzheimer-related changes. *Acta Neuropathol (Berl)* 82:239-59
4. Fox NC, Scahill RI, Crum WR et al (1999) Correlation between rates of brain atrophy and cognitive decline in AD. *Neurology* 52:1687-9
5. Jack CR, Shiung MM, Weigand SD et al (2005) Brain atrophy rates predict subsequent clinical conversion in normal elderly and amnesic MCI. *Neurology* 65:1227-1231
6. Jack CR, Jr., Petersen RC, Xu Y et al (2000) Rates of hippocampal atrophy correlate with change in clinical status in aging and AD. *Neurology* 55:484-89
7. Tapiola T, Pennanen C, Tapiola M et al (2006) MRI of hippocampus and entorhinal cortex in mild cognitive impairment: A follow-up study. *Neurobiol Aging* 29: 31-38
8. van de Pol LA, van Der Flier WM, Korf ES et al (2007) Baseline predictors of rates of hippocampal atrophy in mild cognitive impairment. *Neurology* 69:1491-7
9. Jack CR, Shiung MM, Gunter JL et al (2004) Comparison of different MRI brain atrophy, rate measures with clinical disease progression in AD. *Neurology* 62:591-600
10. Sluimer JD, van Der Flier WM, Karas GB et al (2007) Whole-brain atrophy rate and cognitive decline: a longitudinal MRI study of memory clinic patients. *Radiology* 248:590-598
11. Folstein MF, Folstein SE, Mchugh PR (1975) "Mini-mental state". A practical method for grading the cognitive state of patients for the clinician. *J Psychiatr Res* 12:189-98
12. Petersen RC, Stevens JC, Ganguli M et al (2001) Practice parameter: early detection of dementia: mild cognitive impairment (an evidence-based review). Report of the Quality Standards Subcommittee of the American Academy of Neurology. *Neurology* 56:1133-42
13. McKhann G, Drachman D, Folstein M et al (1984) Clinical diagnosis of Alzheimer's disease: report of the NINCDS-ADRDA Work Group under the auspices of Department of Health and Human Services Task Force on Alzheimer's Disease. *Neurology* 34:939-44
14. Neary D, Snowden JS, Gustafson L et al (1998) Frontotemporal lobar degeneration: a consensus on clinical diagnostic criteria. *Neurology* 51:1546-54

15. van Straaten EC, Scheltens P, Knol DL et al (2003) Operational definitions for the NINDS-AIREN criteria for vascular dementia: an interobserver study. *Stroke* 34:1907-12
16. McKeith IG, Dickson DW, Lowe J et al (2005) Diagnosis and management of dementia with Lewy bodies: third report of the DLB Consortium. *Neurology* 65:1863-72
17. Freeborough PA and Fox NC (1998) Modeling brain deformations in Alzheimer disease by fluid registration of serial 3D MR images. *J Comput Assist Tomogr* 22:838-43
18. Fox NC, Crum WR, Scahill RI et al (2001) Imaging of onset and progression of Alzheimer's disease with voxel-compression mapping of serial magnetic resonance images. *Lancet* 358:201-5
19. Sled JG, Zijdenbos AP, Evans AC (1998) A nonparametric method for automatic correction of intensity nonuniformity in MRI data. *IEEE Trans Med Imaging* 17:87-97
20. Smith SM, Zhang Y, Jenkinson M et al (2002) Accurate, robust, and automated longitudinal and cross-sectional brain change analysis. *Neuroimage* 17:479-89
21. Lewis EB and Fox NC (2004) Correction of differential intensity inhomogeneity in longitudinal MR images. *Neuroimage* 23:75-83
22. Smith SM, Jenkinson M, Woolrich MW et al (2004) Advances in functional and structural MR image analysis and implementation as FSL. *Neuroimage* 23:S208-19
23. Tzourio-Mazoyer N, Landeau B, Papathanassiou D et al (2002) Automated anatomical labeling of activations in SPM using a macroscopic anatomical parcellation of the MNI MRI single-subject brain. *Neuroimage* 15:273-89
24. Carmichael OT, Kuller LH, Lopez OL et al (2007) Ventricular volume and dementia progression in the Cardiovascular Health Study. *Neurobiol Aging* 28:389-397
25. van de Pol LA, Hensel A, Barkhof F et al (2006) Hippocampal atrophy in Alzheimer disease: Age matters. *Neurology* 66:236-238
26. Apostolova LG, Steiner CA, Akopyan GG et al (2007) Three-dimensional gray matter atrophy mapping in mild cognitive impairment and mild Alzheimer disease. *Arch Neurol* 64:1489-95
27. Baron JC, Chetelat G, Desgranges B et al (2001) *In vivo* mapping of gray matter loss with voxel-based morphometry in mild Alzheimer's disease. *Neuroimage* 14:298-309

28. Karas GB, Burton EJ, Rombouts SA et al (2003) A comprehensive study of gray matter loss in patients with Alzheimer's disease using optimized voxel-based morphometry. *Neuroimage* 18:895-907
29. Davatzikos C, Fan Y, Wu X et al (2006) Detection of prodromal Alzheimer's disease via pattern classification of MRI. *Neurobiol Aging* 29:514-523
30. Whitwell JL, Shiung MM, Przybelski SA et al (2007) MRI patterns of atrophy associated with progression to AD in amnesic mild cognitive impairment. *Neurology* 70:512-520
31. Karas G, Sluimer J, Goekoop R et al (2008) Amnesic Mild Cognitive Impairment: Structural MR Imaging Findings Predictive of Conversion to Alzheimer Disease. *AJNR Am J Neuroradiol* 29:944-949
32. Carmichael OT, Kuller LH, Lopez OL et al (2007) Cerebral ventricular changes associated with transitions between normal cognitive function, mild cognitive impairment, and dementia. *Alzheimer Dis Assoc Disord* 21:14-24
33. Ridha BH, Barnes J, Bartlett JW et al (2006) Tracking atrophy progression in familial Alzheimer's disease: a serial MRI study. *Lancet Neurol* 5:828-834
34. Scahill RI, Schott JM, Stevens JM et al (2004) Fluid registration of serial MRI: Identifying regional changes in Alzheimer's disease. *Neurobiol Aging* 25:269-269
35. Lam LC, Lui VW, Tam CW et al (2005) Subjective memory complaints in Chinese subjects with mild cognitive impairment and early Alzheimer's disease. *Int J Geriatr Psychiatry* 20:876-82
36. Visser PJ, Kester A, Jolles J et al (2006) Ten-year risk of dementia in subjects with mild cognitive impairment. *Neurology* 67:1201-7
37. Berg L, Mckeel DW, Jr, Miller JP et al (1998) Clinicopathologic studies in cognitively healthy aging and Alzheimer's disease: relation of histologic markers to dementia severity, age, sex, and apolipoprotein E genotype. *Arch Neurol* 55:326-35
38. multicentre, community-based population in England and Wales. *Neuropathology Group of the Medical Research Council Cognitive Function and Ageing Study (MRC CFAS). Lancet* 357:169-75
39. Barnes J, Whitwell JL, Frost C et al (2006) Measurements of the amygdala and hippocampus in pathologically confirmed Alzheimer disease and frontotemporal lobar degeneration. *Arch Neurol* 63:1434-1439
40. Fearing MA, Bigler ED, Norton M et al (2007) Autopsy-confirmed Alzheimer's disease versus clinically diagnosed Alzheimer's disease in the Cache County Study on Memory and Aging: a comparison of quantitative MRI and neuropsychological findings. *J Clin Exp Neuropsychol* 29:553-60

Chapter 5

Hippocampal atrophy rates in Alzheimer disease: Added value over whole-brain volume measures

Neurology 2009

W.J.P. Henneman
J.D. Sluimer
J. Barnes
W.M. van der Flier
I.C. Sluimer
N.C. Fox
Ph. Scheltens
H. Vrenken
F. Barkhof

Abstract

Objective: To investigate the added value of hippocampal atrophy rates over whole brain volume measurements on MRI in patients with AD, mild cognitive impairment (MCI) and controls.

Methods: We included 64 AD patients (67 ± 9 yrs.; f/m 38/26), 44 MCI patients (71 ± 6 yrs.; 21/23) and 34 controls (67 ± 9 yrs.; 16/18). Two MR-scans were performed (scan interval: 1.8 ± 0.7 yrs., 1.0T), using a coronal 3D T1-weighted gradient echo sequence. At follow-up, three controls and 23 MCI patients had progressed to AD. Hippocampi were manually delineated at baseline. Hippocampal atrophy rates were calculated using regional, non-linear 'fluid' registration. Whole brain baseline volumes and atrophy rates were determined using automated segmentation and registration tools.

Results: All MRI measures differed between groups ($p < 0.005$). For the distinction of MCI from controls, larger effect sizes of hippocampal measures were found compared to whole brain measures. Between MCI and AD, only whole brain atrophy rate differed significantly. Cox proportional hazards models (variables dichotomized by median) showed that within all non-demented patients, hippocampal baseline volume (hazard ratio [HR]: $5.7[95\%CI:1.5-22.2]$), hippocampal atrophy rate ($5.2[1.9-14.3]$) and whole brain atrophy rate ($2.8[1.1-7.2]$) independently predicted progression to AD; the combination of low hippocampal volume and high atrophy rate yielded a HR of 61.1 ($6.1-606.8$). Within MCI patients, only hippocampal baseline volume and atrophy rate predicted progression.

Conclusion: Hippocampal measures, especially hippocampal atrophy rate, best discriminate MCI from controls. Whole brain atrophy rate discriminates AD from MCI. Regional measures of hippocampal atrophy are the strongest predictors of progression to AD.

Introduction

Underlying clinical progression in Alzheimer's disease are neuropathological changes that follow a pattern of regional spread throughout the brain, starting at the medial temporal lobe and gradually effecting other parts of the cerebral cortex in later stages.¹ Especially with the prospect of disease-modifying therapies, early detection and monitoring of progression are important research goals in AD. Two frequently studied *in vivo* markers for diagnosis and disease progression in AD are whole brain atrophy and hippocampal atrophy on MRI. Both whole brain atrophy²⁻⁴ and hippocampal atrophy⁴ distinguish AD patients from controls and correlate with cognitive decline.^{5,6} Within MCI patients, hippocampal atrophy predicts future progression to AD,^{7,8} and in a recent study, we showed that whole brain atrophy rate distinguished groups and predicted progression to dementia in a cohort of AD, MCI and controls.⁹ Former studies mostly focused on either hippocampal or whole brain measurements in isolation. There are few studies that directly compared the predictive value of hippocampal and whole brain measures, and they yield inconsistent results.^{3,10} The discrepancy between studies may in part reflect technical difficulties in measuring change, especially for the hippocampal region, which is often determined using manual outlining. In the present study, we applied a novel, semi-automated regional registration method to measure hippocampal atrophy rate, that was shown to be superior to manual segmentation.¹¹ We directly compare the hippocampal atrophy rates with whole brain volume measurements and hippocampal baseline volume in the same sample.

Methods

Patients and clinical assessment

We studied a cohort of 154 subjects attending our memory clinic, with a diagnosis of probable AD, MCI as well as controls, of whom we had obtained serial MRI scans. Patients with evidence of other (concomitant) disease on MRI ($n=7$), or with insufficient scan quality ($n=5$) were excluded. In total, 142 patients were available for the present study: 64 patients with AD, 44 patients with MCI and 34 controls; this control group consisted of 26 patients with subjective complaints and 8 healthy volunteers. The study was approved by the institutional ethical committee and all subjects or their caregivers gave written informed consent for their clinical and MRI data to be used for research purposes.

All patients underwent a standardized clinical assessment, including medical history taking, neurological examination, neuropsychological examination, and MRI. Diagnoses were made in a multidisciplinary consensus meeting. The NINCDS-ADRDA criteria¹² were used for the diagnosis of AD. MCI subjects met the Petersen criteria,¹³ based on subjective and objective cognitive impairment, predominantly affecting memory, in the absence of dementia or significant functional loss, with a Clinical Dementia Rating¹⁴ of 0.5. Visual association test (VAT)¹⁵ was used to assess memory. Language and executive functioning were tested using the category fluency test, where patients had to produce the name of as many animals as possible within one minute. Activities of daily living were assessed by an interview, structured by the instrumental activities of daily living scale.¹⁶ The group of controls contained patients presenting with cognitive complaints in the absence of cognitive deficits on neuropsychological examination. We additionally included volunteers without memory complaints, mostly caregivers of patients visiting our memory clinic. Because there were no differences in age, sex, baseline MMSE or scan interval between patients with subjective complaints and volunteers, these two groups were pooled into one group (controls). Baseline demographic and clinical data by diagnostic group are shown in Table 1. Patients with MCI were slightly older than patients with AD and controls. There were no differences between groups in the distribution of sex or the length of the scan interval.

Non-demented participants (MCI and controls) visited the memory clinic annually. At follow-up visit, diagnostic classification was re-evaluated according to published consensus criteria. Within the group of MCI patients,²³ patients progressed to AD during follow-up, and five patients were diagnosed with another type of dementia; two with vascular dementia (VaD)¹⁷, two with fronto-temporal lobar degeneration (FTLD)¹⁸ and one with dementia with Lewy bodies¹⁹. Of the controls, three subjects progressed to AD during follow-up and one progressed to FTLD.

MRI scan acquisition and image processing

MRI scans were acquired at 1.0Tesla (Siemens Magnetom Impact Expert System, Siemens AG, Erlangen, Germany). All patients were actively invited for a follow-up MRI scan, using the same scanner and exactly the same scan protocol. Mean \pm SD scan interval was 1.8 ± 0.7 years. Scan protocol included a coronal, 3D, heavily T1-weighted single slab volume sequence (magnetization-prepared, rapid acquisition gradient echo sequence [MP-RAGE]); rectangular 250mm FOV with a 256x256 matrix; 1.5mm slice thickness; 168 slices; 1x1mm in plane resolution; TR=15ms; TE=7ms; TI=300ms; flip angle 15o.

Baseline 3DT1-weighted volume scans were reformatted in 2mm slices (in plane resolution 1x1mm) perpendicular to the long axis of the left hippocampus. Hippocampi on both sides were manually delineated using the software package Show_Images 3.7.0 (in-house developed at VU University Medical Center, 2003), by three trained technicians (coefficients of variation: Inter-rater<8%, intra-rater<5%). The technicians were blinded to diagnosis. Previously described criteria were used for the segmentation of the hippocampus.^{20,21} The region of interest (ROI) includes the dentate gyrus, cornu ammonis, subiculum, fimbriae and alveus. Baseline hippocampal volume was calculated by multiplying the total area of all ROIs of each hippocampus by slice thickness. Baseline hippocampal volumes were adjusted for intracranial volume, using the scaling factor derived from SIENAX (see below).

For the measurement of hippocampal atrophy rate, regional non-linear 'fluid' registration was used.²²⁻²⁴ First, a global, linear brain to brain registration (six degrees of freedom [dof]) was performed using the in-house developed

registration tool ‘visual register’. Subsequently, the software package MIDAS²⁵ was used to perform two consecutive regional registration steps. A local six dof registration was performed, to further align the hippocampal region on baseline and repeat scans. Subsequently, a cuboid extending 16 voxels in all three perpendicular directions from the extreme margins of the baseline hippocampal ROI was applied to the baseline and locally registered follow-up scan. A linear intensity drop-off was created in the outer eight voxels of this cuboid to facilitate the non-linear registration. Finally, non-linear ‘fluid’ registration was performed within the same region, as described previously.¹¹ The volume change was calculated by quantification of the Jacobian values, derived from the deformation matrix. This quantification was restricted to voxels within the baseline hippocampal region that showed contraction at follow-up.¹¹ Atrophy rate was expressed as percentage change from baseline volume.

Normalized brain volume (NBV) and percentage brain volume change (PBVC) over time were calculated from the 3DT1 weighted images, as previously described,⁹ using SIENAX (structural image evaluation, using normalization, of atrophy, cross-sectional) and SIENA (structural image evaluation, using normalization, of atrophy), both part of FMRIB’s Software Library (FSL www.fmrib.ox.ac.uk/analysis/research/siena).²⁶ In short, brain extraction tool (BET) was used to create brain and skull masks for the baseline and follow-up images. A scaling factor was derived from an affine (12dof) registration of the baseline brain to a reference image (MNI-152)²⁷, using the skull to constrain the scaling and skew. NBV was derived from a tissue-type segmentation of brain tissue, using the scaling factor to normalize the baseline brain volume. For PBVC, baseline and follow-up images were registered half-way to each other. Tissue-type segmentation was performed, and the brain surface was estimated on both scans based on the border between brain and CSF. The displacement of follow-up brain surface compared with baseline was calculated as the edge-point displacement perpendicular to the surface. Subsequently, the mean edge-point displacement was converted into a global estimate of PBVC.

Statistical analyses

Statistical analyses were performed using SPSS 15.0 for Windows. Atrophy rates were divided by scan interval to obtain annualized atrophy rates. For hippocampal measures, we used the mean of left and right values. Differences between groups for categorical variables were assessed using Chi-squared tests. Analysis of variance (ANOVA), corrected for age and sex, was used to assess differences between groups for continuous variables. Post-hoc analysis of between-group differences was performed using t-tests with Bonferroni correction. To compare sensitivity to the contrasts between controls and MCI and between MCI and AD, effect sizes were calculated using the difference of the means, divided by root of the mean square error of the difference (adapted from Cohen's d, to adjust for group differences in variance). Partial correlations, controlling for age and sex, were performed between MRI measures and baseline scores on cognitive tests. Subsequently, we estimated the risk of progression, related to the four measures, using Cox proportional hazards models. The MRI measures were dichotomized, based on their median value (hippocampal baseline volume 3652mm³, atrophy rate -3.3%/yr; whole brain baseline volume 1487ml, atrophy rate -0.3%/yr). Primary outcome was progression to AD, excluding six patients who progressed to another type of dementia. Each MRI measure was entered separately, unadjusted for covariates (model 1), adjusted for age, sex and MMSE (model 2), and together with age, sex, MMSE and the other MRI variables (model 3). We repeated the Cox-regression analysis with progression to dementia as outcome, including all patients. Finally, to explore the combined effect of baseline volume and atrophy rates within the non-demented subjects, we constructed 4 groups by median values of each variable: (1) high baseline volume and low atrophy rate, (2) high baseline volume and high atrophy rate, (3) low baseline volume and low atrophy rate and (4) low baseline volume and high atrophy rate. These were entered as categorical variables into the analysis, together with the covariates age, sex and MMSE. All Cox-regression analyses were performed within all non-demented patients and within MCI patients separately.

Results

Baseline volumes and atrophy rates for each diagnostic group are presented in Table 1. Figure 1 represents box plots of the four MRI markers per diagnostic group and atrophy rates in MCI patients that remained stable and had progressed to AD at follow-up. Adjusted for age and sex, all four MRI markers differed between groups ($p < 0.005$). Post-hoc analyses with Bonferroni correction (adjusted for age and sex) showed that all four MRI markers differed between controls and patients with AD ($p < 0.005$). MCI patients had lower hippocampal baseline volumes and higher hippocampal atrophy rates than controls ($p < 0.005$), but hippocampal baseline volumes and atrophy rates did not distinguish AD from MCI patients.

Table 1: Population descriptors and MRI measures per diagnostic group

| | Controls | MCI | AD | Total |
|------------------------------------|------------|--------------|-----------------|------------|
| Number of subjects (n) | 34 | 44 | 64 | 142 |
| Progression to AD (n) | 3 | 23 | - | 26 |
| Progression to dementia (n) | 4 | 28 | - | 32 |
| Age | 67 (9) | 71 (6) † | 67 (9) * | 68 (8) |
| Sex (n [%] male) | 18 (53%) | 23 (52%) | 26 (41%) | 67 (47%) |
| scan interval | 1.9 (0.9) | 1.9 (0.7) | 1.7 (0.6) | 1.8 (0.7) |
| MMSE on baseline | 28 (2) | 26 (3) † | 22 (5) *, † | 25 (4) |
| Visual association test | 11 (1) | 8 (3) † | 5 (3) *, † | 7 (4) |
| Category fluency | 21 (7) | 17 (5) † | 13 (5) *, † | 16 (6) |
| Hippocampus | | | | |
| Baseline volume | 4065 (357) | 3633 (489) † | 3537 (634) † | 3693 (572) |
| Atrophy rate | -2.2 (1.4) | -3.8 (1.2) † | -4.0 (1.2) † | -3.5 (1.4) |
| Whole brain | | | | |
| Baseline volume | 1534 (93) | 1480 (77) | 1453 (89) † | 1480 (92) |
| Atrophy rate | -0.6 (0.6) | -1.3 (0.9) † | -1.9 (0.9) *, † | -1.4 (1.0) |

Data represent mean \pm SD, unless indicated otherwise. Baseline hippocampal volume is represented in mm³, baseline brain volume in mL, hippocampal and brain atrophy rate in %/year volume change. For visual association test and category fluency, data was available for 103 subjects. MCI: mild cognitive impairment; MMSE: Mini-mental status examination

* $p < 0.05$ compared with MCI

† $p < 0.05$ compared with controls

The two outliers with the highest hippocampal atrophy rate in controls (Figure 1B) represent two subjects that had progressed to AD at follow-up. Baseline whole brain volume did not differ between controls and MCI, nor between patients with MCI and AD. In contrast, whole brain atrophy rates were higher in MCI than in controls ($p < 0.005$), and were again higher in AD ($p < 0.005$). The four outliers with highest whole brain atrophy rate within MCI (Figure 1D) had progressed to either AD ($n=3$) or FTLN ($n=1$) at follow-up. MCI patients that had progressed to AD at follow-up showed higher hippocampal atrophy rates than MCI patients that remained stable (Figure 1E), and there was no difference for whole brain atrophy rate (Figure 1F).

For the difference between controls and MCI, effect size (95% CI) of baseline hippocampal volume (0.73 [0.17-1.30]) was higher than that of baseline whole brain volume (0.49 [0.17-1.30]). Likewise, the effect size of hippocampal atrophy rate (1.17 [0.60-1.73]) was higher than that of whole brain atrophy rate (0.86 [0.30-1.43]). These results suggest a greater value of regional hippocampal measures, especially atrophy rates, in discriminating MCI from controls. In contrast, when looking at the difference between MCI and AD, effect sizes for both whole brain measures (baseline volume: 0.47 [-0.02-0.96]; atrophy rate: 0.67 [0.17-0.1.16]) were larger than for hippocampal measures (baseline volume: 0.33 [-0.16-0.82]; atrophy rate 0.25 [-0.24-0.74]), implying that whole brain measures provide more discriminatory value when comparing patients with AD and MCI.

Within the total population, we found correlations of hippocampal volume with baseline scores on VAT (r : 0.35; $p < 0.05$), of hippocampal atrophy rate with baseline MMSE, VAT and category fluency (r : 0.25, 0.38 and 0.26; $p < 0.05$), of baseline whole brain volume with baseline MMSE and VAT (r : 0.26 and 0.29; $p < 0.05$) and of whole brain atrophy rate with baseline MMSE, VAT and category fluency (r : 0.41, 0.32 and 0.36; $p < 0.05$).

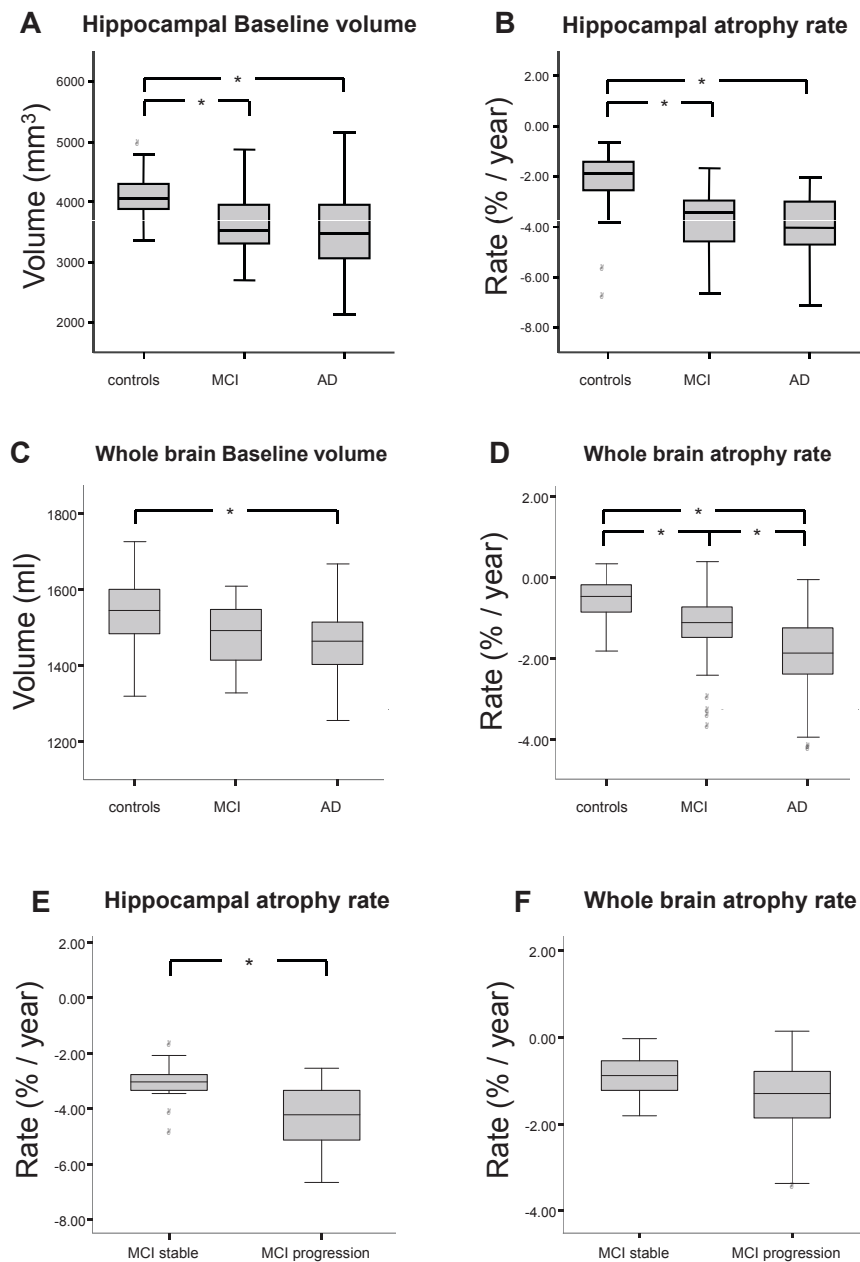


Figure 1. Mean volumes and atrophy rates. Box plots per diagnostic groups of (A) baseline hippocampal volume, (B) hippocampal atrophy rate, (C) baseline whole brain volume and (D) whole brain atrophy rate per diagnostic group (controls, MCI and AD), and box plots of MCI patients that remained stable and those who progressed to AD for (E) hippocampal atrophy rate and (F) whole brain atrophy rate. Lines represent median, boxes interquartile range and whiskers range; o: outliers * $p < 0.005$

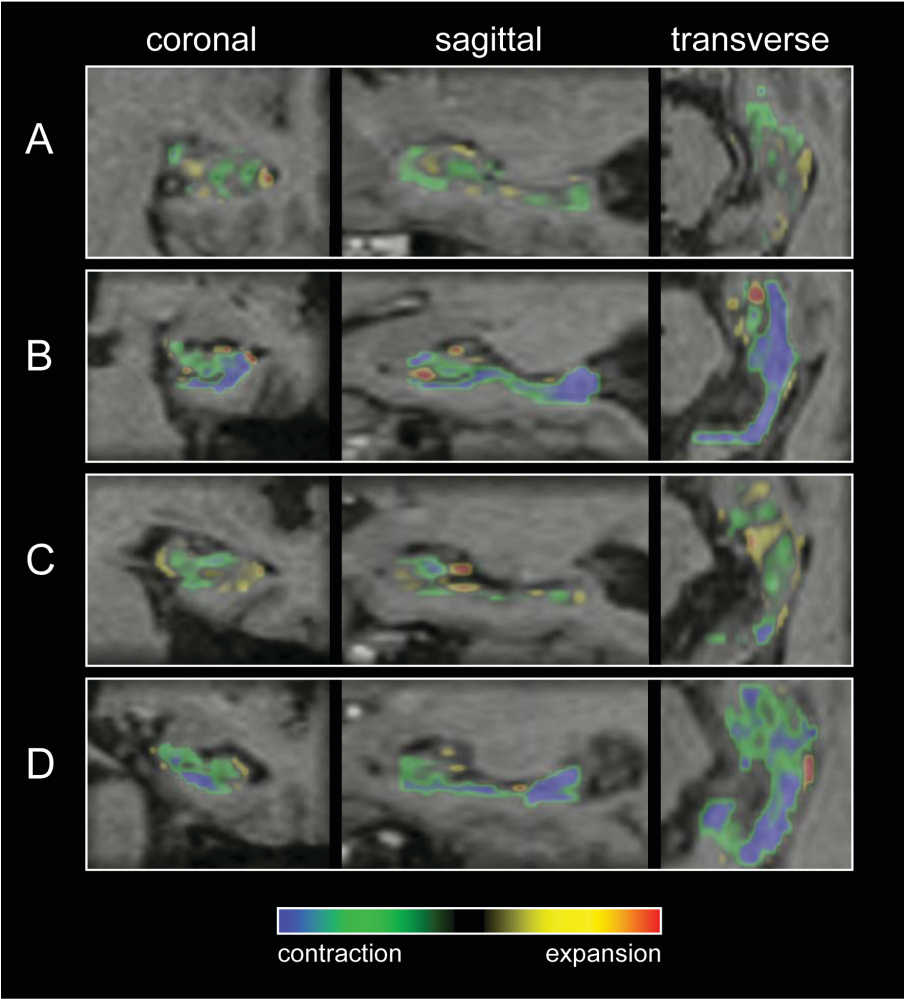


Figure 2. Individual examples of color overlay, representing contraction (green and blue) and expansion (yellow and red) within the right hippocampal ROI's of (A) a control that remained stable, (B) a control that had progressed to AD at follow-up (C) a MCI patient that remained stable and (D) a MCI patient that progressed to AD during follow-up.

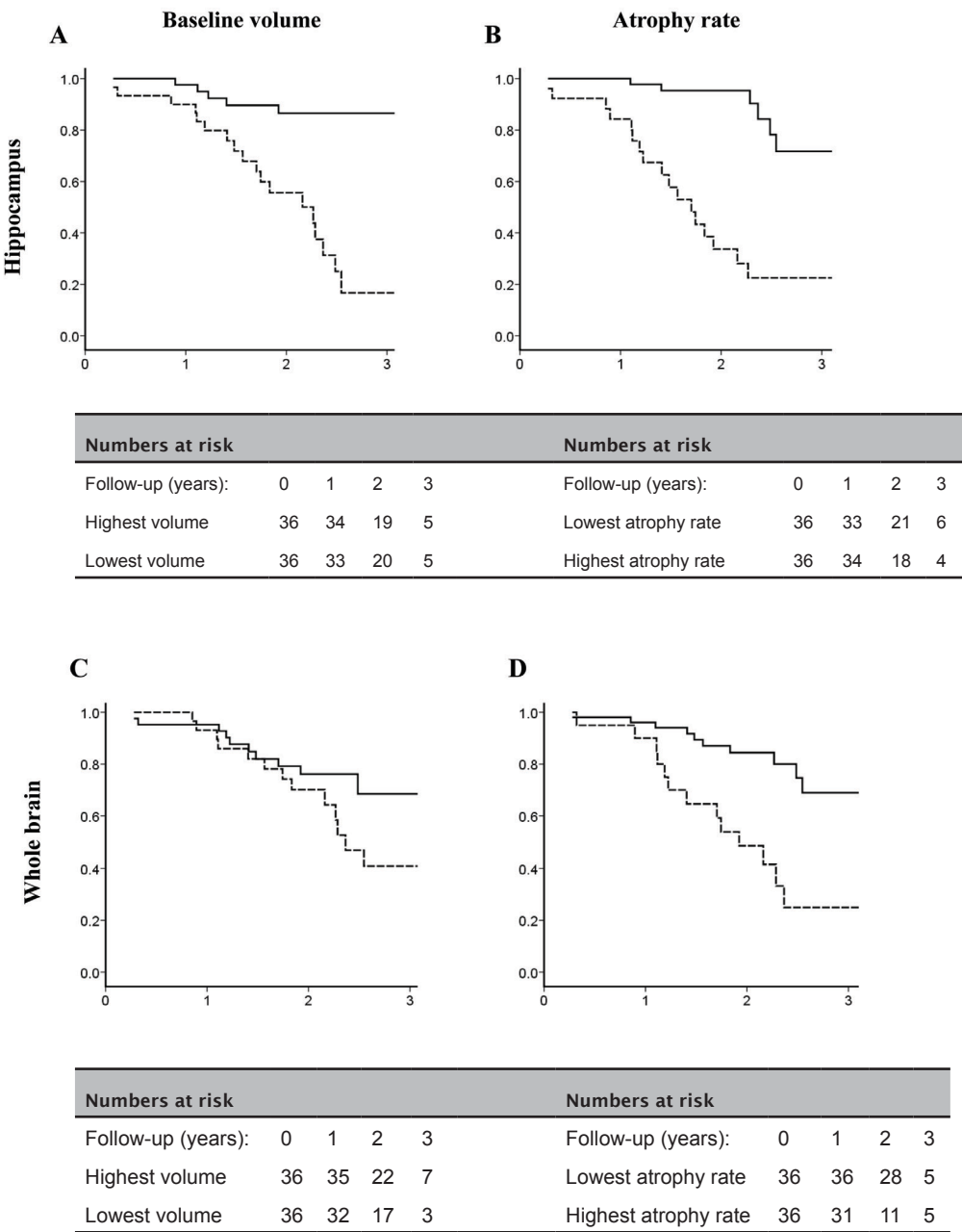


Figure 3. Kaplan-Meier curves of time to conversion within all non-demented subjects at baseline. MRI markers were dichotomised based on the median value: (A) baseline hippocampal volume, (B) hippocampal atrophy rate, (C) baseline whole brain volume and (D) whole brain atrophy rate. On the X-axis: follow-up duration (years); on the Y-axis: proportion of subjects that remained stable. Filled line: highest baseline volume (A; C) or lowest atrophy rate (B; D). Dotted line: lowest baseline volume (A; C) or highest atrophy rate (B; D). Tables represent the number of patients exposed to risk at the intervals of 0; 1; 2 and 3 years

Cox proportional hazard models (Table 2) show that within non-demented patients (MCI and controls), lower baseline hippocampal volume and higher hippocampal atrophy rate, as well as higher whole brain atrophy rate, independently predicted progression to AD. Baseline brain volume did not predict clinical progression. Hippocampal markers seemed to be stronger predictors than whole brain markers, with a roughly twofold higher risk. Kaplan-Meier curves for the MRI markers are shown in Figure 3. When the analysis was restricted to MCI patients, hippocampal baseline volume had the highest predictive value. Hippocampal atrophy rate was an independent, additional predictor. However, neither whole brain volume measure predicted progression to AD. Using progression to dementia as an outcome instead of progression to AD, hippocampal baseline volume (HR [95% CI]: 2.3 [1.1-6.2]), hippocampal atrophy rate (3.8 [1.7-8.6]) and whole brain atrophy rate (2.4 [1.1-5.3]) predicted progression to dementia in model 2, and only hippocampal atrophy rate (3.0 [1.3-7.0]) was an independent predictor of progression in model 3. Within MCI patients, hippocampal baseline volume (model 2: 5.0 [2.0-12.6], model 3: 4.9 [1.8-13.2]) and hippocampal atrophy rate (model 2: 2.7 [1.2-6.3], model 3: 2.1 [0.9-5.0]) predicted progression to dementia.

Table 2: Risk of progression to AD

| | | Model 1 | Model 2 | Model 1 |
|--|-----------------|------------------|-------------------|------------------|
| A. all non-demented patients (n=72) | | | | |
| Hippocampus | Baseline volume | 6.7 (2.5-18.1) * | 5.0 (1.5-16.1) * | 5.7 (1.5-22.2) * |
| | Atrophy rate | 8.6 (3.4-21.9) * | 6.2 (2.4-16.2) * | 5.2 (1.9-14.3) * |
| Whole brain | Baseline volume | 2.2 (1.0-5.0) | 1.4 (0.6-3.6) | 1.4 (0.5-4.2) |
| | Atrophy rate | 3.3 (1.5-7.3) * | 3.5 (1.5-8.2) * | 2.8 (1.1-7.2) * |
| B. MCI patients (n=39) | | | | |
| Hippocampus | Baseline volume | 7.4 (2.4-23.0) * | 10.4 (3.1-34.8) * | 9.0 (2.5-32.3) * |
| | Atrophy rate | 3.9 (1.6-9.9) * | 4.5 (1.7-11.9) * | 3.6 (1.2-10.7) * |
| Whole brain | Baseline volume | 1.1 (0.5-2.5) | 1.1 (0.5-2.7) | 1.0 (0.4-2.5) |
| | Atrophy rate | 1.3 (0.6-3.1) | 1.2 (0.5-3.1) | 1.0 (0.4-2.7) |

Data represent hazard ratio (95% confidence interval) of each MRI measure for the progression to Alzheimer's disease in (A) all non-demented subjects (n=72; 26 progressed to AD) and in (B) MCI patients, (n=39; 23 progressed to AD). Model 1: unadjusted; Model 2: individual MRI measure, adjusted for age, sex and baseline MMSE; Model 3: includes all MRI measures, adjusted for age, sex and baseline MMSE.

* p<0.05

Finally, we addressed the combined effect of baseline volume and atrophy rate on the prediction of progression to AD. Within all non-demented subjects, patients with a combination of both low baseline hippocampal volume and high hippocampal atrophy rate (median split) had a far more increased risk of progression to AD (HR 61.1 [95% CI: 6.1-606.8]), compared with patients with either a low baseline volume (11.2 [1.1-111.1]) or a high atrophy rate (12.8 [1.4-112.9]). Within MCI patients, we observed a comparable, yet less pronounced effect; HR (95%CI) 20.4 (3.9-107.2) for the combination of low hippocampal baseline volume and high atrophy rate versus 11.3 (2.0-62.8; only low baseline volume) and 5.6 (1.0-30.9; only high atrophy rate). For whole brain measures, we did not observe this increased risk for the combination of low baseline volume and high atrophy rate.

Discussion

Hippocampal baseline volume, in particular hippocampal atrophy rate, were better able to discriminate MCI patients from controls than whole brain measures. Whole brain volume measures better discriminated AD from MCI. Within non-demented subjects, regional hippocampal measures were the strongest predictors of progression to AD, but whole brain atrophy rate had an additional independent predictive effect. Within MCI patients, baseline hippocampal atrophy was the strongest predictor of progression to AD.

The atrophy rates we report are consistent with atrophy rates reported by other studies.^{2, 28-30} One previous study that directly compared the sensitivity of hippocampal and whole brain atrophy rates reported that both hippocampal and whole brain measures discriminated AD from controls and cognitively impaired subjects, but neither measure distinguished controls from the cognitively impaired.¹⁰ The apparent difference with our findings can be explained by the fact that their group of cognitively impaired did not meet MCI criteria¹³, and contained no subjects that progressed to dementia at follow-up. We found stronger correlations with baseline scores on cognitive tests for whole brain measures than for hippocampal measures, which is congruent with findings by other studies.³¹

Where hippocampal measurements are more sensitive markers early in the disease, we observe a shift towards an advantage of the use of whole brain volume measurements at a later stage. Moreover, we show that both hippocampal baseline volume and atrophy rate can be used to distinguish controls from MCI and predict progression, whereas of the whole brain measurements, only atrophy rate is able to do this. This finding seems to reflect that at the stage of MCI, considerable hippocampal atrophy has already taken place. Within MCI patients, baseline hippocampal volume was an even stronger predictor than hippocampal atrophy rate, and whole brain volume did not predict progression at all in this group. We showed that combining hippocampal baseline volume and atrophy rate leads to a much higher risk on progression than when either one is present. The predictive value of whole brain and hippocampal atrophy rates was lower in MCI patients than in the group of all non-demented subjects. This implies that the predictive effects of

these longitudinal measures are strongly driven by those patients that were at a very early stage (controls) at baseline, and showed fast progression from control to AD at follow-up, with concomitant high atrophy rates.

The fact that our controls included patients with subjective cognitive complaints might be seen as a limitation of our study. Indeed, with three of the 34 controls progressing to AD, our group contained a relatively high number of patients with pre-symptomatic pathology. Although the proportion of subjects that progress to AD or dementia in our MCI and control groups are higher than reported in community-based studies,³² they are comparable with other studies within memory clinic populations.³³ Furthermore, we think it is a strength that our groups represent a typical memory clinic population, covering the complete cognitive continuum of AD and its preceding stages.

Our findings extend on previous studies focussing on the progressive regional distribution of atrophy in AD and its preceding stages. Between MCI patients and controls, differences in atrophy (rates) have been described in medial temporal lobe structures.^{4,34,35} Increased hippocampal atrophy rates have even been found in patients with familial AD before clinical symptoms occur.^{34,36} In patients with AD, more widespread atrophy in other cortical areas occurs.^{4,34,35} This pattern of widespread atrophy is already evident in MCI patients later progressing to AD.³⁷ We show that hippocampal atrophy (rate) does not differentiate AD patients from MCI, as has also been reported by others.⁸ This supports earlier findings that AD-like hippocampal atrophy rate is already established in a transitional stage (MCI).^{8,34} After this stage, because whole brain atrophy rates still increase with progressing disease severity,^{38,39} whole brain atrophy rate becomes a better marker of disease progression than hippocampal volume measurements.

Reference list

1. Braak H, Braak E, Neuropathological staging of Alzheimer-related changes. *Acta Neuropathol* 1991;82:239-259.
2. Fotenos AF, Snyder AZ, Girton LE, Morris JC, Buckner RL. Normative estimates of cross-sectional and longitudinal brain volume decline in aging and AD. *Neurology* 2005;64:1032-1039.
3. Jack CR, Shiung MM, Weigand SD et al. Brain atrophy rates predict subsequent clinical conversion in normal elderly and amnesic MCI. *Neurology* 2005;65:1227-1231.
4. Karas GB, Scheltens P, Rombouts SA et al. Global and local gray matter loss in mild cognitive impairment and Alzheimer's disease. *Neuroimage* 2004;23:708-716.
5. Mungas D, Reed BR, Jagust WJ et al. Volumetric MRI predicts rate of cognitive decline related to AD and cerebrovascular disease. *Neurology* 2002;59:867-873.
6. Rusinek H, De SS, Frid D et al. Regional brain atrophy rate predicts future cognitive decline: 6-year longitudinal MR imaging study of normal aging. *Radiology* 2003;229:691-696.
7. Devanand DP, Pradhaban G, Liu X et al. Hippocampal and entorhinal atrophy in mild cognitive impairment: prediction of Alzheimer disease. *Neurology* 2007;68:828-836.
8. Jack CR, Jr., Petersen RC, Xu Y et al. Rates of hippocampal atrophy correlate with change in clinical status in aging and AD. *Neurology* 2000;55:484-489.
9. Sluimer JD, van der Flier WM, Karas GB et al. Whole-Brain Atrophy Rate and Cognitive Decline: Longitudinal MR Study of Memory Clinic Patients. *Radiology* 2008.
10. Cardenas VA, Du AT, Hardin D et al. Comparison of methods for measuring longitudinal brain change in cognitive impairment and dementia. *Neurobiol Aging* 2003;24:537-544.
11. van de Pol LA, Scahill RI, Frost C et al. Improved reliability of hippocampal atrophy rate measurement in mild cognitive impairment using fluid registration. *Neuroimage* 2007;34:1036-1041.
12. McKhann G, Drachman D, Folstein M et al. Clinical diagnosis of Alzheimer's disease: report of the NINCDS-ADRDA Work Group under the auspices of Department of Health and Human Services Task Force on Alzheimer's Disease. *Neurology* 1984;34:939-944.
13. Petersen RC, Doody R, Kurz A et al. Current concepts in mild cognitive impairment. *Arch Neurol* 2001;58:1985-1992.
14. Morris JC. The Clinical Dementia Rating (CDR): current version and scoring rules. *Neurology* 1993;43:2412-2414.

15. Lindeboom J, Schmand B, Tulner L, Walstra G, Jonker C. Visual association test to detect early dementia of the Alzheimer type. *J Neurol Neurosurg Psychiatry* 2002;73:126-133.
16. Lawton MP, Brody EM. Assessment of older people: self-maintaining and instrumental activities of daily living. *Gerontologist* 1969;9:179-186.
17. Roman GC, Tatemichi TK, Erkinjuntti T et al. Vascular dementia: diagnostic criteria for research studies. Report of the NINDS-AIREN International Workshop. *Neurology* 1993;43:250-260.
18. Neary D, Snowden JS, Gustafson L et al. Frontotemporal lobar degeneration: a consensus on clinical diagnostic criteria. *Neurology* 1998;51:1546-1554.
19. McKeith IG, Galasko D, Kosaka K et al. Consensus guidelines for the clinical and pathologic diagnosis of dementia with Lewy bodies (DLB): report of the consortium on DLB international workshop. *Neurology* 1996;47:1113-1124.
20. Jack CR, Jr. - MRI-based hippocampal volume measurements in epilepsy. - *Epilepsia* 1994;35 Suppl 6:S21-9.
21. van de Pol LA, van der Flier WM, Korf ES et al. Baseline predictors of rates of hippocampal atrophy in mild cognitive impairment. *Neurology* 2007;69:1491-1497.
22. Barnes J, Lewis EB, Scahill RI et al. Automated measurement of hippocampal atrophy using fluid-registered serial MRI in AD and controls. *J Comput Assist Tomogr* 2007;31:581-587.
23. Crum WR, Scahill RI, Fox NC. Automated hippocampal segmentation by regional fluid registration of serial MRI: validation and application in Alzheimer's disease. *Neuroimage* 2001;13:847-855.
24. Freeborough PA, Fox NC. Modeling brain deformations in Alzheimer disease by fluid registration of serial 3D MR images. *J Comput Assist Tomogr* 1998;22:838-843.
25. Freeborough PA, Fox NC, Kitney RI. Interactive algorithms for the segmentation and quantitation of 3-D MRI brain scans. *Comput Methods Programs Biomed* 1997;53:15-25.
26. Smith SM, Zhang Y, Jenkinson M et al. Accurate, robust, and automated longitudinal and cross-sectional brain change analysis. *Neuroimage* 2002;17:479-489.
27. Mazziotta J, Toga A, Evans A et al. A probabilistic atlas and reference system for the human brain: International Consortium for Brain Mapping (ICBM). *Philos Trans R Soc Lond B Biol Sci* 2001;356:1293-1322.
28. Barnes J, Bartlett JW, van de Pol LA et al. A meta-analysis of hippocampal atrophy rates in Alzheimer's disease. *Neurobiol Aging* 2008.

29. O'Brien JT, Paling S, Barber R et al. Progressive brain atrophy on serial MRI in dementia with Lewy bodies, AD, and vascular dementia. *Neurology* 2001;56:1386-1388.
30. Fox NC, Freeborough PA. Brain atrophy progression measured from registered serial MRI: validation and application to Alzheimer's disease. *J Magn Reson Imaging* 1997;7:1069-1075.
31. Ridha BH, Anderson VM, Barnes J et al. Volumetric MRI and cognitive measures in Alzheimer disease - Comparison of markers of progression. *Journal of Neurology* 2008;255:567-574.
32. Petersen RC. Mild cognitive impairment as a diagnostic entity. *J Intern Med* 2004;256:183-194.
33. Zetterberg H, Wahlund LO, Blennow K. Cerebrospinal fluid markers for prediction of Alzheimer's disease. *Neurosci Lett* 2003;352:67-69.
34. Scallan RI, Schott JM, Stevens JM, Rossor MN, Fox NC. Mapping the evolution of regional atrophy in Alzheimer's disease: unbiased analysis of fluid-registered serial MRI. *Proc Natl Acad Sci U S A* 2002;99:4703-4707.
35. Whitwell JL, Przybelski SA, Weigand SD et al. 3D maps from multiple MRI illustrate changing atrophy patterns as subjects progress from mild cognitive impairment to Alzheimer's disease. *Brain* 2007;130:1777-1786.
36. Schott JM, Fox NC, Frost C et al. Assessing the onset of structural change in familial Alzheimer's disease. *Ann Neurol* 2003;53:181-188.
37. Whitwell JL, Shiung MM, Przybelski SA et al. MRI patterns of atrophy associated with progression to AD in amnesic mild cognitive impairment. *Neurology* 2008;70:512-520.
38. Chan D, Janssen JC, Whitwell JL et al. Change in rates of cerebral atrophy over time in early-onset Alzheimer's disease: longitudinal MRI study. *Lancet* 2003;362:1121-1122.
39. Jack CR, Weigand SD, Shiung MM et al. Atrophy rates accelerate in amnesic mild cognitive impairment. *Neurology* 2008;70:1740-1752.

Chapter 6

Whole-brain atrophy rate in Alzheimer's disease: identifying fast progressors

Neurology 2008

J.D. Sluimer
H. Vrenken
M.A. Blankenstein
N.C. Fox
Ph. Scheltens
F. Barkhof
W.M. van der Flier

Abstract

Objective: To assess which baseline clinical and MRI measures influence whole-brain atrophy rates, measured from serial MR imaging.

Patients & Methods: We recruited 65 AD patients (age mean \pm sd 70 \pm 8y, 58% women, MMSE 22 \pm 5), scanned with an average interval of 1.7 \pm 0.6 years. Whole-brain atrophy rates were used as outcome measure. Baseline normalized brain volume, hippocampal volume and whole-brain atrophy rates were measured using 3D T1-weighted imaging. The influence of age, sex, apolipoprotein E genotype (APOE), baseline Mini-Mental State Examination (MMSE), baseline hippocampal volume, and baseline normalized brain volume on whole-brain atrophy rates was assessed using linear regression.

Results: The mean whole-brain atrophy rate was -1.9 \pm 0.9% per year. In the multivariate model, younger age (β (SE)=0.03(0.01); $p=0.04$), absence of APOE (β (SE)=0.61(0.28); $p=0.03$), and a low MMSE (β (SE)=0.11(0.03); $p<0.001$) were associated with a higher whole-brain atrophy rate. Furthermore, a relatively spared hippocampus predicted faster decline for patients with a smaller baseline brain volume ($p=0.09$), and with a lower MMSE ($p=0.07$). Finally, a smaller brain volume was associated with a higher rate of atrophy in younger patients ($p=0.03$).

Conclusions: Our results suggest that is possible to characterise a subgroup of AD patients, that are at risk of faster loss of brain volume. Patients with more generalized, rather than focal hippocampal atrophy, who often have an onset before the age of 65, and are APOE ϵ 4 negative, seem to be at risk of faster whole-brain atrophy rates than the more commonly seen AD patients, who are older, APOE ϵ 4 positive and have pronounced hippocampal atrophy.

Introduction

Alzheimer's disease is characterised by progressive cognitive impairment.¹ However, the course of AD is variable: not all patients progress at the same rate and the factors that influence or predict progression are not well understood.^{2,3} Most commonly, progression of the disease is measured by change in cognition over time.²⁻⁵ However, clinical and neuropsychological measures may lack sensitivity to change, are subject to day-to-day variability, and are influenced by behavioral fluctuations and intercurrent illness and medication. Neuroimaging markers provide an alternative and objective assessment of progression. The use of whole-brain atrophy rates, measured from serial MR imaging, correlates well with clinical progression in untreated subjects.⁶⁻¹⁰

Rates of whole brain atrophy within AD are most typically reported to amount to 2% per year¹¹, with substantial variability among populations studied (1% to 4%).^{7,12} Little is known about the determinants of this variability. We wished to assess which baseline demographic, clinical, and MRI variables influence whole-brain atrophy rates in AD.

Material and methods

Patients

We recruited 65 patients with clinically diagnosed AD attending our memory clinic. Patients underwent a standardized clinical assessment at baseline, including medical history, physical and neurological examination, laboratory tests, psychometric evaluation, and brain MRI. The mini-mental state examination (MMSE) was used as a measure of general cognitive function.¹³ Diagnoses were established during a multidisciplinary consensus meeting according to the NINCDS-ADRDA (National Institute of Neurological and Communicative Diseases and Stroke/Alzheimer's Disease and Related Disorders Association) criteria for probable AD.¹⁴ Based on age at baseline MRI (roughly corresponding to age at diagnosis), patients were dichotomised in early onset (≤ 65 years) and late onset (> 65 years) AD. The study was approved by the institutional ethical review board and all subjects gave written informed consent.

APOE

DNA was isolated from 10 ml EDTA blood. Apolipoprotein E (APOE) genotype was determined with the Light Cycler APOE mutation detection method (Roche Diagnostics GmbH, Mannheim, Germany). APOE was available from 53 of 65 patients (82%) and was dichotomized according to APOE $\epsilon 4$ status (one or more versus no $\epsilon 4$ alleles present).

MRI

Between 2004 and 2006 all patients were invited for a repeat MR scan, so each of the subjects had 2 MR scans. Follow-up time is defined as time between the two MRI scans (mean interval 1.7 years, standard deviation 0.6; range 11m-4y2m). MR imaging was performed on a 1.0-T Siemens Magnetom Impact Expert scanner (Siemens AG, Erlangen, Germany) and included coronal T1-weighted 3D MPRAGE volumes (magnetization prepared rapid acquisition gradient echo; single slab 168 slices; voxel size 1x1x1.5 mm; repetition time=15ms; echo time=7ms; inversion time=300ms; flip angle 15°). Subjects were included only if they had two scans of adequate quality, performed on the same scanner using the same imaging protocol. Scans were reviewed by a

radiologist to exclude non-neurodegenerative pathology that could explain the cognitive impairment. NINDS-AIREN criteria¹⁵ were used to exclude patients with vascular dementia (3 patients).

Whole-brain volume and whole-brain atrophy rates

Normalized baseline brain volume (NBV) and percentage brain volume change (PBVC) between two time-points were determined using SIENAX and SIENA (Structural Image Evaluation, using Normalisation, of Atrophy), two fully automated techniques part of FSL (for a detailed explanation see: www.fmrib.ox.ac.uk/analysis/research/siena/).^{16,17}

Whole-brain atrophy rates were measured with SIENA. Briefly, the brain was extracted using the brain extraction tool.¹⁷ Compared to standard SIENAX and SIENA, the procedure to remove non-brain tissue was slightly modified, because the brain extraction tool often leaves significant amounts of non-brain tissue (e.g. skull, meninges), while also removing cortex in some areas.¹⁸ To remove all non-brain tissue without losing cortex, we incorporated registration of a template mask to the individual scans. After this modified brain extraction procedure, the standard SIENA pipeline was continued. Using affine registration, the two scans were resampled in a common space to allow the change analysis. The skull was used as a scaling constraint in this step, in order to prevent the registration from introducing differences in head size between the two time points. The change analysis was then performed by applying automated tissue type segmentation, identifying edge points between brain tissue and other substances, and then estimating the perpendicular motion of the brain edge at these edge points. Finally, the average edge motion was converted to a percentage brain volume change (PBVC) between the two timepoints

Baseline brain volume, normalized for subject head size, was measured with a cross-sectional modification of SIENA called SIENAX. Briefly, after brain extraction tissue-type segmentation with partial volume estimation was carried out in order to calculate total volume of brain tissue. In addition, to correct for inter individual differences in head size, a volumetric scaling factor was obtained by affine-registering the brain image to MNI152 space, using

the skull contour to determine the registration scaling. Baseline brain volume, normalized for subject head size, was then obtained by multiplying the volume of brain tissue by the volumetric scaling factor.

For SIENAX (cross-sectional) a brain volume accuracy of 0.5 to 1% has been reported, whereas for SIENA (longitudinal), an error of 0.15 to 0.20% on the PBVC scale has been reported.¹⁶ All individual scans, registration results, and SIENA(X) output were reviewed by a rater who was blinded to the diagnosis. Two scans were excluded from analysis, because movement artefacts in the original MRI data led to spurious results.

Baseline hippocampal volume

The in-house developed software package Show Images 3.7.0 was used for manual delineation of the baseline left and right hippocampus. The hippocampus was resliced and measured according to previously published criteria.^{19,20} Briefly, the slice on which the hippocampal formation is first visible ventral to the amygdala was the most anterior slice measured. The ventral border is formed by the white matter of the parahippocampal gyrus. The dorsal border is formed by the amygdala in the anterior slices, more posterior cerebrospinal fluid (CSF) and the choroid plexus. The slice in which the crux of the fornix is visible in its total length was the most posterior slice measured. The dentate gyrus, cornu ammonis, subiculum, fimbria and alveus were measured (referred to as hippocampus). Measurements were performed by two operators, blinded to all clinical data. Reliability was assessed by measuring 10 brains twice: the mean intra-rater variability was below 5%, and mean inter-rater variability was below 8%. Hippocampal volume was computed by summing the delineated area of the region of interest on each slice and multiplying by the slice thickness. Left and right hippocampal volumes were averaged.

Table 1. Baseline demographics, clinical and MRI characteristics

| | Total | Early onset AD (age≤65y) | Late onset AD (age>65) |
|---|------------|-----------------------------|---------------------------|
| N patients | 65 | 26 | 39 |
| Sex (women / men) | 38 / 27 | 16 / 10 | 22 / 17 |
| Age, years | 70 (8) | 58 (3) | 73 (4) |
| Disease duration, years | 3 (2) | 3 (2) | 3 (2) |
| No. apolipoprotein E genotype (ϵ 4- / ϵ 4+) ^a | 13 / 40 | 7 / 16 | 5 / 23 |
| Baseline MMSE score | 22 (5) | 22 (5) | 22 (4) |
| Average hippocampal volume, mL | 2.7 (0.4) | 2.8 (0.4) | 2.6 (0.4) * |
| Normalized brain volume, mL | 1453 (88) | 1452 (81) | 1454 (94) |
| Follow-up time, years | 1.7 (0.6) | 1.7 (0.8) | 1.7 (0.5) |
| MMSE change (points/year) ^b | -2.1 (2) | -2.4 (1.6) | -1.9 (2.1) |
| Whole-brain atrophy rate, %/year | -1.9 (0.9) | -2.2 (1.1) | -1.7 (0.8) * |

Data are displayed as mean (sd), unless indicated otherwise. To test for differences between dichotomised age-groups (young: ≤ 65 and old: > 65) chi-squared test and ANOVA were used where appropriate. ^a = available for n=53; ^b= available for n=60; * $p<0.05$ versus early onset AD; MMSE = Mini-Mental State Examination

Statistics

Statistical analysis was performed with SPSS 12.0. Whole-brain atrophy rates (PBVC) were annualized by dividing by the time interval in years. A more negative whole-brain atrophy rate represents a larger relative brain volume loss per year. To test for differences between dichotomised age-groups (young: ≤ 65 and old: > 65) chi-squared test and t-test were used. Associations between MMSE change and whole-brain atrophy rates were assessed using bivariate correlation. We used linear regression analysis to assess the effects of age, sex, APOE, baseline MMSE, hippocampal volume and normalized brain volume (independent variables) on whole-brain atrophy rate (dependent variable). In model 1, influence for each variable was assessed separately, univariate analyses are presented. In model 2 each variable is corrected for age and sex, which are known to influence many of the predictor variables (these two variables are tested in model containing only age and sex). Model 3 is the full model,

where the influence of all variables was tested simultaneously. Subsequently, interactions between baseline predictors were assessed, by entering bivariate interaction terms into a model containing all variables, except for APOE, as APOE data were not available for all patients. Interactions with APOE were calculated separately in the full model. When assessing interactions, dichotomised age was used (young: ≤ 65 and old: > 65). In general, statistical significance was set at $p < 0.05$. Interactions were considered significant if p-values were lower than 0.10.

Results

Baseline demographic, clinical and MRI characteristics are presented in Table 1. AD patients in this study on average were 70 ± 8 years old, 39 patients were above the age of 65 years, and 26 were 65 years or younger. Mean baseline MMSE was 22 ± 5 , indicating mild to moderate AD. The mean whole-brain atrophy rate for the AD group was $-1.9 \pm 0.9\%$ per year. Older AD patients had smaller baseline hippocampi ($p < 0.05$), and a lower whole-brain atrophy rate ($p < 0.05$) compared to young AD patients. Whole-brain atrophy rate correlated with annualized change in MMSE score ($r = 0.38$; $p < 0.01$).

The effects of baseline demographic, clinical and MRI characteristics on whole-brain atrophy rate were evaluated using linear regression analyses (Table 2). In the univariate model, age, APOE, MMSE and hippocampal volume were associated with whole-brain atrophy rate. These effects remained comparable after correction for age and sex, and showed that earlier onset AD patients had a higher whole-brain atrophy rate, with an increase in whole-brain atrophy rate of 0.3% per year for every decade AD patients were younger. Compared with APOE $\epsilon 4$ positive patients, APOE $\epsilon 4$ negative patients had a 0.7% per year higher whole-brain atrophy rate. For every point lower on baseline MMSE, patients subsequently lost 0.1% more brain per year. There was an inverse relation between baseline hippocampal volume and whole-brain atrophy rate, with larger hippocampal volume being associated with a higher whole-brain atrophy rate. In model 3 (full model) the effects of age, APOE and MMSE remained significant.

Subsequently, bivariate interaction terms were entered into the model. First, we observed an interaction between hippocampal volume and normalized brain volume ($p=0.09$), indicating that in patients with a relatively spared hippocampal volume, a lower normalized brain volume was associated with a higher whole-brain atrophy rate, while this effect was not seen in patients with hippocampal atrophy at baseline (Figure 1). Secondly, there was an interaction between hippocampal volume and MMSE ($p=0.07$): a lower baseline MMSE was associated with a higher whole-brain atrophy rate in patients with a relatively large hippocampal volume, while this effect was not seen in patients with a smaller hippocampal volume (Figure 2). Finally, there was an interaction between age and normalized brain volume ($p=0.03$), indicating that among patients with a younger age a lower baseline normalized brain volume was associated with a higher whole-brain atrophy rate, while in patients with a higher age, normalized brain volume was not associated with whole-brain atrophy rate (Figure 3).

Table 2. Influence of baseline demographics, clinical and MRI characteristics on whole-brain atrophy rate

| | Model 1: univariate | Model 2: age, sex | Model 3: full model |
|--|------------------------|----------------------|------------------------|
| Age, per 1-year increment | 0.03 (0.01) * | 0.03 (0.01) * | 0.03 (0.01) * |
| Sex, women | 0.12 (0.24) | 0.04 (0.23) | -0.01 (0.24) |
| Apolipoprotein E genotype, ϵ 4 present ^a | 0.77 (0.30) * | 0.71 (0.31) * | 0.61 (0.28) * |
| Mini-Mental State Examination, per 1-point increment | 0.09 (0.02) * | 0.10 (0.02) * | 0.11 (0.03) * |
| Hippocampal volume, per 1-mL increment | -0.60 (0.26) * | -0.46 (0.28) + | -0.03 (0.28) |
| Normalized brain volume, per 1-mL increment | 0.002 (0.001) | 0.002 (0.001) + | 0.002 (0.001) |

Data are presented as β (SE) per unit. Model 1 represents the univariate analysis. In model 2 the analysis is corrected for age and sex. Model 3 is the full model ($n=53$). Negative estimates imply a higher whole-brain atrophy rate; positive estimates imply a lower whole-brain atrophy rate.

* $p<0.05$; + $p<0.10$; ^a= available for $n=53$

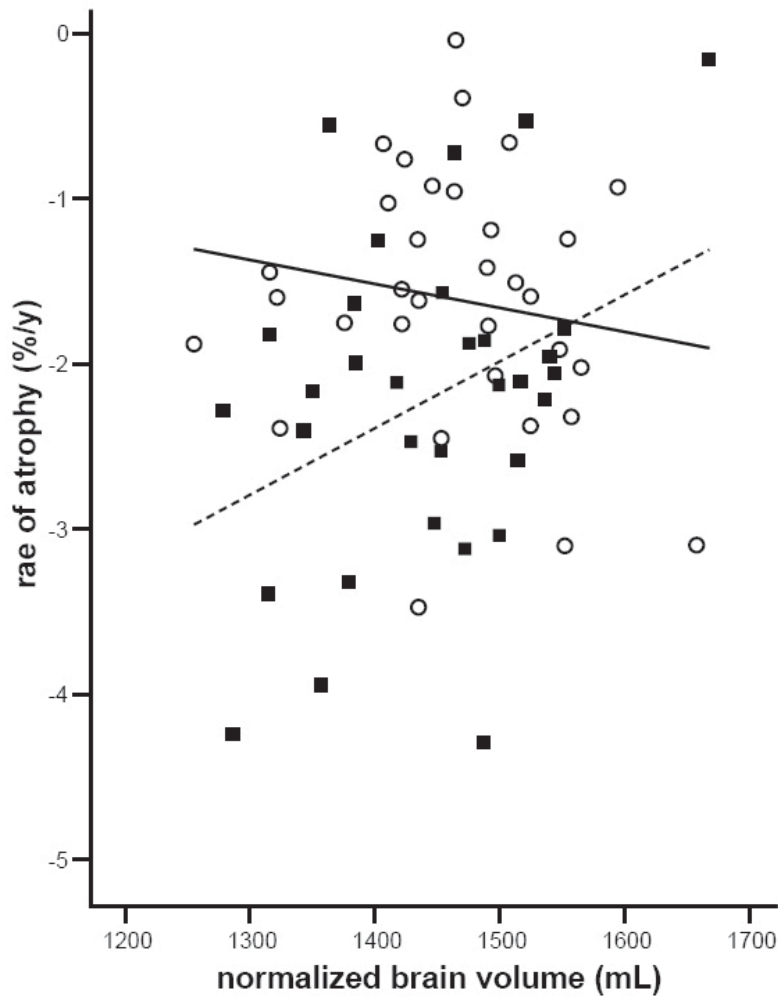


Figure 1. Scatter plot of whole-brain atrophy rate (%/y) by normalized brain volume (mL). For display purposes only, hippocampal volume has been dichotomized into small and large volume, based on median split. The intersecting regression lines of large (line) and small (dotted line) hippocampal volume indicate that the association between normalized brain volume and whole-brain atrophy rate is modified by the extent of hippocampal atrophy. While a low baseline brain volume is associated with a higher whole-brain atrophy rate for patients with a relatively spared hippocampus, this effect is not observed in the patient group with hippocampal atrophy.

Scatter: ○ = small hippocampus; ■ = large hippocampus

Regression line: — = small hippocampus; --- = large hippocampus

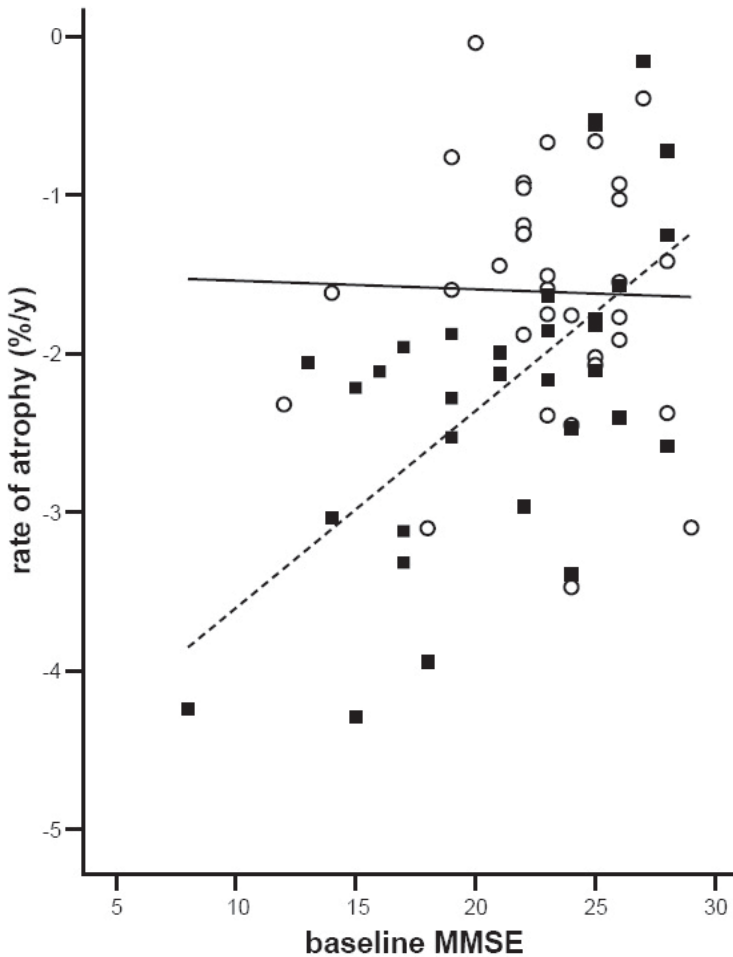


Figure 2. Scatter plot of whole-brain atrophy rate (%/y) by baseline MMSE.

For display purposes only, hippocampal volume has been dichotomized into large and small volume, based on median split. The intersecting regression lines of large (line) and small (dotted line) hippocampal volume indicate that whole-brain atrophy rate is differently affected by a low MMSE for patients with or without hippocampal atrophy. While a low MMSE is associated with a higher whole-brain atrophy rate for patients with a relatively spared hippocampus, this effect is not observed in patients with hippocampal atrophy.

Scatter: ▲ = small hippocampus; □ = large hippocampus

Regression line: — = small hippocampus; --- = large hippocampus

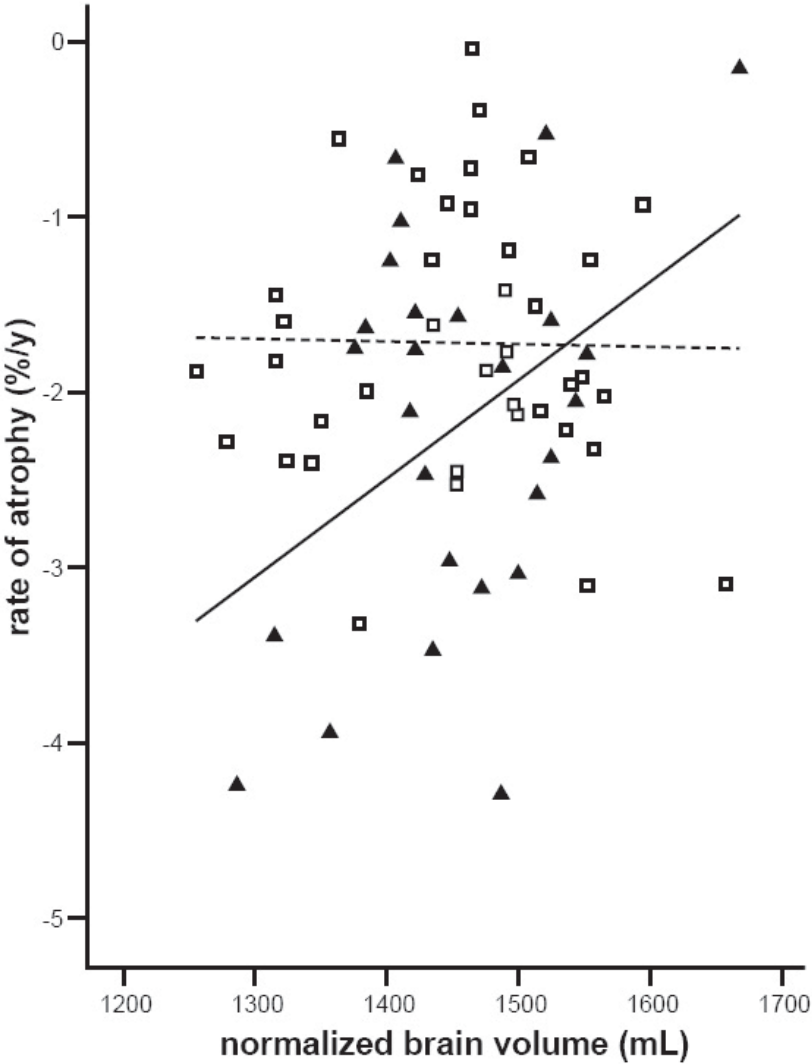


Figure 3. Scatter plot of whole-brain atrophy rate (%/y) by normalized brain volume (mL). Age has been dichotomized into young (≤ 65 y) versus old (> 65 y) Alzheimer's disease (AD) patients. The intersecting regression lines of young (line) versus old (dotted line) indicate that whole-brain atrophy rate is differently affected by the normalized brain volume in both age groups. While a low baseline brain volume for younger patients is associated with a higher whole-brain atrophy rate, indicating a faster decline, this effect is not observed in the older patient group.

Scatter: ▲ = young AD; ◻ = old AD
Regression line: — = young AD; --- = old AD

Discussion

In this study we assessed which MRI and demographic factors influence whole-brain atrophy rate in a sample of patients with a clinical diagnosis of AD. The main findings are that an earlier age, absence of APOE ϵ 4 and a low MMSE at baseline were associated with higher whole-brain atrophy rate, as measured using serial MR imaging. Furthermore, a relatively spared baseline hippocampus predicted faster decline for AD patients with a smaller baseline brain volume and a lower MMSE score. Finally, a smaller brain volume was associated with a higher rate of whole brain atrophy in patients with a relatively younger age. Most studies focus on the early diagnosis of AD trying to identify diagnostic markers. Few studies have aimed at the identification of prognostic markers that influence the variation in rate of decline after patients have received the diagnosis of AD. In the majority of available studies that assess the progression of AD, change in cognitive function is used as a marker for disease progression.^{2,5} These studies report that there is substantial heterogeneity in the progression of AD. The severity of cognitive impairment at diagnosis is suggested to be an important predictor of progression.^{2,3} Furthermore, patients with a slow rate of cognitive decline in the early stage of AD were unlikely to show a subsequent fast progression rate.^{2,5}

We found younger age, absent APOE ϵ 4 and low MMSE to be associated with a higher whole-brain atrophy rate. It has been suggested that the course of presenile dementia is more rapid.²¹ Papers that address familial AD (mostly early onset) report that patients progress more rapidly compared to sporadic AD (mostly late onset).²² We extend these findings by showing in a group of sporadic AD with a large variation in age, that an earlier age by itself predicts a faster whole-brain atrophy rate.

Within our sample of AD patients the presence of APOE ϵ 4 – the most important genetic risk for AD – was associated with a lower whole-brain atrophy rate. Although in the non-demented elderly population APOE ϵ 4 has shown to be associated with a higher rate of decline, this is attributable to APOE ϵ 4 being a risk factor for AD and does not necessarily imply an effect on progression in established disease.^{23,24} The few studies that assess the effects of APOE ϵ 4 on the rate of progression within AD tend to have comparable findings with our study. One study of AD patients reported that APOE ϵ 4 carriers performed better on the MMSE.⁴ In another paper the proportion of APOE ϵ 4 carriers

was not different between fast and slow progressing AD patients, though this was not formally tested.⁷ This would imply that APOE ϵ 4 carriers, once they reach the AD stage, do not have atrophy rates that are more rapid than AD non-carriers.

Finally, inspection of interactions showed that a smaller brain volume was associated with a higher whole-brain atrophy rate in patients with an early age. Furthermore a relatively spared hippocampal volume was predictive of a higher whole-brain atrophy rate in AD patients with a smaller normalized brain volume and a lower MMSE. At first sight, it seems counterintuitive, that patients with a large hippocampal volume were predisposed to a higher whole-brain atrophy rate. However, this effect was specific for those patients who in addition had a small baseline brain volume or low MMSE. These results suggest that patients with early brain volume loss due to atrophy in other regions than the medial temporal lobe, are at risk of faster decline, especially when they have an earlier age. Among the strengths of this study is the number of AD patients, who were collected in one center and underwent serial MR imaging on the same scanner. Patients were characterized in a uniform manner and the relatively large diagnosis was determined by a multidisciplinary team. Limitations of the study include that, even though we included a relatively large number of AD patients, these were not pathologically proven and not more than one repeated MRI scan was obtained per patient to monitor the course of the disease. Furthermore, APOE genotyping was missing in a minority of patients. Our AD patient sample was relatively young, with a mean age of 70 years. This can be explained by the fact that patients were recruited at a tertiary referral center, where many patients with early onset dementia are evaluated. The broad age range of our patient sample provided us with the unique opportunity to explore the effect of age on clinical characteristics of AD.

Clinically, different phenotypes of AD have been described.^{25,26} It has been suggested that AD patients with an onset before the age of 65, who are APOE ϵ 4 negative often have a distinct clinical profile, with prominent parietal dysfunction.^{27,28} It is tempting to think that these patients have early biparietal and more generalized atrophy, rather than focal medial temporal lobe atrophy. Our data suggest that these patients may be at risk of faster global disease progression than the more commonly seen sporadic AD patients, who are older, APOE ϵ 4 positive and have pronounced hippocampal atrophy.

Reference list

1. Waldemar G, Dubois B, Emre M, Georges J, McKeith IG, Rossor M et al. - Recommendations for the diagnosis and management of Alzheimer's disease and other disorders associated with dementia: EFNS guideline. - *Eur J Neurol* 2007 Jan;14(1):e1-26.
2. Kraemer HC, Tinklenberg J, Yesavage JA. - 'How far' vs 'how fast' in Alzheimer's disease. The question revisited. - *Arch Neurol* 1994 Mar;51(3):275-9.
3. Marra C, Silveri MC, Gainotti G. - Predictors of cognitive decline in the early stage of probable Alzheimer's disease. - *Dement Geriatr Cogn Disord* 2000 Jul-Aug;11(4):212-8.
4. Adak S, Illouz K, Gorman W, Tandon R, Zimmerman EA, Guariglia R et al. Predicting the rate of cognitive decline in aging and early Alzheimer disease. *Neurology* 2004; 63(1):108-114.
5. Capitani E, Cazzaniga R, Francescani A, Spinnler H. - Cognitive deterioration in Alzheimer's disease: is the early course predictive of the later stages? - *Neurol Sci* 2004 Oct;25(4):198-204.
6. Fox NC, Scahill RI, Crum WR, Rossor MN. - Correlation between rates of brain atrophy and cognitive decline in AD. - *Neurology* 1999 May 12;52(8):1687-9.
7. Jack CR, Shiung MM, Gunter JL, O'Brien PC, Weigand SD, Knopman DS et al. Comparison of different MRI brain atrophy, rate measures with clinical disease progression in AD. *Neurology* 2004; 62(4):591-600.
8. Mungas D, Harvey D, Reed BR, Jagust WJ, DeCarli C, Beckett L et al. Longitudinal volumetric MRI change and rate of cognitive decline. *Neurology* 2005; 65(4):565-571.
9. Fox NC, Black RS, Gilman S, Rossor MN, Griffith SG, Jenkins L et al. Effects of A beta immunization (AN1792) on MRI measures of cerebral volume in Alzheimer disease. *Neurology* 2005; 64(9):1563-1572.
10. Erten-Lyons D, Howieson D, Moore MM, Quinn J, Sexton G, Silbert L et al. - Brain volume loss in MCI predicts dementia. - *Neurology* 2006 Jan 24;66(2):233-5.
11. Schott JM, Price SL, Frost C, Whitwell JL, Rossor MN, Fox NC. Measuring atrophy in Alzheimer disease - A serial MRI study over 6 and 12 months. *Neurology* 2005; 65(1):119-124.
12. Boyes RG, Rueckert D, Aljabar P, Whitwell J, Schott JM, Hill DLG et al. Cerebral atrophy measurements using Jacobian integration: Comparison with the boundary shift integral. *Neuroimage* 2006; 32(1):159-169.
13. Folstein MF, Folstein SE, Mchugh PR. - "Mini-mental state". A practical method for grading the cognitive state of patients for the clinician. - *J Psychiatr Res* 1975 Nov;12(3):189-98.

14. McKhann G, Drachman D, Folstein M, Katzman R, Price D, Stadlan EM. - Clinical diagnosis of Alzheimer's disease: report of the NINCDS-ADRDA Work Group under the auspices of Department of Health and Human Services Task Force on Alzheimer's Disease. - *Neurology* 1984 Jul;34(7):939-44.
15. Roman GC, Tatemichi TK, Erkinjuntti T, Cummings JL, Masdeu JC, Garcia JH et al. - Vascular dementia: diagnostic criteria for research studies. Report of the NINDS-AIREN International Workshop. - *Neurology* 1993 Feb;43(2):250-60.
16. Smith SM, Zhang Y, Jenkinson M, Chen J, Matthews PM, Federico A et al. - Accurate, robust, and automated longitudinal and cross-sectional brain change analysis. - *Neuroimage* 2002 Sep;17(1):479-89.
17. Smith SM, Jenkinson M, Woolrich MW, Beckmann CF, Behrens TE, Johansen-Berg H et al. - Advances in functional and structural MR image analysis and implementation as FSL. - *Neuroimage* 2004;23 Suppl 1:S208-19.
18. Hartley SW, Scher AI, Korf ESC, White LR, Launer LJ. Analysis and validation of automated skull stripping tools: A validation study based on 296 MR images from the Honolulu Asia aging study. *Neuroimage* 2006; 30(4):1179-1186.
19. van de Pol LA, Barnes J, Scallhill RI, Frost C, Lewis EB, Boyes RG et al. - Improved reliability of hippocampal atrophy rate measurement in mild cognitive impairment using fluid registration. - *Neuroimage* 2007 Feb 1;34(3):1036-41 Epub 2006 Dec 15.
20. Jack CR, Jr. - MRI-based hippocampal volume measurements in epilepsy. - *Epilepsia* 1994;35 Suppl 6:S21-9.
21. Greicius MD, Geschwind MD, Miller BL. - Presenile dementia syndromes: an update on taxonomy and diagnosis. - *J Neurol Neurosurg Psychiatry* 2002 Jun;72(6):691-700.
22. Schott JM, Fox NC, Frost C, Scallhill RI, Janssen JC, Chan D et al. - Assessing the onset of structural change in familial Alzheimer's disease. - *Ann Neurol* 2003 Feb;53(2):181-8.
23. Enzinger C, Fazekas F, Matthews PM, Ropele S, Schmidt H, Smith S et al. Risk factors for progression of brain atrophy in aging - Six-year follow-up of normal subjects. *Neurology* 2005; 64(10):1704-1711.
24. Yip AG, Brayne C, Easton D, Rubinsztein DC. - Apolipoprotein E4 is only a weak predictor of dementia and cognitive decline in the general population. - *J Med Genet* 2002 Sep;39(9):639-43.
25. Ross SJ, Graham N, Stuart-Green L, Prins M, Xuereb J, Patterson K et al. - Progressive biparietal atrophy: an atypical presentation of Alzheimer's disease. - *J Neurol Neurosurg Psychiatry* 1996 Oct;61(4):388-95.
26. Galton CJ, Patterson K, Xuereb JH, Hodges JR. - Atypical and typical presentations of Alzheimer's disease: a clinical,

- neuropsychological, neuroimaging and pathological study of 13 cases. - Brain 2000 Mar;123 Pt 3:484-98.
27. van Der Flier WM, Schoonenboom SN, Pijnenburg YA, Fox NC, Scheltens P. - The effect of APOE genotype on clinical phenotype in Alzheimer disease. - Neurology 2006 Aug 8;67(3):526-7.
28. Schott JM, Ridha BH, Crutch SJ, Healy DG, Uphill JB, Warrington EK et al. - Apolipoprotein e genotype modifies the phenotype of Alzheimer disease. - Arch Neurol 2006 Jan;63(1):155-6.

Chapter 7

Whole-brain atrophy rate and CSF biomarker levels in MCI and AD: a longitudinal study

Neurobiology of Aging 2010

J.D. Sluimer
F.H. Bouwman
H. Vrenken
M.A. Blankenstein
F. Barkhof
W.M. van der Flier
Ph. Scheltens

Abstract

Objectives: To assess associations between cerebrospinal fluid (CSF) biomarker levels and MRI-based whole-brain atrophy rate in mild cognitive impairment (MCI) and Alzheimer's disease (AD).

Methods: We included 99 patients (47 AD, 29 MCI, 23 controls) who underwent lumbar puncture at baseline and repeat MRI. A subgroup of 48 patients underwent a second lumbar puncture. CSF levels of beta-amyloid1-42 ($A\beta_{1-42}$), tau and tau phosphorylated at threonine-181 ($P\text{-tau}_{181}$), and whole-brain atrophy rate were measured.

Results: Across groups, baseline $A\beta_{1-42}$ and tau were modestly associated with whole-brain atrophy rate. Adjusted for age, sex and diagnosis, we found no association between $A\beta_{1-42}$ or tau, and whole-brain atrophy rate. By contrast, high CSF levels of $P\text{-tau}_{181}$ showed a mild association with a lower whole-brain atrophy rate in AD but not in controls or MCI patients. Finally, whole-brain atrophy rate was associated with change in MMSE, but change in CSF biomarker levels was not.

Conclusions: Whole-brain atrophy rate and CSF levels of $A\beta_{1-42}$, tau or $P\text{-tau}_{181}$ provide complementary information in patients with MCI and AD.

Introduction

Both cerebrospinal fluid biomarkers and magnetic resonance imaging are increasingly used to detect and characterise brain changes associated with Alzheimer's disease *in vivo*. In CSF, decreased $A\beta_{1-42}$ levels and increased tau, and P-tau₁₈₁ levels are thought to reflect the presence of AD pathology.¹ These CSF biomarkers have been shown to differentiate patients with AD from control subjects with reasonable accuracy.³⁷ Moreover, these changes can be detected in patients with mild cognitive impairment (MCI) who will progress to AD.^{2;15} Brain tissue loss (atrophy) secondary to the neurodegenerative disease process can be visualized and measured using MRI. Whole-brain atrophy rate, measured from serial MRI, correlates well with disease and clinical progression in patients with MCI and AD.^{10;11;18}

Although both MRI and CSF biomarkers have been shown to be valuable markers of disease in MCI and AD^{36,37}, the relation between these markers has been less well studied. In cross-sectional studies, CSF biomarkers have been reported not to be related to MRI measures of atrophy, suggesting that these markers reflect different aspects of Alzheimer type neuropathology.^{25,26} However, longitudinal studies are needed, to clarify the relationship between these markers. The few studies that have reported CSF biomarkers and MRI measures in a longitudinal design, have used relatively small sample sizes, and have shown conflicting results in terms of whether or not these markers are associated.^{7,13,35}

The objective of the present investigation was to assess whether MRI measures and CSF biomarkers are related or provide independent information. We therefore assessed the relationship between baseline levels of CSF $A\beta_{1-42}$, tau, and P-tau₁₈₁ and whole-brain atrophy rate in patients with AD, MCI, and controls. In addition, we studied the association between longitudinal change of these CSF biomarker levels, whole-brain atrophy rates, and change in cognitive function.

Material and methods

Patients

We included 47 patients with AD, 29 patients with MCI and 23 controls with baseline CSF and repeat MRI scans from our memory clinic. All patients underwent lumbar puncture (LP) at baseline and MRI at baseline and follow up. At follow-up, 48 patients (20 AD, 17 MCI, 11 controls) agreed to undergo a second lumbar puncture. Follow-up time was defined as time between the two MRI scans (mean interval 1.7 years, standard deviation 0.7; range 11 m-4y). Patients underwent a standardized clinical assessment including medical history, physical and neurological examination, psychometric evaluation, and brain MRI. The Mini-Mental State Examination (MMSE) was used as a measure of general cognitive function.⁹ Diagnoses were established during a multidisciplinary consensus meeting according to the Petersen criteria for MCI²³ and the NINCDS-ADRDA (National Institute of Neurological and Communicative Diseases and Stroke/Alzheimer's Disease and Related Disorders Association) criteria for probable AD.¹⁹ The team involved in the diagnostic work-up was not aware of the results of the CSF analyses or the whole-brain atrophy rates. The control group consisted of 18 patients who presented to our memory clinic with subjective complaints, but who –after careful investigation– were considered to be cognitively normal. Additionally, we included 5 volunteers without cognitive complaints, who underwent the same diagnostic procedure as patients attending our memory clinic. The study was approved by the institutional ethical review board and all subjects gave written informed consent.

Clinical assessment at follow-up

Non-demented subjects (MCI and controls) visited the memory clinic annually (maximum: 4 visits). Diagnostic classification was re-evaluated at follow-up. The clinical diagnosis of dementia was determined according to published consensus criteria.^{19,21} Within the MCI group, 12 patients remained stable, and 17 progressed to AD¹⁹, one to fronto-temporal lobar degeneration (FTLD).²¹ Within the control group two patients with subjective complaints progressed to MCI, two to AD and one to FTLD, while 14 controls remained stable. Among the 48 patients with repeated LP, one control progressed to MCI (10 remained stable), and 11 patients with MCI progressed to AD, while 6 remained stable. The two patients converting to FTLD were excluded from analysis, leaving a sample size of 99 patients.

MRI

MR imaging was performed on a 1.0-T Siemens Magnetom Impact Expert scanner (Siemens AG, Erlangen, Germany) and included coronal T1-weighted 3D MPRAGE volumes (magnetization prepared rapid acquisition gradient echo; single slab 168 slices; matrix 256x256; FOV 250mm; voxel size 1x1x1.5 mm; repetition time=15ms; echo time=7ms; inversion time=300ms; flip angle 15°). All subjects included had two scans of adequate quality, performed on the same scanner using an identical imaging protocol. Scans were reviewed by a radiologist to exclude non-neurodegenerative pathology that could explain the cognitive impairment. Scans that fulfilled radiological criteria of the NINDS-AIREN for vascular dementia were excluded.³²

Whole-brain atrophy rates were measured with SIENA (Structural Image Evaluation, using Normalisation, of Atrophy), a fully automated technique part of FSL (for a detailed explanation see: www.fmrib.ox.ac.uk/analysis/research/siena).³¹ Briefly, the brain was extracted using the brain extraction tool.³⁰ Compared to standard SIENA, the procedure to remove non-brain tissue was slightly modified, because the brain extraction tool often leaves significant amounts of non-brain tissue (e.g. skull, meninges), while also removing cortex in some areas.¹⁶ To remove all non-brain tissue without losing cortex, we incorporated in the procedure the registration of a template mask to the individual scans. After this modified brain extraction procedure, the standard SIENA pipeline was continued. Using affine registration, the two scans were resampled in a common space to allow the change analysis. The skull was used as a scaling constraint in this step, in order to prevent the registration from introducing differences in head size between the two time points. The change analysis was then performed by applying automated tissue type segmentation, identifying edge points between brain tissue and other substances, and then estimating the perpendicular motion of the brain edge at these edge points. Finally, the average edge motion was converted to a percentage brain volume change (PBVC) between the two time points. For SIENA, an error of 0.15 to 0.20% on the PBVC scale has been reported.³¹ All individual scans, registration results, and SIENA output were reviewed by a rater who was blinded to the diagnosis.

CSF

CSF was obtained by LP between the L3/L4 or L4/L5 intervertebral space, using a 25-gauge needle, and collected in 12-mL polypropylene tubes. Within two hours, CSF samples were centrifuged at 2100g for 10 minutes at 4 °C. A small amount of CSF was used for routine analysis, including total cells (leucocytes and erythrocytes), total protein and glucose. CSF was aliquoted in polypropylene tubes of 0.5 or 1 ml, and stored at -80 °C until further analysis. CSF A β_{1-42} , tau and P-tau₁₈₁ were measured as described previously.³ The intra-assay coefficient of variation (CV) was 2.8% for A β_{1-42} , 3.7% for tau and 1.6% for P-tau₁₈₁. The inter-assay coefficient of variation (CV) was 13.5% for A β_{1-42} , 10.2% for tau and 12.8% for P-tau₁₈₁. To circumvent inter-assay variability, baseline and follow-up samples were run in the same assay at the time of the second spinal tap.⁴

Statistics

Statistical analysis was performed with SPSS 12.0 (2003, Chicago, IL). Whole-brain atrophy rate (PBVC), change in CSF biomarker levels, and change in MMSE over time were annualized by dividing by the time interval in years. A more negative whole-brain atrophy rate represents a larger relative brain volume loss per year. CSF biomarker levels were log-transformed. Frequency distributions for sex were compared with chi-squared tests. One way Analysis of Variance (ANOVA) adjusted for age and sex, with post hoc Bonferroni tests was used to compare continuous variables between the diagnostic groups. To assess associations between baseline CSF biomarker levels and whole-brain atrophy rate, we first calculated Pearson's correlations across the whole group. We then used linear regression analyses with baseline CSF biomarkers as independent variables, and whole-brain atrophy rate as dependent variable. We used three models, one for each CSF biomarker. Age, sex and diagnosis (using dummy variables) were entered as covariates. To check if associations with CSF biomarker levels differed according to diagnostic group, interaction terms (dummy-diagnosis * CSF biomarker) were included in the model. If there was a significant interaction between diagnosis and CSF biomarker ($p \leq 0.05$), β [SE] are displayed for each diagnostic group separately. When no significant interaction was found, the overall β is reported. Finally, associations between

annualized whole-brain atrophy rate, annualized change in CSF biomarker levels, and annualized change in MMSE score were assessed using bivariate correlations (available for 46 patients).

Results

Demographic and clinical data are presented by patient group in Table 1. MCI patients were older when compared to AD patients. We found no difference in sex or follow-up time. Annualized whole-brain atrophy rate differed between diagnostic groups ($p < 0.001$). We also found group differences for baseline $A\beta_{1-42}$ ($p < 0.001$), tau, and P-tau₁₈₁ (both $p < 0.01$). By contrast, annualized change in CSF c, tau, and P-tau₁₈₁ levels over time did not differ between patient groups (all $p > 0.49$).

To investigate associations between baseline CSF levels of $A\beta_{1-42}$, tau, and P-tau₁₈₁ and whole-brain atrophy rate, we first performed bivariate correlations across the whole sample, as shown in Figure 1. Lower baseline CSF levels of $A\beta_{1-42}$ ($r = 0.36$, $p < 0.001$) and higher tau levels ($r = -0.27$, $p < 0.01$) were associated with a higher whole-brain atrophy rate, while CSF P-tau₁₈₁ levels were not ($r = -0.16$, $p = 0.10$). After adjustment for age, sex, and diagnosis in linear regression analyses we found no association between $A\beta_{1-42}$ and whole-brain atrophy rate (β [SE] 0.34[0.26], $p = 0.19$). The interaction terms for CSF biomarker and diagnosis were significant for tau ($p = 0.02$) and P-tau₁₈₁ ($p = 0.02$), implying that associations of these CSF biomarkers and whole-brain atrophy rate were different for the diagnostic groups. In the control group there was a trend for increased tau to be associated with a higher whole-brain atrophy rate (β [SE] -0.62 [0.32], $p = 0.06$), however after exclusion of the two patients who progressed to AD the effect disappeared. Furthermore, this effect was not observed in MCI (β [SE] -0.39 [0.33], $p = 0.24$), or AD (β [SE] 0.43 [0.27], $p = 0.11$). By contrast, increased P-tau₁₈₁ levels were associated with a lower whole-brain atrophy rate (β [SE] 0.78 [0.35], $p = 0.03$) in the AD group. The effects in the control group (β [SE] -0.54[0.40], $p = 0.18$) and MCI group (β [SE] -0.52 [0.40], $p = 0.19$), though not significant, were in the opposite direction of that in the AD group.

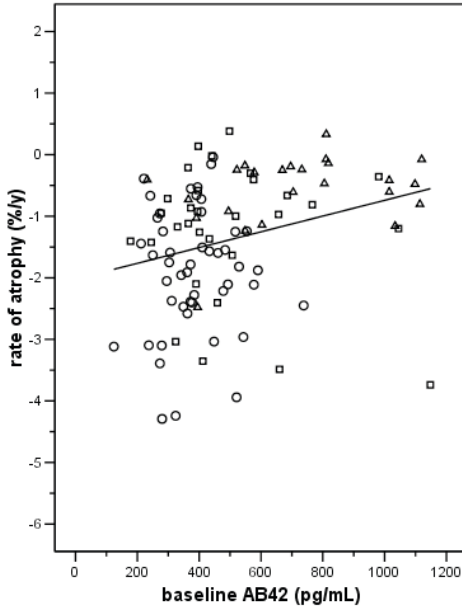
Finally, we studied associations between change in CSF biomarker levels over time, and whole-brain atrophy rate. Across groups, change in $A\beta_{1-42}$ ($r=0.02$, $p=0.90$), tau ($r=0.08$, $p=0.59$), and P-tau₁₈₁ ($r=0.06$, $p=0.68$) levels were not associated with whole-brain atrophy rate. In addition, we assessed longitudinal associations of change in CSF biomarker levels, whole-brain atrophy rate, and change in MMSE score over time. While whole-brain atrophy rate was associated with change in MMSE score ($r=0.43$, $p<0.01$), change in CSF levels of $A\beta_{1-42}$, ($r=0.18$, $p=0.23$), tau ($r=-0.03$, $p=0.83$), and P-tau₁₈₁ ($r=-0.07$, $p=0.96$) were not.

Table 1 Demographic and clinical variables by diagnostic group

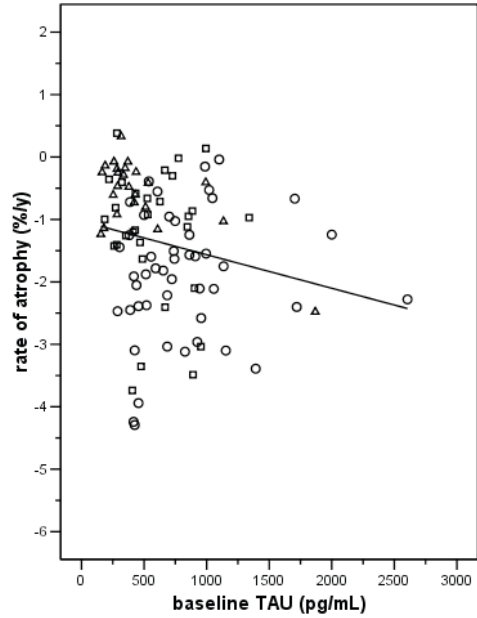
| | Control | MCI | AD |
|---|------------|-------------------------|---------------------------|
| N | 23 | 29 | 47 |
| Age-at-diagnosis (y) | 66 (9) | 71 (6) | 65 (8) ^b |
| Sex (w/m) | 11 / 12 | 15 / 14 | 25 / 22 |
| Baseline MMSE score | 29 (2) | 26 (3) ^a | 22 (5) ^{d,e} |
| Follow-up time (MRI) (y) | 1.9 (1.0) | 1.7 (0.6) | 1.6 (0.5) |
| Time to last diagnosis (y) | 2.2 (0.8) | 1.8 (0.7) | - |
| Diagnosis at follow up | 2 AD | 17 AD | - |
| Baseline $A\beta_{1-42}$ | 696 (249) | 481 (201) ^d | 384 (119) ^d |
| Baseline tau | 457 (390) | 589 (286) | 819 (463) ^c |
| Baseline P-tau₁₈₁ | 64 (34) | 80 (33) | 91 (34) ^c |
| Annualized change in CSF $A\beta_{1-42}$ level+ | 32 (68) | 18 (35) | 35 (32) |
| Annualized change in CSF tau level+ | 25 (43) | 36 (52) | 63 (129) |
| Annualized change in CSF P-tau₁₈₁ level + | 1 (2) | 2 (4) | 0.0 (6) |
| Annualized whole-brain atrophy rate (%/y) | -0.6 (0.6) | -1.1 (1.0) ^a | -1.9 (1.0) ^{b,d} |
| Annualized change in MMSE score | -0.2 (1.1) | -1.5 (2.7) ^a | -2.2 (1.8) ^c |

Data are presented as mean (sd), unless indicated otherwise. Differences between groups were assessed using ANOVA (age and sex as covariates where appropriate, post-hoc Bonferroni correction $p<0.05$). Please note that raw values are shown for CSF biomarkers (pg/mL), while log-transformed variables were used for statistical analysis. MCI=mild cognitive impairment; AD=Alzheimer's disease; FTL=Frontotemporal Lobar Degeneration; MMSE=mini-mental state examination; CSF=Cerebrospinal fluid; $A\beta_{1-42}$ =beta-amyloid₁₋₄₂; P-tau₁₈₁=tau phosphorylated at threonine-181; MRI=Magnetic Resonance Imaging. ^a $p<0.05$ compared to controls; ^b $p<0.05$ compared to MCI; ^c $p<0.01$ compared to controls; ^d $p<0.001$ compared to controls; ^e $p<0.001$ compared to MCI + = longitudinal data available for 48 patients.

A



B



C

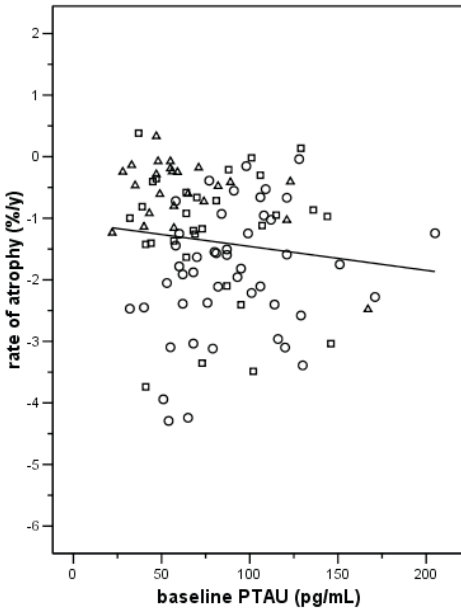


Figure 1. CSF biomarker levels and annualized whole-brain atrophy rates. Scatter plots of baseline CSF biomarker levels versus annualized whole-brain atrophy rate. (A.) Across diagnostic groups baseline $A\beta_{1-42}$ levels and whole-brain atrophy rate were associated ($r=0.36$, $p<0.001$). In diagnostic groups no association was found. (B.) Across diagnostic groups tau levels and whole-brain atrophy rate were associated ($r=-0.27$, $p=0.01$). In the control group there was a trend for increased tau to be associated with a higher whole-brain atrophy rate (β [SE] -0.62 [0.32], $p=0.06$). However, this effect disappeared when the three patients, who progressed to dementia were excluded. (C.) Across diagnostic groups P-tau₁₈₁ levels were not associated ($r=-0.16$, $p=0.10$). By contrast, there was a modest effect of an increased P-tau₁₈₁ level in the AD group (β [SE] 0.78 [0.35], $p=0.03$) being associated with a lower whole-brain atrophy rate.

_ = fit line across groups

Δ = controls; \square = MCI; \circ = AD

Discussion

The major finding of this study is that, notwithstanding modest correlations of baseline CSF biomarker levels and whole-brain atrophy rate across groups, hardly any association within diagnostic groups was found. Whole-brain atrophy rate was associated with clinical progression, measured by change in MMSE score, but longitudinal changes in the CSF biomarker levels were not. Thus, MRI and CSF biomarkers appear to reflect different aspects of AD: whole-brain atrophy rate appears to be linked to the clinical progression of the disease, whereas CSF biomarkers seem to reflect disease state rather than rate of progression.

Both CSF biomarker levels and atrophy on MRI are used in the diagnostic work-up of AD.^{10,36,37} Moreover, both marker types are predictive of dementia in patients with MCI.^{2,8,15,17} Previous studies typically report lowered CSF levels of $A\beta_{1-42}$, and elevated tau and P-tau, and higher rates of whole brain atrophy in MCI and AD.^{1,27} Our study confirms these results, which have been published previously in overlapping samples, derived from the same memory clinic population.^{3,29} Relatively few studies have combined CSF biomarker levels and atrophy measured from MRI, using a cross-sectional design^{2,25,26} or a longitudinal design.^{7,13,35} Of the longitudinal studies, one study described positive correlations between baseline CSF biomarkers and change in MRI measures in a group with a wide variation in cognitive impairment.³⁵ A second study described the relation between increase in tau phosphorylated at threonine-231 (P-tau₂₃₁) and $A\beta_{1-42}$ and decrease in hippocampal volume in seven patients with MCI.⁷ Finally, a study involving 22 AD patients found high baseline CSF levels of P-tau₂₃₁ to be associated with a higher rate of hippocampal atrophy.¹³ In the present study, however, we were not able to confirm these findings despite our larger patient sample.

For tau we found an association across groups with, as expected, higher levels of tau being related to a faster rate of atrophy; however we did not find this association within diagnostic groups. A trend towards higher tau being associated with higher whole-brain atrophy rates within the control group, could be ascribed to a few subjects showing clinical progression, since the effect disappeared after exclusion of three subjects who progressed to dementia. It might be argued that these subjects should not have been

included in the control group. However, because the risk of dementia increases with age, healthy elderly may progress to dementia.³³ Moreover, the cognitive continuum of dementia shows a gradual decline, and boundaries between AD and MCI are somewhat arbitrary.¹² We therefore think by including these progressing patients, we included the whole cognitive spectrum and studied a typical heterogeneous memory clinic population.

In contrast to $A\beta_{1-42}$ and tau, baseline P-tau₁₈₁ was weakly associated with whole-brain atrophy rate within the AD group, but not across groups. When we started this study, we hypothesised that patients with a larger load of senile plaques and neurofibrillary tangles (reflected by CSF biomarker levels), would have a higher rate of neuronal loss, consequently leading to a higher whole-brain atrophy rate. Our study did not confirm this. In fact, we found a modest effect in the opposite direction, with a higher (more abnormal) P-tau₁₈₁ being related to a lower (less abnormal) whole-brain atrophy rate. We are unsure how to interpret this finding. We cannot exclude the possibility that some of our AD patients were misdiagnosed, especially since no post mortem verification of diagnosis was available. However, all patients fulfilled NINDS-ADRDA clinical criteria for probable AD, which was confirmed both at baseline and at follow-up in multidisciplinary consensus meetings. Our findings might suggest the existence of subtypes of AD with differential combinations of levels of p-tau and atrophy rates. These results are comparable to our finding that, while for MCI patients the APOE ϵ 4 genotype is a predictor of faster subsequent progression, we observe the opposite in AD patients, as APOE ϵ 4 positive patients show a slower atrophy rate.²⁸ These results suggest that patients who – despite their favourable APOE ϵ 3 status – still develop AD, have a more aggressive form of the disease. Likewise, it seems that those who show clinical AD in spite of relatively low levels of p-tau, are likely to have slightly higher atrophy rates.

Post mortem studies have shown considerable overlap in the neuropathological features associated with AD, regardless of whether or not dementia was actually present during life.²⁰ This implies that other factors than senile plaques and neurofibrillary tangles must be involved in the development of the clinical syndrome of dementia. Indeed, it has been reported that brain volume

by itself is a good predictor of dementia, independent of senile plaque and neurofibrillary tangle load.²⁰ Our results are in line with these neuropathological findings, since we hardly found any association of whole-brain atrophy rates and CSF biomarker levels. This could imply that brain volume loss *in vivo*, measured with MRI, and CSF biomarker levels, which are thought to represent senile plaque and neurofibrillary tangle load, reflect different aspects of AD.

Among the strengths of this study is that we investigated the association of two widely used markers (CSF and MRI) in a large cohort of MCI, AD patients and controls derived from a memory clinic, in a prospective longitudinal fashion. For every patient, baseline CSF and longitudinal MRI were available. Follow up CSF data were available for a large subgroup. A limitation of this study may be that we used MRI scans that were obtained on a 1T scanner. We feel however that T1 scans have sufficient contrast of parenchyma-CSF, while the gain of scans obtained at a higher field strength largely lies in increased gray-white matter contrast. As we assessed the whole-brain, rather than gray and white matter separately, we feel that our scans had sufficient quality. In addition, it could be argued that hippocampal atrophy is a more specific marker for AD than whole-brain atrophy rate²⁴, which is increased in a number of different diseases that cause dementia.^{6,22} However, senile plaques and neurofibrillary tangles accumulate throughout the brain, and are not exclusively found in the medial temporal lobe.⁵ Our control group that included patients with subjective complaints may limit the generalisability of the results, since patients with subjective complaints are known to have an increased risk of progression to dementia.³⁴ However, the present study did not focus on differences between groups, but rather, on associations between two different types of biomarkers. We deliberately included the entire cognitive spectrum, and showed that – across the entire cognitive spectrum, MRI atrophy rate and CSF biomarkers were modestly correlated. Within diagnostic groups however, there was hardly any relationship. When healthy controls only would have been included, these results would be unaltered. Another possible limitation is our relatively high number of converters. All patients were assessed in a standardized way and diagnosed according to the criteria of Petersen.²³ Compared to the conversion rate of 12% per year reported by Petersen et al, the conversion rate of 59% over a period of almost two years in our group of MCI patients seems rather high.

However, our results are comparable to the conversion rate of other memory clinics¹⁴, while the conversion rate reported by Petersen et al was found in a general community setting.

In contrast to whole-brain atrophy rates which were associated with change in MMSE score over time, longitudinal changes in CSF biomarker levels were not. These results suggest that for tracking the rate of progression of AD, whole-brain atrophy rates are more useful than CSF levels of $A\beta_{1-42}$, tau, and P-tau₁₈₁; by contrast these CSF markers can be considered to be disease state markers, which may be more sensitive as diagnostic tools, possibly in earlier stages of AD.

Reference list

1. Blennow K, Hampel H. - CSF markers for incipient Alzheimer's disease. - *Lancet Neurol* 2003 Oct;2(10):605-13.
2. Bouwman FH, Schoonenboom SNM, van Der Flier WM, Van Elk EJ, Kok A, Barkhof F, Blankenstein MA, Scheltens P. CSF biomarkers and medial temporal lobe atrophy predict dementia in mild cognitive impairment. *Neurobiol Aging* 2007; 28: 1070-1074.
3. Bouwman FH, van Der Flier WM, Schoonenboom NS, Van Elk EJ, Kok A, Rijmen F, Blankenstein MA, Scheltens P. Longitudinal changes of CSF biomarkers in memory clinic patients. - *Neurology* 2007 Sep 4;69(10):1006-11 2007.
4. Bouwman FH, van Der Flier WM, Schoonenboom NS, Van Elk EJ, Kok A, Scheltens P, Blankenstein MA. - Usefulness of longitudinal measurements of beta-amyloid₁₋₄₂ in cerebrospinal fluid of patients with various cognitive and neurologic disorders. - *Clin Chem* 2006 Aug;52(8):1604-6.
5. Braak H, Braak E. - Neuropathological staging of Alzheimer-related changes. - *Acta Neuropathol (Berl)* 1991;82(4):239-59.
6. Chan D, Fox NC, Jenkins R, Scahill RI, Crum WR, Rossor MN. - Rates of global and regional cerebral atrophy in AD and frontotemporal dementia. - *Neurology* 2001 Nov 27;57(10):1756-63.
7. de Leon MJ, DeSanti S, Zinkowski R, Mehta PD, Pratico D, Segal S, Rusinek H, Li J, Tsui W, Saint Louis LA, Clark CM, Tarshish C, Li Y, Lair L, Javier E, Rich K, Lesbre P, Mosconi L, Reisberg B, Sadowski M, DeBernadis JF, Kerkman DJ, Hampel H, Wahlund LO, Davies P. - Longitudinal CSF and MRI biomarkers improve the diagnosis of mild cognitive impairment. - *Neurobiol Aging* 2006 Mar;27(3):394-401 Epub 2005 Aug 26.
8. Erten-Lyons D, Howieson D, Moore MM, Quinn J, Sexton G, Silbert L, Kaye J. - Brain volume loss in MCI predicts dementia. - *Neurology* 2006 Jan 24;66(2):233-5.
9. Folstein MF, Folstein SE, Mchugh PR. - "Mini-mental state". A practical method for grading the cognitive state of patients for the clinician. - *J Psychiatr Res* 1975 Nov;12(3):189-98.
10. Fox NC, Black RS, Gilman S, Rossor MN, Griffith SG, Jenkins L, Koller M. Effects of A beta immunization (AN1792) on MRI measures of cerebral volume in Alzheimer disease. *Neurology* 2005; 64: 1563-1572.
11. Fox NC, Scahill RI, Crum WR, Rossor MN. - Correlation between rates of brain atrophy and cognitive decline in AD. - *Neurology* 1999 May 12;52(8):1687-9.
12. Gauthier S, Reisberg B, Zaudig M, Petersen RC, Ritchie K, Broich K, Belleville S, Brodaty H, Bennett D, Chertkow H, Cummings JL, de LM, Feldman H, Ganguli M, Hampel H,

- Scheltens P, Tierney MC, Whitehouse P, Winblad B. - Mild cognitive impairment. - Lancet 2006 Apr 15;367(9518):1262-70.
13. Hampel H, Burger K, Pruessner JC, Zinkowski R, DeBernardis J, Kerkman D, Leinsinger G, Evans AC, Davies P, Moller HJ, Teipel SJ. - Correlation of cerebrospinal fluid levels of tau protein phosphorylated at threonine 231 with rates of hippocampal atrophy in Alzheimer disease. - Arch Neurol 2005 May;62(5):770-3.
14. Hampel H, Teipel SJ, Fuchsberger T, Andreasen N, Wiltfang J, Otto M, Shen Y, Dodel R, Du Y, Farlow M, Moller HJ, Blennow K, Buerger K. Value of CSF beta-amyloid₁₋₄₂ and tau as predictors of Alzheimer's disease in patients with mild cognitive impairment. Mol Psychiatry 2004; 9: 705-710.
15. Hansson O, Zetterberg H, Buchhave P, Londos E, Blennow K, Minthon L. - Association between CSF biomarkers and incipient Alzheimer's disease in patients with mild cognitive impairment: a follow-up study. - Lancet Neurol 2006 Mar;5(3):228-34.
16. Hartley SW, Scher AI, Korf ESC, White LR, Launer LJ. Analysis and validation of automated skull stripping tools: A validation study based on 296 MR images from the Honolulu Asia aging study. Neuroimage 2006; 30: 1179-1186.
17. Herukka SK, Helisalmi S, Hallikainen M, Tervo S, Soininen H, Pirttila T. - CSF Abeta42, Tau and phosphorylated Tau, APOE epsilon4 allele and MCI type in progressive MCI. - Neurobiol Aging 2007 Apr;28(4):507-14 Epub 2006 Mar 20.
18. Jack CR, Shiung MM, Gunter JL, O'Brien PC, Weigand SD, Knopman DS, Boeve BF, Ivnik RJ, Smith GE, Cha RH, Tangalos EG, Petersen RC. Comparison of different MRI brain atrophy, rate measures with clinical disease progression in AD. Neurology 2004; 62: 591-600.
19. McKhann G, Drachman D, Folstein M, Katzman R, Price D, Stadlan EM. - Clinical diagnosis of Alzheimer's disease: report of the NINCDS-ADRDA Work Group under the auspices of Department of Health and Human Services Task Force on Alzheimer's Disease. - Neurology 1984 Jul;34(7):939-44.
20. MRC CFAS. Pathological correlates of late-onset dementia in a multicentre, community-based population in England and Wales. Neuropathology Group of the Medical Research Council Cognitive Function and Ageing Study (MRC CFAS). - Lancet 2001 Jan 20;357(9251):169-75 2001.
21. Neary D, Snowden JS, Gustafson L, Passant U, Stuss D, Black S, Freedman M, Kertesz A, Robert PH, Albert M, Boone K, Miller BL, Cummings J, Benson DF. - Frontotemporal

- lobar degeneration: a consensus on clinical diagnostic criteria. - *Neurology* 1998 Dec;51(6):1546-54.
22. O'Brien JT, Paling S, Barber R, Williams ED, Ballard C, McKeith IG, Gholkar A, Crum WR, Rossor MN, Fox NC. - Progressive brain atrophy on serial MRI in dementia with Lewy bodies, AD, and vascular dementia. - *Neurology* 2001 May 22;56(10):1386-8.
23. Petersen RC, Stevens JC, Ganguli M, Tangalos EG, Cummings JL, DeKosky ST. - Practice parameter: early detection of dementia: mild cognitive impairment (an evidence-based review). Report of the Quality Standards Subcommittee of the American Academy of Neurology. - *Neurology* 2001 May 8;56(9):1133-42.
24. Ridha BH, Barnes J, Bartlett JW, Godbolt A, Pepple T, Rossor MN, Fox NC. Tracking atrophy progression in familial Alzheimer's disease: a serial MRI study. *Lancet Neurology* 2006; 5: 828-834.
25. Schonknecht P, Pantel J, Hartmann T, Werle E, Volkmann M, Essig M, Amann M, Zanabali N, Bardenheuer H, Hunt A, Schroder J. - Cerebrospinal fluid tau levels in Alzheimer's disease are elevated when compared with vascular dementia but do not correlate with measures of cerebral atrophy. - *Psychiatry Res* 2003 Oct 15;120(3):231-8.
26. Schoonenboom NS, van Der Flier WM, Blankenstein MA, Bouwman FH, Van Kamp GJ, Barkhof F, Scheltens P. - CSF and MRI markers independently contribute to the diagnosis of Alzheimer's disease. - *Neurobiol Aging* 2007 Jan 4.
27. Silbert LC, Quinn JF, Moore MM, Corbridge E, Ball MJ, Murdoch G, Sexton G, Kaye JA. - Changes in premorbid brain volume predict Alzheimer's disease pathology. - *Neurology* 2003 Aug 26;61(4):487-92.
28. Sluimer JD, Vrenken H, Blankenstein MA, Fox NC, Scheltens P, Barkhof F, van der Flier WM. Whole-brain atrophy rate in Alzheimer disease: Identifying fast progressors. *Neurology* 2008.
29. Sluimer JD, van Der Flier WM, Karas G, Fox N, Scheltens P, Barkhof F, Vrenken H. Whole-brain atrophy rate and cognitive decline: a longitudinal MRI study of memory clinic patients. In: 2007.
30. Smith SM, Jenkinson M, Woolrich MW, Beckmann CF, Behrens TE, Johansen-Berg H, Bannister PR, De LM, Drobnjak I, Flitney DE, Niazy RK, Saunders J, Vickers J, Zhang Y, De SN, Brady JM, Matthews PM. - Advances in functional and structural MR image analysis and implementation as FSL. - *Neuroimage* 2004;23 Suppl 1:S208-19.
31. Smith SM, Zhang Y, Jenkinson M, Chen J, Matthews PM, Federico A, De SN. - Accurate, robust, and automated longitudinal and cross-sectional brain change analysis. - *Neuroimage* 2002 Sep;17(1):479-89.
32. van Straaten EC, Scheltens P, Knol DL, van Buchem MA, van Dijk EJ, Hofman PA, Karas G, Kjartansson O, de Leeuw FE, Prins

- ND, Schmidt R, Visser MC, Weinstein HC, Barkhof F. - Operational definitions for the NINDS-AIREN criteria for vascular dementia: an interobserver study. - Stroke 2003 Aug;34(8):1907-12 Epub 2003 Jul 10.
33. Visser PJ, Kester A, Jolles J, Verhey F. - Ten-year risk of dementia in subjects with mild cognitive impairment. - Neurology 2006 Oct 10;67(7):1201-7.
34. Visser PJ, Kester A, Jolles J, Verhey F. - Ten-year risk of dementia in subjects with mild cognitive impairment. - Neurology 2006 Oct 10;67(7):1201-7.
35. Wahlund LO, Blennow K. - Cerebrospinal fluid biomarkers for disease stage and intensity in cognitively impaired patients. - Neurosci Lett 2003 Mar 20;339(2):99-102.
36. Waldemar G, Dubois B, Emre M, Georges J, McKeith IG, Rossor M, Scheltens P, Tariska P, Winblad B. - Recommendations for the diagnosis and management of Alzheimer's disease and other disorders associated with dementia: EFNS guideline. - Eur J Neurol 2007 Jan;14(1):e1-26.
37. Wiltfang J, Lewczuk P, Riederer P, Grunblatt E, Hock C, Scheltens P, Hampel H, Vanderstichele H, Iqbal K, Galasko D, Lannfelt L, Otto M, Esselmann H, Henkel AW, Kornhuber J, Blennow K. - Consensus paper of the WFSBP Task Force on Biological Markers of Dementia: the role of CSF and blood analysis in the early and differential diagnosis of dementia. - World J Biol Psychiatry 2005;6(2):69-84.

Chapter 8

**General Discussion, Summary &
Future perspectives**

General Discussion, Summary & Future perspectives

The general objective of this thesis was to expand insights in the use of longitudinal whole-brain and regional MR imaging in the early detection, diagnosis and prognosis of AD. Furthermore, it explored the association of these atrophy markers with clinical, genetic and cerebrospinal fluid biomarkers, aiming to develop a better understanding of the course of the disease. In this thesis, we showed that the clinical role of longitudinal neuroimaging extends beyond diagnosis, and can play an important part in prognosis as well. In the present chapter, the main findings of the thesis are summarized, followed by a discussion of the disease pathology, methodology, and implications of these findings for research and clinical practice. Finally, recommendations for future research are given.

Summary of findings

In chapter 2 we used VBM to find out whether structural differences on MR imaging offer insight in the development of clinical AD in patients with amnesic MCI at 3-year follow-up. By studying the converting versus the non-converting MCI population, we found atrophy beyond the medial temporal lobe to be characteristic of patients with MCI prone to progress to dementia. Atrophy of several gray matter structures, including the left lateral temporal lobe and left parietal cortex independently predicted conversion.

In chapter 3, we prospectively determined baseline brain volume and whole-brain atrophy rate, using SIENAX and SIENA respectively. We assessed their association with cognitive decline, and also investigated the risk of progression to dementia in initially non-demented patients, based on whole-brain volume at baseline and whole-brain atrophy rate. We showed that whole-brain atrophy rate discriminates between controls, patients with subjective complaints, MCI and AD, better than cross-sectional brain volume does. Furthermore, whole-brain atrophy rate was strongly associated with the rate of cognitive decline. In non-demented participants, a high whole-brain atrophy rate (fast volume loss) was associated with an increased risk of progression to dementia. The

association with cognitive decline indicates that rate of atrophy could be valuable as a measure for tracking disease progression. Moreover, whole-brain atrophy rates might be used to predict conversion to dementia.

In chapter 4, we used Fluid, a robust and accurate non-linear registration algorithm, to estimate regional atrophy rates. Our objective was to track the regional lobar atrophy pattern in the progression from normal aging to AD. We observed that atrophy spreads through the brain with development of AD: MCI is marked by temporal lobe atrophy. In AD, the medial temporal lobe atrophy rate remains comparable to MCI, whilst the other parts of the temporal lobe demonstrate an even higher atrophy rate. Moreover, atrophy also accelerates in parietal, frontal, insular and occipital lobes when patients reach the AD stage. Finally, we showed that in non-demented elderly, the rate of medial temporal lobe atrophy was most predictive of progression to AD, demonstrating the importance of this region in the early detection of AD.

In chapter 5, we looked into the added value of hippocampal atrophy rates over whole brain atrophy measurements. We examined the applicability of different types of measurements hippocampal and whole-brain atrophy by comparing their ability to distinguish between controls, MCI and AD, and their ability to predict progression to AD within controls and MCI. Finally, we compared cross-sectional and longitudinal measurement of the hippocampus and whole brain. We demonstrated that hippocampal measures, especially hippocampal atrophy rate, best discriminate MCI from controls. Whole brain atrophy rate discriminates AD from MCI. Hippocampal atrophy is the strongest predictor of progression to AD. We conclude that hippocampal atrophy rates have added value of over whole brain volume measurements in the early diagnosis of AD.

In chapter 6, we evaluated which baseline clinical and MRI measures influence rate of progression within AD, using whole-brain atrophy rates measured from serial MR imaging, derived with SIENA as outcome measure. Our results suggest it is possible to characterise a subgroup of AD patients that are at risk of faster loss of brain volume. Patients with more generalized atrophy, rather than focal hippocampal atrophy, with an onset of disease before the age of 65, and who are APOE ϵ 4 negative, seem to be at risk of faster whole-brain

atrophy rates than the more commonly seen AD patients, who are generally older, APOE ϵ 4 positive and mainly have pronounced hippocampal atrophy. This implies there are different phenotypes within AD.

In chapter 7 we investigated associations between cross-sectional and longitudinal CSF biomarker levels and MRI-based whole-brain atrophy rate in MCI and AD. We found that across groups, baseline $A\beta_{1-42}$ and tau were modestly associated with whole-brain atrophy rate. Adjusted for age, sex and diagnosis, we found no association between $A\beta_{1-42}$ or tau, and whole-brain atrophy rate. By contrast, high CSF levels of P-tau₁₈₁ showed a mild association with a lower whole-brain atrophy rate in AD but not in controls or MCI patients. Finally, whole-brain atrophy rate was associated with change in MMSE, but change in CSF biomarker levels was not. We concluded that whole-brain atrophy rate and CSF levels of $A\beta_{1-42}$, tau or P-tau₁₈₁ provide complementary information in patients with MCI and AD.

General discussion & Conclusions

Disease pathology

Neuropathological studies report that AD pathology spreads through the brain in a predictable fashion.¹ For neurofibrillary tangles the accumulation can be described in six stages: Stages I-II show alterations in the transentorhinal regions, stages III-IV are known as the limbic stage, while stage V-VI are marked by isocortical destruction. The accumulation of amyloid deposits can be divided in three stages: Stage A shows initial deposits in the basal portions of the isocortex, stage B shows amyloid in virtually all isocortical association areas, but the hippocampal formation is only mildly involved, while in stage C end-stage deposits can be observed throughout the isocortex. However, by definition, autopsy studies are post hoc and cross-sectional in design. Even though they are essential in uncovering the biological basis of clinical AD, they clearly cannot provide clinical-histological correlations in the individual during life.

This thesis shows that atrophy rates accelerate throughout the brain with the progression of cognitive decline, as observed *in vivo* using serial MRI. In controls, only a mild acceleration of medial temporal lobe atrophy is seen, in

concurrence with previous studies,^{2,4} which is thought to be associated with normal ageing.⁵ In MCI, the temporal lobe shows the greatest atrophy rate, but atrophy already extends beyond the medial temporal lobe, as atrophy rates in the remaining part of the temporal lobe are equally high. Atrophy rates in the medial temporal lobe were no higher in the AD patients than in the MCI patients, implying that rate of neurodegeneration in this region may already be at a maximum prior to the clinical diagnosis of AD. The progression to AD is characterised by increasing atrophy rates in the rest of the temporal lobe, and atrophy also accelerating in parietal, frontal and occipital lobes. This entails that neocortical involvement is an important characteristic of progression from MCI to clinical AD.^{6,7} We conclude that the pattern of regional atrophy rates changes with the development of neurodegenerative disease. In addition, we show that the regional atrophy pattern closely follows the pattern of accumulating neurofibrillary tangles as described by Braak.¹

Methodology

Cohort

We strived to create a cohort that included the whole cognitive spectrum. We included a relatively large number of subjects from one center where all subjects have been carefully defined using a standardized diagnostic battery. As a consequence, subjects are characterized in a uniform manner and the diagnosis was determined by a multidisciplinary team. Besides patients with AD and MCI, we included both patients with subjective complaints and volunteers without complaints. At baseline, we found no differences between healthy volunteers and patients with subjective complaints, and we therefore pooled these subjects in one control group. However, patients presenting at a memory clinic with subjective complaints are known to have a higher risk of developing AD.⁸⁻¹⁰ In fact, during follow-up three patients converted to AD and one to FTLD. One could argue that these patients should have been excluded, as they did not remain control-like throughout the study. However, we feel that, since they fulfilled initial inclusion criteria, excluding these patients would have biased the results. Nevertheless, their influence on the overall results is limited and exclusion of these patients had no major effects.

Computational analyses

In this thesis we analyzed 3D volumes acquired using MR imaging with three different neurocomputational analyses. Firstly, we used VBM,¹¹ which uses a moderate non-linear registration, and is driven by both voxel-intensity and anatomical probability maps. Statistical analysis entails a voxel-wise comparison between or within groups, and if desired, differences in volume can be quantified within defined standardized brain regions. An advantage of VBM is the unbiased way in which atrophy throughout the brain is assessed throughout the brain. The main disadvantage of VBM as applied in this thesis is the cross-sectional nature of the analysis, which suffers from inter-individual variety in brain structure and ageing. Nowadays, the application of longitudinal VBM has become available. Secondly, we acquired whole brain volumes and atrophy rates with SIENA(X),¹² a volumetric analysis that uses a linear registration, which can be performed cross-sectional as well as longitudinal. An advantage is the low calculation time. A disadvantage is the fact that only whole-brain atrophy measures were available. Nevertheless, it can be used to distinguish patients on a group level. Thirdly, we used Fluid,¹³ a robust non-linear registration algorithm driven by voxel-intensity, developed at the Dementia Research Centre (University College London). A disadvantage of this technique is the long calculation time. We have overcome this problem by using a powerful network of parallel computers for analyses (Virtual Laboratory for e-Science; www.vl-e.nl). Clear advantages of this technique are the robust nature and the detailed information generated about regional atrophy in the individual, which makes it possible to accurately track the pattern of atrophy throughout the course of the disease.^{9,10}

Implications for Clinical practice and Research

At present the diagnosis of AD is made according to clinical criteria, in these guidelines neuroimaging is mainly used to exclude non-neurodegenerative pathology.¹⁴ Currently in clinical practice cross-sectional neuroimaging -amongst clinical, neuropsychological and other biomarkers- is used more often to establish a diagnosis, by gathering positive evidence to support the diagnosis.^{10,15} Nevertheless, diagnostic accuracy leaves room for improvement, as there is substantial overlap between groups.¹⁶ In this thesis we use two approaches to improve the diagnostic accuracy. Firstly, it is known that

cross-sectional imaging suffers the confounding influence of inter-individual variability in brain structure and ageing. Longitudinal imaging offers a means to overcome this problem. Secondly, more sensitive methods can be used to analyze the data. We demonstrate that longitudinal MRI measures are more sensitive than cross-sectional volumes, as atrophy rates were able to separate AD from MCI, and MCI from controls. The clinical relevance of longitudinal atrophy rates is further demonstrated by the association with cognition and cognitive decline. Moreover, since individuals with a higher whole-brain and regional atrophy rate had greater risks of progression to dementia, repeat MR imaging can be helpful in the diagnostic work-up of patients suspected of having dementia. Within subjects without dementia, regional hippocampal measures were the strongest predictors of progression to AD, but whole brain and regional atrophy rates had an additional independent predictive effect. In this thesis we confirm the early involvement of the medial temporal lobe, as observed in neuropathological and clinical studies,^{17,18} and its clinical importance in the detection of incipient AD.¹⁹ Furthermore, we show that neocortical involvement is an important characteristic of progression from MCI to clinical AD.^{6,19}

Moreover, there is need for prognostic factors, and biomarkers that can accurately track disease progression. We show that longitudinal MRI might be used in clinical practice to give an accurate prognosis, and can track disease progression, as it is strongly associated with cognitive decline. In research, longitudinal neuroimaging can play an important role in more effective patient selection for trials. In addition, atrophy rates can provide valuable objective information about disease progression. The effect of newly developed therapies can be monitored, according to changes in the brain tissue loss. This is particularly important considering that disease-modifying therapies, early detection and monitoring of progression are main research goals in AD.

Fast progressors: a specific subgroup

Clinically, different phenotypes of AD have been described.²⁰ We show that a younger age, absence of APOE ϵ 4 and a low MMSE at baseline were associated with higher whole-brain atrophy rate, as measured using serial MR imaging. Furthermore, a relatively spared baseline hippocampus predicted faster decline for AD patients with a smaller baseline brain volume and a lower MMSE score.

Moreover, a smaller brain volume was associated with a higher rate of whole brain atrophy in patients with a relatively younger age. It has been suggested that AD patients with an onset before the age of 65, who are APOE ϵ 4 negative often have a distinct clinical profile, with prominent parietal dysfunction.²¹ It is tempting to think that these patients have early biparietal and more generalized atrophy, rather than focal medial temporal lobe atrophy. Our data suggest that these patients may be at risk of faster global disease progression than the more commonly seen sporadic AD patients, who are older, APOE ϵ 4 positive and have pronounced hippocampal atrophy.

Association of MRI en CSF biomarkers

Furthermore, in this thesis the association between MRI and CSF biomarkers was studied. Notwithstanding modest correlations of baseline CSF biomarker levels and whole-brain atrophy rate across groups, hardly any association within diagnostic groups was found. Whole-brain atrophy rate was associated with clinical progression, but longitudinal changes in the CSF biomarker levels were not. Thus, MRI and CSF biomarkers appear to reflect different aspects of AD: whole-brain atrophy rate appears to be linked to the clinical progression of the disease, whereas CSF biomarkers seem to reflect disease state rather than rate of progression.⁹ We conclude that for tracking the rate of progression of AD, atrophy rates are more useful than CSF levels of $A\beta_{1-42}$, tau, and P-tau₁₈₁; by contrast these CSF markers can be considered to be disease state markers, which may be more sensitive as diagnostic tools, possibly in earlier stages of AD.

Future recommendations

Important goals in future neurodegenerative research are to improve the methods to detect incipient AD, to monitor disease progression, and unravel underlying neuropathological changes. To achieve this, firstly larger cohorts are needed to increase power and sensitivity. This can be achieved by either large multicentre and / or population studies. Uniform data should be collected, including at least clinical and neuropsychological data, and serial MR imaging. Preferably, CSF biomarkers and PET imaging could be obtained as well. Secondly, patients could undergo multiple consecutive MR examinations to gain more insight in the development of brain tissue loss in the individual

in *vivo*. MR examinations ought to be collected with constant intervals, using identical protocols, throughout the disease. Protocols should at least contain 3D volumes. This protocol could be expanded with Diffusion Weighted Imaging, which gives information about the white matter tracts, functional MRI, which can be used to measure functional connectivity of brain networks, and ASL (arterial spin labeling), a non-invasive MRI technique for the quantification of cerebral perfusion. Thirdly, analysis methods could be optimized to detect pathology as accurately as possible. Non-linear registration seems to perform best; data should be analyzed regionally, as it is able to more accurately distinguish patients. Furthermore, this adds to the understanding of the pattern of atrophy throughout the disease. Depending on the goal research should focus on the medial temporal lobe and/or key neocortical regions. Fourthly, for the detection of early AD research should center on patients with subjective complaints, as patients and their relatives are still the most sensitive in detecting their cognitive decline, especially at the earliest stages. Finally, post-mortem verification should be obtained, as it still is the gold standard, even if it is by definition post-hoc. Perhaps by combining different techniques which can be applied in *vivo*, a new gold standard can be developed.

In conclusion, this thesis expands insights in the use of longitudinal imaging in the early detection of incipient AD, and nosological diagnosis. We showed that the clinical role of neuroimaging extends beyond diagnosis, and can play an important part in prognosis as well. The association of atrophy markers with clinical, genetic and cerebrospinal fluid biomarkers was studied, aiming to develop a better understanding of the course of the disease. In research, longitudinal imaging can help to select patients eligible for specific treatment, and monitor the effect for disease modifying therapy. The combination of neuroimaging markers with other biomarkers will play an important role in future research and clinical practice, in establishing an accurate early diagnosis and prognosis.

Reference list

1. Braak H, Braak E. Neuropathological staging of Alzheimer-related changes. - *Acta Neuropathol (Berl)*. 1991;82(4):239-59.
2. Tapiola T et al. MRI of hippocampus and entorhinal cortex in mild cognitive impairment: A follow-up study. - *Neurobiol Aging*. 2006 Nov 9;.
3. van de Pol LA et al. Hippocampal atrophy in Alzheimer disease: Age matters. *Neurology* 66, 236-238.
4. Barnes J et al. Measurements of the amygdala and hippocampus in pathologically confirmed Alzheimer disease and frontotemporal lobar degeneration. *Arch. Neurol*. 63, 1434-1439.
5. Fjell AM et al. - CSF biomarker pathology correlates with a medial temporo-parietal network affected by very mild to moderate Alzheimer's disease but not a fronto-striatal network affected by healthy aging. - *Neuroimage*. 2010 Jan 15;49(2):1820-30.
6. Desikan RS et al. - MRI measures of temporoparietal regions show differential rates of atrophy during prodromal AD. - *Neurology*. 2008 Sep 9;71(11):819-25.
7. Fennema-Notestine C et al. - Structural MRI biomarkers for preclinical and mild Alzheimer's disease. - *Hum Brain Mapp*. 2009 Oct;30(10):3238-53.
8. Visser PJ, Kester A, Jolles J, Verhey F, Ten-year risk of dementia in subjects with mild cognitive impairment. - *Neurology*. 2006 Oct 10;67(7):1201-7.
9. Jack CR Jr et al. Hypothetical model of dynamic biomarkers of the Alzheimer's pathological cascade. - *Lancet Neurol*. 2010 Jan;9(1):119-28.
10. Frisoni GB, Fox NC, Jack CR Jr, Scheltens P, Thompson PM. The clinical use of structural MRI in Alzheimer disease. - *Nat Rev Neurol*. 2010 Feb;6(2):67-77.
11. Karas GB et al. A comprehensive study of gray matter loss in patients with Alzheimer's disease using optimized voxel-based morphometry. - *Neuroimage*. 2003 Apr;18(4):895-907.
12. Smith SM et al. Accurate, robust, and automated longitudinal and cross-sectional brain change analysis. - *Neuroimage*. 2002 Sep;17(1):479-89.
13. Fox NC et al. Imaging of onset and progression of Alzheimer's disease with voxel-compression mapping of serial magnetic resonance images. - *Lancet*. 2001 Jul 21;358(9277):201-5.
14. McKhann G et al. Clinical diagnosis of Alzheimer's disease: report of the NINCDS-ADRDA Work Group under the auspices of Department of Health and Human Services Task Force on Alzheimer's Disease. - *Neurology*. 1984 Jul;34(7):939-44. (1984).

15. Scheltens P, Fox N, Barkhof F, De CC
Structural magnetic resonance imaging
in the practical assessment of dementia:
beyond exclusion. - *Lancet Neurol*. 2002
May;1(1):13-21.
16. Jack CR et al. Comparison of different MRI
brain atrophy, rate measures with clinical
disease progression in AD. *Neurology* 62,
591-600.
17. Jack CR et al. Brain atrophy rates predict
subsequent clinical conversion in normal
elderly and amnesic MCI. *Neurology* 65,
1227-1231.
18. MRC CFAS Pathological correlates of
late-onset dementia in a multicentre,
community-based population in England
and Wales. Neuropathology Group of
the Medical Research Council Cognitive
Function and Ageing Study (MRC CFAS). -
Lancet. 2001 Jan 20;357(9251):169-75.
19. Risacher, S. L. et al. - Baseline MRI
predictors of conversion from MCI to
probable AD in the ADNI cohort. - *Curr
Alzheimer Res*. 2009 Aug;6(4):347-61.
20. Galton, C. J., Patterson, K., Xuereb, J.
H. & Hodges, J. R. - Atypical and typical
presentations of Alzheimer's disease: a
clinical, neuropsychological, neuroimaging
and pathological study of 13 cases. - *Brain*.
2000 Mar;123 Pt 3:484-98.
21. Ross SJ et al. - Progressive biparietal
atrophy: an atypical presentation of
Alzheimer's disease. - *J Neurol Neurosurg
Psychiatry*. 1996 Oct;61(4):388-95.

Nederlandse Samenvatting

Curriculum Vitae

List of Publications

Theses Alzheimercentrum

Dankwoord / Acknowledgements

Nederlandse samenvatting

Het visualiseren van de krimpende hersenen: Longitudinaal MRI onderzoek in het spectrum van cognitieve achteruitgang

Dementie is een groeiend sociaal, maatschappelijk en economisch probleem, als gevolg van een toename van het aantal mensen en de langere levensverwachting. De ziekte van Alzheimer begint jaren voordat de klinische diagnose gesteld kan worden. Neuropathologisch wordt stapeling gezien van eiwitten in de hersenen, de zogenaamde amyloid-beta plaques buiten de cellen en tau-fosfaat kluwen binnen de neuronen. De huidige opvatting is dat deze eiwitstapeling leidt tot schade aan neuronen, de functionele eenheden van de hersenen. Deze neuronen worden geacht zich nauwelijks te kunnen herstellen of vermenigvuldigen. Daarom is het van belang in een zo vroeg mogelijk stadium het neuronenverlies te beperken en de hersenen te beschermen. Er is dus behoefte aan middelen voor vroegdiagnostiek. Er is echter niet één diagnosticum om altijd in vroeg stadium de juiste diagnose te stellen.

Beeldvorming is de laatste jaren een steeds prominentere rol gaan spelen bij de diagnostiek van dementie. Waar het eerst met name gebruikt werd om andere oorzaken van cognitieve stoornissen uit te sluiten, wordt beeldvorming steeds vaker gebruikt om het met dementie samenhangende celverlies (atrofie) aan te tonen. Meestal wordt beeldvorming cross-sectioneel gebruikt -op een tijdstip vergeleken met leeftijdsgenoten-, echter dit heeft zijn beperkingen. Er zijn namelijk grote verschillen in hersenstructuur en de normale veroudering tussen individuen. Longitudinaal onderzoek heeft veel minder last van deze beperkingen.

De doelstelling van dit proefschrift is inzicht te verschaffen in de bruikbaarheid van longitudinale globale en regionale structurele beeldvorming van de hersenen met behulp van MRI (Magnetic Resonance Imaging) bij de vroege detectie, nosologische diagnostiek en prognose van de ziekte van Alzheimer. Bovendien onderzoekt het de wijze waarop deze atrofie markers met klinische,

genetische en hersenvocht biomarkers samenhangen, met als doel het ontwikkelen van een beter begrip van het verloop van de ziekte, en uiteindelijk het verbeteren van de patientzorg.

In hoofdstuk 2 hebben we met voxel-based morphometry uitgezocht of structurele verschillen van de hersenen op MRI bij patienten met amnestische MCI (mild cognitive impairment), inzicht kunnen geven in het ontwikkelen van klinische ziekte van Alzheimer na 3-jaar follow-up. Door het bestuderen van de naar de ziekte van Alzheimer converterende versus de niet-converterende MCI populatie, vonden we dat de atrofie buiten de mediale temporaal kwab het kenmerk is van patienten met MCI, die het risico hebben om op kortere termijn dementie te ontwikkelen. Atofie van structuren als de linker laterale temporaalkwab en linker parietale cortex voorspelden onafhankelijk conversie naar de ziekte van Alzheimer.

In hoofdstuk 3 bepaalden we prospectief het hersenvolume op baseline -bij het begin van het onderzoek- en de snelheid van atrofie van de hersenen -over de tijd gemeten-, met respectievelijk SIENAX en SIENA. Wij hebben het verband met cognitieve achteruitgang onderzocht, en het risico op progressie naar klinische dementie berekend op basis van het hersenvolume op baseline en snelheid van atrofie van de hersenen bij patiënten die bij aanvang van het onderzoek niet dement waren. We toonden aan dat de longitudinaal gemeten snelheid van atrofie beter discrimineert tussen gezonde controles, patiënten met subjectieve klachten, MCI en de ziekte van Alzheimer, dan hersenvolume op één tijdstip. Bovendien was snelheid van atrofie van de hersenen sterk geassocieerd met cognitieve achteruitgang. In op baseline niet-demente deelnemers was een hoge snelheid van atrofie geassocieerd met een verhoogd risico om dementie te ontwikkelen. De correlatie met cognitieve achteruitgang geeft aan dat snelheid van atrofie als marker voor ziekteprogressie kan worden gebruikt. Bovendien kan de atrofie snelheid worden gebruikt om conversie naar klinische dementie te voorspellen.

In hoofdstuk 4 gebruikten we fluid, een niet-lineair registratie algoritme, om robuust en nauwkeurig de regionale atrofie snelheid te berekenen. Onze doelstelling was om het regionale lobaire atrofie patroon vast te leggen in de progressie van normaal veroudering naar de ziekte van Alzheimer. We concluderen op basis van deze gegevens dat atrofie zich volgens een specifiek patroon verspreidt door de hersenen gedurende het ontwikkelen van de ziekte van Alzheimer: MCI wordt gekenmerkt door temporaalkwab atrofie. In de ziekte van Alzheimer blijft de mediale temporaalkwab atrofie vergelijkbaar met MCI, terwijl de atrofie van de extra-mediale temporaalkwab nog verder versnelt. Bovendien versnelt atrofie ook in de pariëtale, frontale, insulaire en occipitale kwabben. Ten slotte bleek dat in niet-demente ouderen, atrofie van de mediale temporaalkwab het meest voorspellend was voor progressie naar de ziekte van Alzheimer, wat wederom het belang van deze regio in de vroegtijdige opsporing van de ziekte van Alzheimer aantoont.

In hoofdstuk 5 keken we naar de toegevoegde waarde van hippocampus atrofie metingen ten opzichte van totale hersenatrofie metingen. Door het onderscheidend vermogen tussen controles, MCI en de ziekte van Alzheimer te vergelijken, onderzochten we de bruikbaarheid van de verschillende soorten metingen van regionale hippocampusatrofie en totale hersenatrofie, en hun vermogen om progressie naar de ziekte van Alzheimer in controles en MCI te voorspellen. Tot slot, vergeleken we de cross-sectionele en longitudinale meting van de hippocampus en de hele hersenen. We toonden aan dat hippocampus atrofie maten, met name snelheid van hippocampus atrofie, het beste discrimineren tussen MCI en controles. Totale hersenatrofie discrimineert de ziekte van Alzheimer van MCI. Regionale hippocampus atrofie maten zijn de sterkste predictoren van progressie naar de ziekte van Alzheimer. We concluderen dat hippocampus atrofie maten meerwaarde hebben boven totaal hersenen volume metingen in de vroegdiagnostiek van de ziekte van Alzheimer.

We evalueerden in hoofdstuk 6 welke klinische en MRI maten op baseline van invloed zijn op progressie in de ziekte van Alzheimer, met als uitkomstmaat snelheid van totale hersenatrofie, berekend van seriële MRI's met SIENA. Onze resultaten suggereren dat er een subgroep van Alzheimer-patiënten

is, die het risico heeft sneller hersenvolume te verliezen. Patiënten met meer gegeneraliseerde in plaats van focale hippocampusatrofie, die vaak een begin hebben vóór de leeftijd van 65, en APOE ϵ 4 negatief zijn, lijken het risico te hebben van een snellere hersenatrofie dan de meer voorkomende Alzheimer-patiënten, die ouder zijn, APOE ϵ 4 positief zijn en uitgesproken hippocampusatrofie hebben. Dit impliceert dat er zijn verschillende fenotypen binnen de ziekte van Alzheimer zijn.

Wij onderzochten in hoofdstuk 7 de samenhang tussen cross-sectionele en longitudinale hersenvocht eiwit spiegels ($A\beta_{1-42}$, tau en P-tau₁₈₁) en op MRI gebaseerde hersenatrofie maten in MCI en de ziekte van Alzheimer. We vonden dat tussen groepen, basis baseline $A\beta_{1-42}$ en tau matig geassocieerd waren met hersenatrofie maten. Gecorrigeerd voor leeftijd, geslacht en diagnose, vonden we geen verband tussen $A\beta_{1-42}$, tau en hersenatrofie snelheid. Daarentegen toonde een hoog P-tau₁₈₁ in de hersenvloeistof een milde associatie met een lagere snelheid van hersenatrofie in de ziekte van Alzheimer, maar niet in controles of MCI patiënten. Tot slot de snelheid van hersenatrofie correleerde met verandering in MMSE, maar verandering in hersenvocht biomarker spiegels niet. Wij concludeerden dat snelheid van hersenatrofie en spiegels van $A\beta_{1-42}$, tau of P-tau₁₈₁ in hersenvocht complementaire informatie bij patiënten met MCI en de ziekte van Alzheimer geven. De snelheid van atrofie is beter te gebruiken voor het vervolgen van de ziekte van Alzheimer, terwijl de eiwitten in hersenvloeistof sensitiever zijn voor het stellen van een vroege diagnose.

Aan de hand van deze bevindingen kan geconcludeerd worden dat longitudinale regionale atrofie maten door hun onderscheidend vermogen, de samenhang met cognitieve achteruitgang, en het hiermee geassocieerde risico op ontwikkelen van de ziekte van Alzheimer in niet-dementen, een belangrijke rol kunnen gaan spelen; zowel in wetenschappelijk onderzoek, bijvoorbeeld bij het selecteren voor, en het vervolgen van het effect bij medicatie trials, als in de klinische praktijk, bij de vroegdiagnostiek en het geven van een accurate prognose.

Curriculum Vitae

Jasper Daniël Sluimer was born on August 10th, 1974 in Vlaardingen, the Netherlands. In 1993 he graduated from the Stedelijk Gymnasium in Schiedam with a β -profile. In his spare time he played basketball, tennis, water polo and did competitive swimming. From 1993 to 2001 he intensely studied medicine, life, and related subjects at the Erasmus University in Rotterdam, where he developed a special interest in Radiology. During his studies, he taught Anatomy to students. Moreover, he was an active member of multiple student societies. During his time as a research assistant at the department of Immunology in 1998, he discovered he did not want to work in a laboratory. After his internship he enjoyed the start of his clinical career as a resident at the department of Neurology at the Sint Franciscus Gasthuis in Rotterdam, in 2002 and 2003. He continued working in the field of Neurology, at the VU University Medical Center, in Amsterdam (of all places). When the opportunity arose, he eagerly decided to become a PhD student at the department of Radiology & the Alzheimer center, in April 2004, resulting in this thesis. Also during that period he worked for the Image Analysis Center on various trials, and did clinical work for the department of Radiology. In October 2007 he started his specialist registrar Radiology training at the VU University Medical Center. In 2008 he studied what it is like to become a patient yourself, when he was diagnosed with diabetes mellitus type I. At the time of writing, he continues his specialist registrar Radiology training at the VU University Medical Center.

List of Publications

Amnesic mild cognitive impairment: structural MR imaging findings predictive of conversion to Alzheimer disease.

Karas G, Sluimer J, Goekoop R, van der Flier W, Rombouts SA, Vrenken H, Scheltens P, Fox N, Barkhof F. *AJNR Am J Neuroradiol*. 2008 May;29(5):944-9.

Whole-brain atrophy rate and cognitive decline: longitudinal MR study of memory clinic patients.

Sluimer JD, van der Flier WM, Karas GB, Fox NC, Scheltens P, Barkhof F, Vrenken H. *Radiology*. 2008 Aug;248(2):590-8.

Whole-brain atrophy rate in Alzheimer disease: identifying fast progressors.

Sluimer JD, Vrenken H, Blankenstein MA, Fox NC, Scheltens P, Barkhof F, van der Flier WM. *Neurology*. 2008 May 6;70(19 Pt 2):1836-41.

Whole-brain atrophy rate and CSF biomarker levels in MCI and AD: A longitudinal study.

Sluimer JD, Bouwman FH, Vrenken H, Blankenstein MA, Barkhof F, van der Flier WM, Scheltens P. *Neurobiol Aging*. 2010 May;31(5):758-64.

Accelerating regional atrophy rates in the progression from normal aging to Alzheimer's disease.

Sluimer JD, van der Flier WM, Karas GB, van Schijndel R, Barnes J, Boyes RG, Cover KS, Olabarriaga SD, Fox NC, Scheltens P, Vrenken H, Barkhof F. *Eur Radiol*. 2009 Dec;19(12):2826-33.

Hippocampal atrophy rates in Alzheimer disease: added value over whole brain volume measures.

Henneman WJ, Sluimer JD, Barnes J, van der Flier WM, Sluimer IC, Fox NC, Scheltens P, Vrenken H, Barkhof F. *Neurology*. 2009 Mar 17;72(11):999-1007.

Prevalence and severity of microbleeds in a memory clinic setting.

Cordonnier C, van der Flier WM, Sluimer JD, Leys D, Barkhof F, Scheltens P. *Neurology*. 2006 May 9;66(9):1356-60.

MRI biomarkers of vascular damage and atrophy predicting mortality in a memory clinic population.

Henneman WJ, Sluimer JD, Cordonnier C, Baak MM, Scheltens P, Barkhof F, van der Flier WM. *Stroke*. 2009 Feb;40(2):492-8.

Incidence of cerebral microbleeds: a longitudinal study in a memory clinic population.

Goos JD, Henneman WJ, Sluimer JD, Vrenken H, Sluimer IC, Barkhof F, Blankenstein MA, Scheltens PH, van der Flier WM. *Neurol*. 2010 Jun 15;74(24):1954-60.

Cognitive and radiological effects of radiotherapy in patients with low-grade glioma: long-term follow-up.

Douw L, Klein M, Fagel SS, van den Heuvel J, Taphoorn MJ, Aaronson NK, Postma TJ, Vandertop WP, Mooij JJ, Boerman RH, Beute GN, Sluimer JD, Slotman BJ, Reijneveld JC, Heimans JJ. *Lancet Neurol*. 2009 Sep;8(9):810-8.

New Research Criteria for the Diagnosis of Alzheimer's Disease Applied in a Memory Clinic Population.

Bouwman FH, Verwey NA, Klein M, Kok A, Blankenstein MA, Sluimer JD, Barkhof F, van der Flier WM, Scheltens P. *Dement Geriatr Cogn Disord*. 2010 Jul 3;30(1):1-7.

Theses Alzheimercentrum

| | |
|---------------------|--|
| L. Gootjes | Dichotic Listening, hemispherical connectivity and dementia (2004) |
| K. van Dijk | Peripheral Nerve Stimulation in Alzheimer's Disease (2005) |
| R. Goekoop | Functional MRI of cholinergic transmission (2006) |
| R. Lazeron | Cognitive aspects in Multiple Sclerosis (2006) |
| N.S.M. Schoonenboom | CSF markers in Dementia (2006) |
| E.S.C. Korf | Medial Temporal Lobe atrophy on MRI: risk factors and predictive value (2006) |
| B. van Harten | Aspects of subcortical vascular ischemic disease (2006) |
| B. Jones | Cingular cortex networks: role in learning and memory and Alzheimer's disease related changes (2007) |
| L. van de Pol | Hippocampal atrophy from aging to dementia: a clinical and radiological perspective (2007) |
| Y.A.L. Pijnenburg | Frontotemporal dementia: towards an earlier diagnosis (2007) |
| A. Bastos Leite | Pathological ageing of the Brain (2007) |
| E.C.W. van Straaten | Vascular dementia (2008) |
| R.L.C. Vogels | Cognitive impairment in heart failure (2008) |
| J. Damoiseaux | The brain at rest (2008) |
| G.B. Karas | Computational neuro-anatomy (2008) |
| F.H. Bouwman | Biomarkers in dementia: longitudinal aspects (2008) |
| A.A. Gouw | Cerebral small vessel disease on MRI: clinical impact and underlying pathology (2009) |
| H. van der Roest | Care needs in dementia and interactive digital information provisioning (2009) |
| C. Mulder | CSF Biomarkers in dementia (2009) |
| W. Henneman | Advances in hippocampal atrophy measurement in dementia: beyond diagnostics (2009) |

Chapter 9

| | |
|------------------|---|
| S.S. Staekenborg | From normal aging to dementia: risk factors and clinical findings in relation to vascular changes on brain MRI (2009) |
| N. Tolboom | Imaging Alzheimer's disease pathology in <i>vivo</i> : towards an early diagnosis (2010) |
| N.A. Verwey | Biochemical markers in dementia: from mice to men. A translational approach (2010) |
| M.I. Kester | Biomarkers for Alzheimer's pathology; Monitoring, predicting and understanding the disease (2011) |

Dankwoord

Een van de eerste zaken die gelezen wordt van een proefschrift is het Dankwoord, waarom zou ik dan juist die pagina's inkorten? Aan mijn promotietraject hebben veel mensen direct of indirect bijgedragen. Speciaal voor hen is hier mijn dankbetuiging, op papier.

Allereerst dank aan alle patiënten en vrijwilligers die een tweetal MRI scans wilden ondergaan.

Graag wil ik mijn promotoren en copromotoren bedanken. Ik ben blij dat ik mocht participeren in een werkomgeving waarin hoogstaande patiëntenzorg en degelijk wetenschappelijk onderzoek is geïntegreerd. Jullie vullen elkaar mooi aan en vormen een goed op elkaar ingespeeld team.

Geachte prof.dr. F. Barkhof, beste Frederik. Je hebt me de kans gegeven te promoveren met cutting-edge technieken in een geweldige sfeer. Gedurende mijn promotie kon ik altijd bij je terecht. Als Radioloog heb je me het belang laten zien van het hebben van klinisch inzicht, als wetenschapper dat je altijd kritisch moet blijven, en als wandelaar en kroegtijger dat je altijd door moet zetten. Het is mooi om te zien hoe het IAC onder jouw handen nog altijd blijft groeien.

Geachte prof.dr. Ph. Scheltens, beste Philip. Bedankt dat je me op het goede pad richting de Radiologie hebt geholpen. De opzet van het Alzheimercentrum is een gouden greep geweest (of is het goud greep) en het is met jou aan kop en dankzij jouw kwaliteiten zo groot geworden. Het MDO was een hoogtepunt van mijn werkweek.

Geachte dr. W.M. van der Flier, beste Wiesje. Je komst bij het Alzheimercentrum was goed merkbaar. Je hebt duidelijke structuur aangebracht en je hebt me veel geleerd. Je stond altijd klaar om te helpen, snel en efficient. Ik waardeer je steun en adviezen zeer.

Geachte dr.ir. H. Vrenken, beste Hugo. Dank je wel voor al je hulp bij het opzetten, verwerken en analyseren van de enorme hoeveelheden data. Goed hoe je het overzicht wist te behouden. Als we weer uren achter elkaar algoritmes moesten aanpassen bleef je rustig, zelfs als een pagina's lang script weer op één haakje te veel of komma te weinig vastliep.

Secondly, I would like to thank the members of the reading committee, Prof.dr. N.C. Fox, Prof.dr. W. Niessen, Prof.dr. ir. S.A.R.B. Rombouts, Dr. M.P. Wattjes, Dr. J. de Munck en Dr. Y.A.L. Pynenburg, for the thorough reading of my thesis and your willingness to participate in the reading committee.

Dear Nick. Thank you for letting me use the algorithms developed at the DRC. You are a pioneer on the field of structural longitudinal imaging, I am grateful that you were always willing to think along. Your hospitality, politeness and patience are much appreciated.

Beste Serge. Jij bent een van de eerste mensen die ik heb leren kennen in het onderzoek, dank voor je hulp bij het verkennen van FSL en VBM.

Beste Mike. Als ik je zou moeten omschrijven dan denk ik dat de hardwerkende Duitser met een goed hart en gevoel voor humor wel volstaat. Ik vind het altijd leuk en nuttig met je samen te werken, als onderzoeker en als Radioloog.

Beste Yolande. Bedankt dat je mijn interesse hebt gewekt om promotie-onderzoek te doen bij het Alzheimercentrum, voor ik het wist werd ik door Philip gebeld tijdens mijn nachtdienst of ik maandagochtend wat te doen had. Ik vond het tijdens het MDO altijd prachtig om te zien hoe je de Radiologie benaderde vanuit het oogpunt van een clinicus.

I want to thank everyone at the DRC for the collaboration, especially Jo for all your support during my thesis. Our nearly normal mail conversations made me laugh a lot, and your cycling skills are unheard of. Richard, thanks for helping me install, and understand Midas and fluid.

Graag wil ik de medewerkers van het IAC bedanken, met name Ronald, Tabe, en Huub voor alle computer gerelateerde ondersteuning, Ellie en Tineke 'of ik al naar dat CDtje had gekeken' en verder iedereen van het IAC die ik nog niet genoemd heb..

Sylvia Olabarriaga and Keith Cover, thank you for enabling us to gain access to VL-E, it speeded up analyses dramatically.

Prof. dr. M.A. Blankenstein, dank voor uw bijdrage aan het integratie-artikel tussen imaging en liquor markers. Femke B, uiteindelijk zijn er toch een aantal mooie papers gekomen, dat had je destijds in het Oude Tramhuis vast niet gedacht.

Beste collega onderzoekers van het Alzheimercentrum, jullie hebben promoveren nog leuker gemaakt.

Wouter, Tim, bedankt dat je paranimf wilde zijn. We zijn gedurende de promotie veel met elkaar opgetrokken, je bent naast een gewaardeerd collega een goede vriend. Dank dat je er ook voor me was toen het minder goed ging! Vind het super om te zien hoe gelukkig je bent met Janna en Lucas.

Beste Alida, 'kamergenootje', ik kon altijd alles bij je kwijt. Uren hebben we zitten discussieren, het merendeel over het werk natuurlijk. Vond het altijd erg gezellig in het Aquarium met je.

Beste Laura en Nelleke of we nu in de Irish pub, Palacio, Metro, Balloons, Meatpackers, of gewoon in ergens Amsterdam waren, jullie waren altijd te porren voor nog één laatste drankje. Superrr gezellig!

Beste Georgios, bedankt dat je me wegwijs hebt gemaakt in de wondere wereld van de computational neuroanatomy, het promoveren, en het VUmc!

Beste Neuromeiden en jongens, het werk, de congressen en borrels waren niet hetzelfde geweest zonder jullie! Salka, Ester Koedam, Jeske, Annelies, Niek, Ilse, Niki, Alie, Esther Pelgrim, Rutger, Antonio Bastos Leite, Daniëlle, Jeroen, Willem, Maartje, Sietske en de anderen, ik heb altijd met veel plezier met jullie samengewerkt en gesocialized!

Dank ook aan de onderzoekers van de slaapgroep, parkinson, neuro-oncologie en MS: Elle, Els, Rebecca, Sanne B, Ricky D, Mirthe, Ingeborg, Bastiaan, Ivo, Stefan, Bas, Jolijn, Jessica, Machtelt, Madeleine en vele anderen voor hun gezelligheid tijdens de koffiepauze, lunch en borrels, maar uiteindelijk bleek toch: Alzheimer de!

Verder wil ik de overige medewerkers van het Alzheimercentrum bedanken, Freek, Rolinka, en vele anderen voor het helpen bij de inclusie, het vergaren van data en de patientenzorg.

Graag wil ik ook mijn huidige opleider bedanken, geachte prof. dr. C van Kuijk, beste Cees. Bedankt voor alle steun en het vertrouwen dat u me hebt gegeven. Ik moet nog vaak denken aan de woorden van Augustinus.

Beste stafleden, AIOS en medewerkers van de Radiologie, te veel om hier persoonlijk op te noemen, ik wil jullie hartelijk danken voor de huidige samenwerking. Het begin van de opleiding was hectisch gezien het afronden van de promotie, en de novo diabetes mellitus. Hartelijk dank voor jullie begrip en de keren dat jullie in zijn gesprongen in de tijd dat ik ziek ben geworden en gedurende mijn herstel. Ik waardeer het zeer dat jullie me de kans hebben gegeven mijn oude leven weer op te pakken, en dat jullie er ook zijn op de mindere momenten.

Tot slot dank voor mijn familie en vrienden. Waar zou ik zijn zonder jullie. Hopelijk kunnen we elkaar in de toekomst blijven opzoeken door heel het land. Allereerst dank voor mijn goede vrienden van de afgelopen jaren, Henri Le Conte, Wooden Charles, Bolle, Rooie, Pikkie, Snorrestaart, Dejeexcx, Benno, Thomas, Eelco Cheval en Jasper W, way to go! Bedankt voor de goede tijden, het lachen en de avonturen.

Gilles, Orfie en Budmeister, jullie maken het makkelijk alles te relativeren, wat maken die rare apen zich toch druk om niets ... slapen, eten, naar buiten en een beetje aandacht is genoeg, en af en toe een schone kattenbak natuurlijk.

Beste Har, bedankt voor alles wat je voor me hebt gedaan! 'What you see is what you get', 'Count your blessings', en 'A man's gotta do, what a man's gotta do' zijn maar een paar van de spreuken die je op het lijf zijn geschreven. Lieve Anne Marie, fijn dat je altijd klaarstaat om naar me te luisteren en adviezen te geven. Ik ben blij dat je meermaals de afstand overbruggt om ons op te zoeken.

Jordi, het is zeldzaam dat je broer toevallig ook je beste vriend is. Bedankt dat je mijn paranimf wil zijn. We hebben aan een half woord (bril) genoeg. Ook al wonen we niet meer op loopafstand, onze band blijft bestaan.

Lieve Oma, Nayat, Adam, Sarah, Emily, John en overige familieleden, bedankt dat jullie er zijn en voor de tijd die we met elkaar delen.

Beste schoonfamilie, Peter, Anneke, Pieter, Christa, Noor, Ernst, dank dat jullie me in jullie gezin hebben opgenomen, voor jullie gastvrijheid, en hulp in en om het huis.

Last but not least mijn lieve gezinnetje. Sanne, ik heb je leren kennen op de laatste dag dat ik nog officieel onderzoeker was, de vonk sloeg meteen over. Ondanks de in het begin roerige tijden bleek dat we heel goed van elkaar op aan kunnen. Het was niet makkelijk met een ontregelde diabeet te leven, desondanks heb jij me altijd gesteund. Je bent een lieve, eerlijke meid en ik voel me blij en vertrouwd bij je. Ik kijk uit naar ons huwelijk, en hoop dat we een lang en gelukkig leven samen zullen hebben. En lieve David, je beseft het nu nog niet, maar alleen al omdat je bestaat ben je het belangrijkste in mijn leven.

